

https://dspace.org/

Molecular mechanics calculations of dimetal bonds.

O'Neill, Francoise Marcelle Mary.

1992
https://hdl.handle.net/10539/27894

Downloaded from a DSpace repository. https://dspace.org/

MOLECULAR MECHANICS CALCULATIONS OF DIMETAL BONDS

Françoise Marcelle Mary O'Neill

A thesis submitted to the Faculty of Science, University of the Witwatersrand, Johannesburg, in fulfilment of the requirements for the degree of Doctor of Philosophy.

August 1992

Abstract

Two aspects of the beautiful conceptual structure of M-M multiple bonding remain puzzling; the large variability of the Cr(II)-Cr(II) quadruple bonds within the $Cr_2(X\text{^}Y)_4L_2$ compounds, and their response to axial ligation.

Most theoretical workers emphasize the inductive effect of the bridging ligand X^Y, while most experimental workers view the influence of the axial ligands L, as most important in determining the Cr-Cr distance. The controversy concerning the relative effects has been difficult to resolve. Previous efforts to understand the bond-length variations in the system have been unfruitful because of added steric distortions on the M-M distance.

A method capable of probing the electronic nature of the M-M bond, in the absence of steric complications, is required. The electronic and steric effects can effectively be separated in molecules with dimetal centres using the methods of molecular mechanics.

Using the Mo_2 system as our model of M-M bonding in these binuclear complexes belonging to group VIA, unique or characteristic (k_r, r_e) couples, where k_r is the force constant and r_e the electronic bond distance, for the Mo-Mo bond of orders 4.0, 3.5, 3.0, 2.0 and 1.0 were generated. Relationships between bond order and either k_r or r_e are then formulated.

Since Mo and Cr are periodically related, the equations modelling Mo-Mo bonding can be transferred to the Cr_2 system to facilitate analysis of its bonding patterns.

The results show that the large variation in Cr-Cr distance is a direct consequence of the cooperative modification of the electron density at the Cr_2 centre by the bridging and axial ligands.

We offer conclusions, based on a molecular mechanics treatment of M-M bonding, which we believe go far towards solving the long standing Cr_2 puzzle. Simultaneously, we have the opportunity of investigating the effect of torsional twist about the M-M bond on the δ^2 component of the quadruple bond.

Declaration

I declare that this dissertation is my own, unaided work. It is being submitted for the degree of Doctor of Philosophy at the University of the Witwatersrand, Johannesburg. It has not been submitted for any degree or examination at any other University.



F.M.M. O'Neill
15th day of August 1992

In loving memory of Joe and Mickey, whom I dearly miss

Acknowledgements

The author wishes to express her sincere appreciation to the following:

* Her supervisor, Professor JCA Boeyens, for his guidance, interest and continuous encouragement in the course of this study.

* The Foundation for Research Development, for the studentships.

* The University of the Witwatersrand for financial support to undertake this project, and for the post as Junior Lecturer in 1988 and 1989.

* Her employer, The Iron and Steel Corporation of South Africa (Iscor Ltd.) for granting study leave, without which much time would have been added to the production of this thesis.

* Her parents, for their love, for being parents, educators and friends, and for all the innumerable ways in which they have contributed to her life.

* Her boyfriend, Peter Fuller, for his continuous moral support, assistance and enduring patience.

* Her colleagues at Iscor (Ltd.) for their interest and encouragement in the final production stages.

* Her 'varsity' friends for being sincere friends, for the advice, encouragement, moral and academic

support, and for all the 'good times'.

* Ebeth van der Berg for the use of her personal computer for the production of the thesis.

Table of Contents

Page

Abstract ii

Acknowledgements vi

CHAPTER 1 1

1.1 The Recognition of the Quadruple Bond 1

1.2 An Overview of Dimetal Bonding 3

1.2.1 A Qualitative Picture of the Quadruple Bond 3

1.2.2 Bonds of Lower Order 7

1.3 Theoretical Advances on the Qualitative Picture 8

1.3.1 The $\sigma^2\pi^4\delta^2$ Configuration 9

(a) $[M_2X_8]^{n-}$ Species 9

(b) $Mo_2(O_2CR)_4$ Compounds 12

1.3.2 The $\sigma^2\pi^4$ Configuration 13

CHAPTER 2 14

2.1 Mo(II)-Mo(II) Quadruple Bonds . . . 14

Page

2.1.1 Compounds with No Bridging Ligands 14

2.1.2 Compounds with Bridging Ligands . . 16

(a) Halide Complexes of the Type $Mo_2X_4(L^{\wedge}L)_2$ 16

(b) The $Mo_2(XZY)_4$ and $Mo_2(XZY)_4L_2$ Compounds 20

2.2 Bonds of Order 3.5 30

2.3 Mo(III)-Mo(III) Triple Bonds 32

2.4 Double Bonds 38

2.5 Unbridged Single Bonds 41

CHAPTER 3 44

3.1 Cr(II)-Cr(II) Quadruple Bonds . . . 44

3.1.1 The Unbridged Chromium Dimer 44

3.1.2 Bridged Dichromium Compounds 45

(a) Dichromium Tetracarboxylates 45

(b) Other Bridged Dichromium Compounds . 52

(i) The Supershort Bonds 53

(ii) The Effect of Axial Ligands on Supershort Bonds 59

Page

(c) The Isolated $Cr_2(O_2CCH_3)_4$ Molecule . . 60

3.2 An Unbridged Single Bond 61

CHAPTER 4 62

4.1 The Effect of Axial Ligands 62

4.2 Formal vs. Effective Bond Order . . 63

4.3 Theoretical Attempts at Resolving the Dichromium Controversy 65

4.4 Another Theoretical Approach via Molecular Mechanics 72

CHAPTER 5 75

5.1 Introduction 75

5.2 Potential Functions of Molecular Mechanics Force Fields 77

5.2.1 Bond Stretching and Angle Bending . 77

5.2.2 Torsional Strain 78

(a) Attractive Torsional Interactions . 79

(i) L_4M-ML_4 Dimers of Order 4.0 and 3.5 79

(ii) Delocalized Interactions 80

(b) Repulsive Torsional Potentials . . . 81

Page

(i) L_4M-ML_4 Dimers of Order Three and Less 81

(ii) L_3M-ML_3 Dimers of Order Three and Less 82

(iii) Torsions About Other X-Y Bonds . . . 83

5.2.3 Out-of-Plane Bending 83

5.2.4 Nonbonded Interactions 84

(a) Coulombic Potential 84

(b) Var der Waals Interactions 84

5.3 Parameterization 88

5.4 Generating Unique, Transferable (k_r, r_o) Values for the Dimetal Centre 89

5.5 Energy Minimization 90

CHAPTER 6 91

6.1 Introduction 91

6.2 Molecular Mechanics Calculations Of the Quadruple Dimolybdenum Compounds 92

6.2.1 The Unbridged $[Mo_2X_8]^{4-}$ and $Mo_2X_4(PR_3)_4$ Compounds 92

Page

(a) Force Field Parameters 93

(b) The Delta Contribution to the Quadruple Bond Strength 96

(c) $\{k_r, r_o\}$ Solution Curves for the Mo_2 Centre 98

(d) Steric Deformations 101

6.2.2 The Bridged $Mo_2(XZY)_4$ and $Mo_2(XZY)_4L_2$ Compounds 102

(a) Force Field Parameters 102

(b) The Delta Contribution to the Quadruple Bond Strength 106

(c) $\{k_r, r_o\}$ Solution Curves for the Mo_2 Centre 107

(d) Steric Deformations 109

6.2.3 The 'Twisted' $Mo_2(XZY)_4L_2$ Molecules . 111

(a) Introduction 111

(b) Force Field Parameters 113

(c) The Delta Contribution to the Quadruple Bond Strength 114

(d) Molecular Mechanics Solution Curves 116

Page

(e) Steric Deformations 118

(i) The ($P-C_1-P$) Bridge 118

(ii) The $P-C_2-P$ Bridge 119

(f) General Conclusions 120

6.2.4 The Unique (k_r, r_o) Couple for Mo-4-Mo 121

6.2.5 Experimental ν_{Mo-Mo} and the Molecular Mechanics 4.07 mdyne/Å . . 122

6.3 Molecular Mechanics Calculations on the Mo-Mo Bond of Order 3.5 127

6.3.1 Introduction 127

6.3.2 Force Field Parameters 127

6.3.3 $\{k_r, r_o\}$ Solution Curves for the Mo_2 Centre 129

6.3.4 Discussion 130

6.3.5 Experimental ν_{Mo-Mo} and the Molecular Mechanics 3.63 mdyne/Å . . 132

6.4 The Triply-bonded Mo_2 Centre 134

6.4.1 The Mo_2L_6 Compounds 134

(a) Force Field Parameters 134

Page

(b) Steric Accommodation of the Electronically Demanded Structure . 136

6.4.2 The $[Mo_2(HPO_4)_4]^{2-}$ Ion 138

(a) Force Field Parameters 138

6.4.3 The $Mo_2(O_2CCH_3)_4(CH_2Bu^t)_2$ Molecule . . 140

(a) Force Field Parameters 140

6.4.4 The $\{k_r, r_o\}_{Mo-Mo}$ Solution Curves . . . 142

6.4.5 Experimental ν_{Mo-Mo} and the k_r(Mo-3-Mo) of 3.37 mdyne/Å 144

6.5 The Mo-Mo Double Bond 145

6.5.1 Molecular Mechanics Modelling . . . 145

6.5.2 The $\{k_r, r_o\}_{Mo-Mo}$ Solution Curves . . . 147

6.6 The Unbridged Mo-Mo Single Bond . . 149

6.6.1 Force Field Parameters 149

6.6.2 The $\{k_r, r_o\}_{Mo-Mo}$ Solution Curves . . . 151

6.6.3 The Equilibrium Structures 153

6.7 Brief Overview of the Mo-Mo Bond . . 154

Page

CHAPTER 7 155

7.1 Previous Analytical Curves 155

7.2 The Relationship between k_r and r_o for the Mo-Mo Bond 156

7.3 The Relationships between N and k_r and N and r_o for the Mo-Mo Bond . 159

7.4 The General Relationships for Dimetal Bonds from Group VIA 161

CHAPTER 8 163

8.1 Introduction 163

8.2 Transfer of Mo_2 Force Field Parameters to the Cr_2 System 164

8.3 The Quadruple Cr-Cr Bond 168

8.3.1 The Delta Contribution to the Quadruple Bond Strength 168

8.3.2 $\{k_r, r_o\}$ Solution Curves for the Cr_2 Centre 169

8.3.3 Steric Deformations 171

8.3.4 The Unique $(k_r, r_o)_{Cr-Cr}$ Couple for Quadruple Bonding 172

Page

8.4 The Relationships between Bonding Variables for Cr_2 173

8.5 Formally Quadruple, but Effectively of Slightly Lower Order 174

8.5.1 Molecular Mechanics Results 174

8.5.2 Discussion 178

8.5.3 The Existence of Fractional Cr-Cr Bond Orders 180

8.5.4 Comparison With Previous Predictions 180

8.6 Further Electronic Weakening of the Cr-Cr Bond by Axial Donation 182

8.6.1 Introduction 182

8.6.2 The Amidato-bridged Cr_2 Bond and Axial Coordination 183

(a) Molecular Mechanics Calculations . . 183

(b) Discussion 186

8.6.3 The Carboxylato-bridged Cr_2 Bond and Axial Coordination 187

(a) Molecular Mechanics Calculations . . 188

(b) Discussion 195

Page

(c) The Cr-Cr Bond Order Trends within the Cr_2 Carboxylates 197

8.6.4 Comparing the Carboxylato- and Amidato-bridged Compounds 202

8.6.5 Comparison with Previous Predictions 202

8.7 The Unsupported Cr-Cr Single Bond . 203

8.7.1 Force Field Parameters 203

8.7.2 Steric Deformations 204

CHAPTER 9 205

9.1 Overview 205

9.1.1 Mo_2 vs. Cr_2 205

9.1.2 Effect of Torsion on the Delta Bond 206

9.1.3 Other Aspects 206

9.2 What Makes Cr_2 Unique 207

9.3 The Value of Molecular Mechanics . . 208

9.4 Further Studies 208

Page

CHAPTER 10 209

10.1 Introduction 209

10.2 Molecular Mechanics Calculations . . 210

10.3 Dicussion 213

Appendix A 216

References 218

Chapter 1

INTRODUCTION TO THE IDEA OF MULTIPLE M-M BONDING

The renaissance of inorganic chemistry that began in the 1950's has its roots in the discovery of new and important classes of inorganic molecules, many of which do not conform to classical bonding theories. Among these landmark discoveries have been the isolation and structural characterization of transition metal compounds that possess multiple metal-metal bonds. From the seminal discoveries in this area in the early 1960's has developed a complex and fascinating chemistry.

1.1 The Recognition of the Quadruple Bond

Until the early 1960's the science of chemistry was devoid of the notion, much less the reality, of discrete multiple bonds between transition metal atoms, and, of course, totally devoid of the concept of quadruple bonds between any atoms whatever.
Then, in a very short space of time the existence of Re-Re double bonds, triple bonds, and quadruple bonds, the first double and triple bonds between transition metal atoms and the first quadruple bonds of any kind, was demonstrated.

With respect to quadruple bonds, a statement [2] made by Pauling in 1960 is interesting:
"It is customary to describe molecules not only in terms of single bonds, each involving a pair of electrons held jointly by two atoms, but also in terms of double bonds

and triple bonds (no one has as yet found evidence justifying the assignment to any molecule of a structure involving a quadruple bond between a pair of atoms)". This statement was entirely accurate at that time, and remained so for approximately four more years, when Cotton found [2,3], for the first time, "evidence justifying the assignment....of a structure involving a quadruple bond between a pair of atoms."

In the now famous structure of $[Re_2Cl_8]^{2-}$ anion [4] we saw for the first time the importance of multiple bonds between metal atoms. Once the crystallographic structure was determined (Figure 1.1), the obvious challenge was to interpret it in terms of bonding and electronic structure.

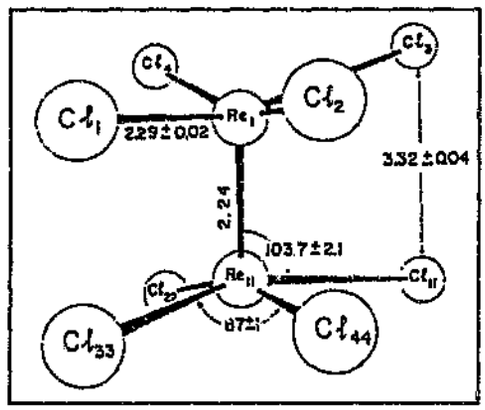


Figure 1.1 The structure of the $[Re_2Cl_8]^{2-}$ ion as originally reported in Ref. 4.

Cotton immediately recognized that, in order to account for the unique shortness of the Re-Re distance and the eclipsed geometry of the two $[ReCl]_4^-$ units, there had to be a strong metal-metal bond and by symmetry and electron counting this had to be comprised of one σ, two π and one δ components. The latter was responsible for the eclipsed geometry and was before that time an unrecognized feature in bonding.

1.2 An Overview of Dimetal Bonding

1.2.1 A Qualitative Picture of the Quadruple Bond

The original discussion [3] of the quadruple bond was based on qualitative considerations of orbital symmetries and rough estimates of overlap integrals.

The Re-Re axis was defined as the z-axis, and the Re-Cl bonds were assumed to project upon the x- and y-axes. Only five non-zero overlaps between pairs of d orbitals on the two metal atoms are possible because of symmetry properties. These are shown in Figure 1.2.

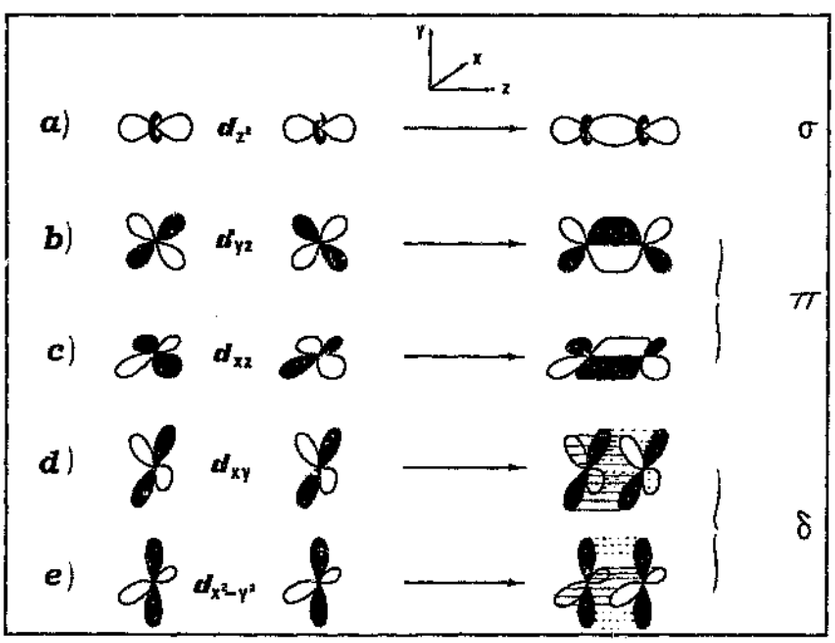


Figure 1.2 The five non-zero d-d overlaps between two metal atoms.

The positive overlap of the two d_{z^2} orbitals, $[d_{z^2}^{(1)} + d_{z^2}^{(2)}]$, gives rise to a σ-bonding orbital. There is of course, a corresponding antibonding σ orbital formed by negative overlap, $[d_{z^2}^{(1)} - d_{z^2}^{(2)}]$. The $[d_{xz}^{(1)} + d_{xz}^{(2)}]$ and the $[d_{yz}^{(1)} + d_{yz}^{(2)}]$ overlaps each give rise to a π

bond; these two are equivalent, but orthogonal, and hence constitute a degenerate pair. Again there are the corresponding π^* orbitals resulting from the negative overlaps. Lastly there are bonding orbitals formed by the $[d_{xy}^{(1)} + d_{xy}^{(2)}]$ and $[d_{x^2-y^2}^{(1)} + d_{x^2-y^2}^{(2)}]$ overlaps; these are also a degenerate pair and form δ (delta) bonds, with the corresponding negatively overlapping combinations giving a pair of δ^* orbitals.

If the set of coordinate axes as shown in Figure 1.3 is used, the $d_{x^2-y^2}$ orbitals differ from the d_{xy} orbitals, because the former point approximately toward the ligands and the latter point between them. In fact, the $d_{x^2-y^2}$ orbitals inevitably become heavily involved in the metal-ligand σ bonds and may be dismissed, leaving only one δ and one δ^* M-M orbital.

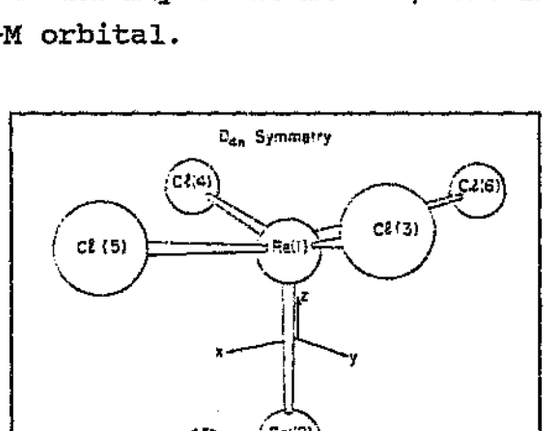


Figure 1.3 The orientation of the Cartesian axes relative to the atoms in the $[Re_2Cl_8]^{2-}$ ion.

Using the basic Hückel concept, namely, that MO (molecular orbital) energies are proportional to overlap integrals, at least for similar types of orbitals, and noting that these integrals must increase in the order $\delta \prec\prec \pi \prec \sigma$, we expect the orbitals to be ordered in energy as

follows, beginning with the most stable:
$\sigma \prec \pi \prec\prec \delta \prec \delta^* \prec\prec \pi^* \prec \sigma^*$.
An energy level diagram for M-M bonding then has the appearance of Figure 1.4.

For the $[Re_2Cl_8]^{2-}$ ion we have eight electrons to be placed in these orbitals, since the rhenium atoms are in the formal oxidation state (III), leaving (7-3)=4 electrons for each metal atom. These eight electrons just fill the bonding orbitals, giving a configuration we can represent as $\sigma^2\pi^4\delta^2$. This results in a formal bond order of four.

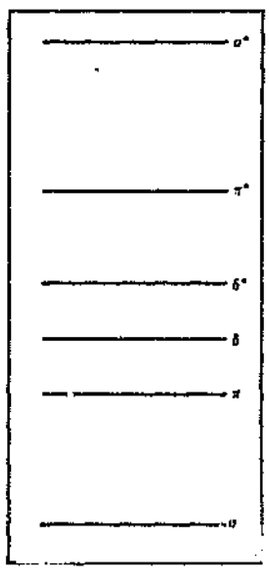


Figure 1.4 The qualitative ordering of the energies of the metal-metal bonding and antibonding orbitals, made up by d-d overlaps.

The $\sigma^2\pi^4\delta^2$ description of a quadruple bond unequivocally accounts for the two most conspicuous features of the dirhenium compound: its extreme shortness and its eclipsed configuration. Obviously the high multiplicity will account for the shortness. The conformational preference is also unambiguously explained. The σ bond is, of course, cylindrically symmetrical. A pair of π bonds is also cylindrically symmetrical. For one of these

the amplitude of the wavefunction as a function of an angle χ, measured from the x-axis around the bond in the xy plane (see Fig. 1.3 for coordinates), is proportional to $\sin^2\chi$. For the other π bond, perpendicular to the first one, the angular dependence is given by $\cos^2\chi$. Thus, the combined wavefunction has an angular dependence of $[\cos^2\chi+\sin^2\chi]$, which is, by a well-known trigonometric identity, a constant, viz., unity. Hence, the $\sigma^2\pi^4$ part of the bond is insensitive to the angle of internal rotation. The δ component of the bond, however, is markedly angle sensitive.

As shown in Figure 1.5, the $[d_{xy}^{(1)}-d_{xy}^{(2)}]$ overlap has its maximum value when the two $ReCl_4$ moieties are precisely eclipsed and it has a value of zero when the rotational conformation is precisely staggered. Thus, any rotation away from the eclipsed conformation causes a loss of δ-bond energy and, when carried to the limit of perfect staggering, causes complete disappearance of the δ bond. It is this dependence of the δ bond on rotation angle that opposes the tendency of nonbonded repulsions to favour a staggered conformation. This argument does not predict that the fully eclipsed conformation is preferred, but only that a conformation approaching the eclipsed one should be preferred.

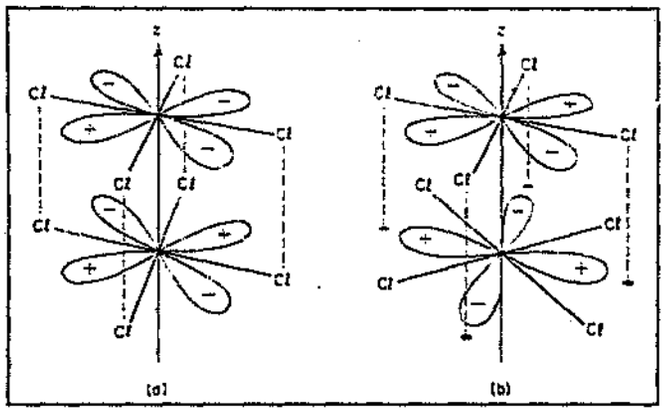


Figure 1.5 The relationship of one d_{xy} orbital to the other for (a) an eclipsed structure and (b) a fully staggered structure.

1.2.2 Bonds of Lower Order

The explicit recognition that quadruple M-M bonds exist and that they may be represented by the ground state electronic configuration $\sigma^2\pi^4\delta^2$ provides a convenient framework upon which to consider bonds of lower orders.

Because of the fact that the δ orbital is only weakly bonding and the δ^* orbital only weakly antibonding, a $\sigma^2\pi^4\delta^2$ quadruple bond is readily subjected to either electron loss or electron gain, as shown below. Thus an entire range of formal bond orders, 4.0 through to 3.0 is accessible.

If still more electrons are added to or removed from the array of MO's formed by d-d overlap, the M-M bond order can be reduced still further. This is true for the addition of as many as five more electrons, which would lead, finally, to a $\sigma^2\pi^4\delta^2\delta^{*2}\pi^{*4}\sigma^{*1}$ configuration; or the removal of five electrons resulting in a σ^1 configuration, with a net bond order of 0.5.

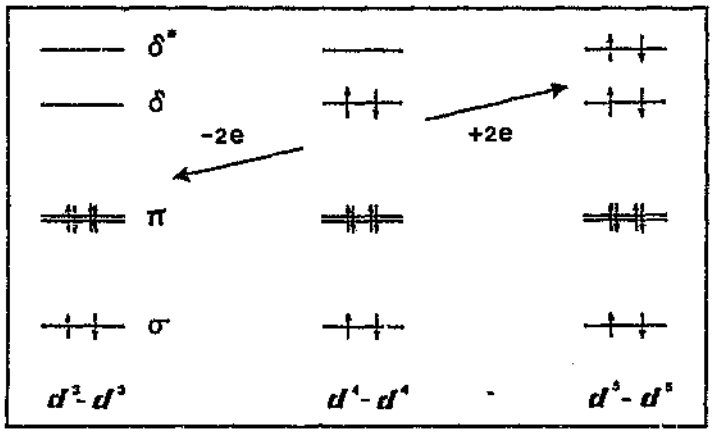


Figure 1.6 A schematic representation of how changes in the occupation of the δ and δ^* orbitals change the M-M bond order.

In short, how many of the five possible nonzero overlaps play a role, and what role they play in binding the metal atoms together depends on the number of electrons available and the number and types of ligands attached to the metal atom.

The above picture of M-M bonding seemed to alarm some organic chemists, who took some time to accept the fact that d orbitals can do things that s and p orbitals cannot.

1.3 Theoretical Advances on the Qualitative Picture

Concomitant with the rapid accumulation of new compounds and the study of their chemistry, there has been a remarkable broadening and deepening of our understanding of the electronic structures of compounds with multiple bonds between metal atoms [32]. This has resulted from both theoretical work and various kinds of physical, especially spectroscopic, measurements and from the interplay between them.

Theory has been continually challenged by these compounds

because of their complexity and the fact that atoms of high atomic number are involved. The nature of the multiply bonded species is such that sophisticated theoretical methods are not easily applied to them. Thus until the early 1970's no significant theoretical advance beyond the simple d-orbital overlap picture was made.

The first encouraging developments began with the modification of certain theoretical techniques, originally developed by Slater's school for dealing with the band theory of metals, to make them applicable to molecular problems. This work, pioneered by John C. Slater and Keith Johnson, resulted in what is commonly called the SCF-Xα-SW method: the abbreviation means self-consistent field Xα scattered wave. The SCF-Xα-SW method of calculation [5] appears to afford a practicable avenue of theoretical approach.

1.3.1 The $\sigma^2\pi^4\delta^2$ Configuration

(a) $[M_2X_8]^{n-}$ Species

The first quantitative calculations were performed by the SCF-Xα-SW method on the $[Mo_2Cl_8]^{4-}$ ion [6,7] and the $[Re_2Cl_8]^{2-}$ ion [8,9]. These calculations are really landmarks in the field because they provided reliable, quantitative, and detailed descriptions of the ground state electronic structures of these ions that are in excellent agreement with the original qualitative description of a quadruple bond based on orbital overlap considerations. They confirmed the primacy of metal d orbitals in the formation of such bonds.

Contour diagrams of the δ, π, and σ orbitals as obtained from the SCF-Xα-SW calculation (Figures 1.7(a)-(c)) have exactly the shapes expected from the qualitative d-orbital overlap picture (cf. Fig. 1.2).

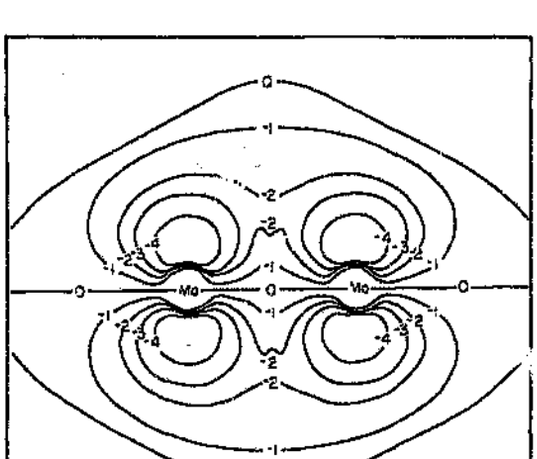


Figure 1.7(a) A contour diagram of the Mo-Mo δ-bonding in $[Mo_2Cl_8]^{4-}$.

When it is noted that the δ, π and σ MO's have 89%, 76%, and 83% metal d-orbital character respectively, this result is completely understandable and satisfying.

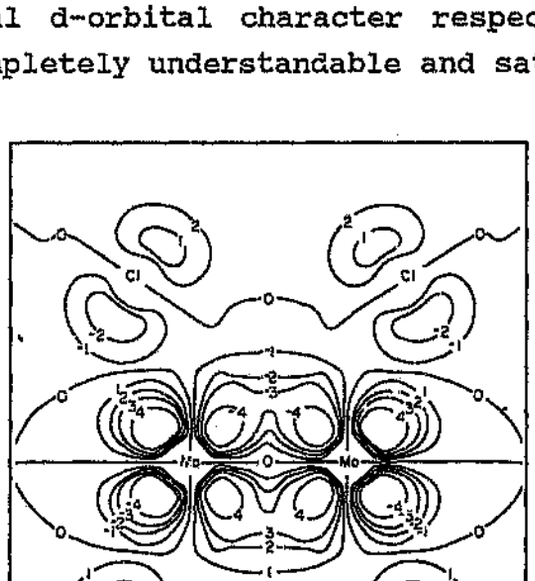


Figure 1.7(b) A contour diagram of one of the Mo-Mo π-bonding orbitals in $[Mo_2Cl_8]^{4-}$.

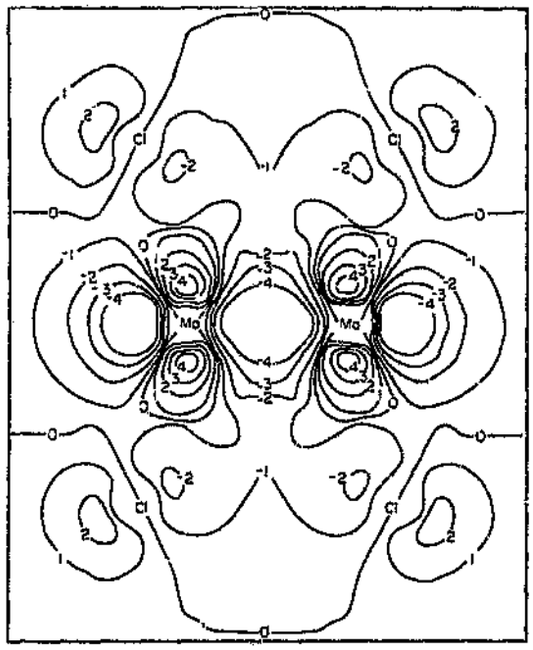


Figure 1.7(c) A contour diagram of the Mo-Mo σ-bonding orbital in $[Mo_2Cl_8]^{4-}$.

Ab initio treatments of dimetal bonding have also been employed. The Hartree-Fock LCAO method has been applied [10,11] to several $[M_2X_8]^{n-}$ species. All calculations on Cr_2 species are best described together in Chapter 4, Section 4.3.

To appreciate the significance of the following discussion, the reader will require some familiarity with the basic concepts of the Hartree-Fock (HF) method. The terms 'SCF calculation' or 'SCF level' are used to mean a HF calculation employing only one configuration and minimizing the energy thereof. The terms 'CI level' or 'CI calculation' designate calculations in which the effects of electron correlation within a single configuration are corrected for (at least partially) by making additional calculations for appropriately chosen higher-energy configurations and employing all of these plus the ground state configuration in a variational minimization of the energy of the system.

For $[Mo_2Cl_8]^{4-}$ the most stable single configuration for the ground state, $\sigma^2\pi^4\delta^2$, was found to be the one corresponding to the quadruple bond. When a limited amount of CI was introduced, the energy of the ground state was lowered by about 2eV, and it was found that the $\sigma^2\pi^4\delta^2$ configuration then made up 61% of the true ground state, the rest consisting principally of other configurations of the types $\pi^4\delta^2\sigma^{*2}$, $\sigma^2\pi^2\delta^2\pi^{*2}$, ..., $\sigma^{*2}\pi^{*4}\delta^{*2}$. Perhaps the most important point for the experimental chemist is that, again, the qualitative picture of the quadruple bond as originally proposed is validated.

(b) $Mo_2(O_2CR)_4$ Compounds

Clear-cut assignment of quadruple bonding to just three discrete σ, π and δ orbitals is not always possible. The situation conforms most closely to such a simple description for the $[Mo_2Cl_8]^{4-}$ case where the metals are in a low formal oxidation state and the ligands are rather simple. More complex ligands lead to complicated patterns of orbital mixing so that in many cases the M-M bonding interactions are distributed over more than one MO of the appropriate symmetry type.

SCF-Xα-SW calculations on the prototype molecule $Mo_2(O_2CH)_4$ [12,13] reveals the retention of high d character for the δ and π MO's, and one can nearly always speak of 'the' δ- and π-bonding orbitals.
For the M-M σ bond there is a mixing with M-O bonding. The Xα-SW calculation yields two components to the σ bond, the $4a_{1g}$ and the $5a_{1g}$ MO's. Both MO's make significant contributions to M-M σ bonding (75% metal character for $4a_{1g}$; 48% Mo for $5a_{1g}$).

1.3.2 The $\sigma^2\pi^4$ Configuration

Calculations by the SCF-Xα-SW method on the Mo_2X_6 species (X = OH, NH_2, NMe_2, and CH_3) have given a very detailed and satisfactory account of the bonding in these molecules [14,15]. For $Mo_2(OH)_6$, the Mo-Mo bonding orbitals are largely made up of metal d-orbital contributions and conform very closely to what is expected from the simple d-orbital overlap picture. The clean separation of the Mo-Mo σ- and π-bonding orbitals from all the lower-lying MO's is lost when we go to the $Mo_2(NR)_6$ and $Mo_2(CH_3)_6$ cases. The lone-pair electrons of the nitrogen atoms and the Mo-C bonding orbitals are in the same energy range as the Mo-Mo π and σ orbitals. As a result one cannot speak of 'pure' M-M bonding.

What is the meaning of this mixing between metal and ligand orbitals?

The answer will become clear as we delve deeper into the subject-matter of this thesis. Suffice it to say that this mixing is, in part, responsible for some inconsistencies observed in the physical data of these dimetal compounds, such as vibronic spectra and observed metal-metal distances.

Chapter 2

BONDS BETWEEN Mo ATOMS: AN OVERVIEW OF STRUCTURAL STUDIES

From the Re-Re quadruple bond, as recognized in $[Re_2Cl_8]^{2-}$ in 1964, the field of metal-metal multiple bonds has steadily grown, so that it now includes many other metals and a considerable variety of ligands.

Only compounds of relevance to this thesis will be discussed. These are the molybdenum dimers of formal orders four through to one, as well as the chromium dimers, for which only formally quadruply- and singly-bonded compounds are known. It should be noted that structure solutions involving any form of disorder that could effect the observed metal-metal bond distance have been excluded. In the studies done, it is of utmost importance to have reliable data concerning the structure of the dimeric compound.

2.1 Mo(II)-Mo(II) Quadruple Bonds

In all of these compounds the formal oxidation number of molybdenum is two. This means that each Mo has (6-2) = 4 electrons available for metal-metal bonding. In effect a total of 8 electrons occupy the d orbitals used for bond formation resulting in a $\sigma^2\pi^4\delta^2$ configuration.

2.1.1 Compounds With No Bridging Ligands

Here, one can assert that a metal-metal bond is present simply because the structure shows that there is nothing

else to hold the metal atoms together.

The first dimolybdenum bond unsupported by ligands was identified as $K_4Mo_2Cl_8.2H_2O$ [16] and characterized as containing the $[Mo_2Cl_8]^{4-}$ anion (Figure 2.1).

The eclipsed configuration, the short Mo-Mo bond (2.138(4) Å), and the fact that it is isoelectronic as well as isostructural with $[Re_2Cl_8]^{2-}$ leave no doubt that it has the type of quadruple bond previously discussed for Re_2. The only reasonable explanation for the eclipsing is the presence of the quadruple bond with its δ component.

The highly symmetrical D_{4h} structure was soon discovered for $(NH_4)_4Mo_2Br_8$ [17] and $Li_4Mo_2(CH_3)_8.4THF$ [18].

Figure 2.1 The structure of the $[Mo_2Cl_8]^{4-}$ anion in $K_4Mo_2Cl_8.2H_2O$.

A large number of neutral mixed ligand complexes, bearing a close structural relationship to $[Mo_2X_8]^{4-}$, have been

isolated and structurally characterized. They can be represented simply with the formula $Mo_2X_4L_4$, where X is a halide (Cl, Br, I) or methyl group (Me), and L is a monodentate phosphine ligand, PR_3 (R_3 = Me_3, Me_2Ph, HPh_2) [19, 20, 21, 22].

The $Mo_2X_4L_4$ core adopts a D_{2d} idealized geometry, as shown in Figure 2.2.
The trans stereochemistry is a consequence of the need to minimize nonbonded repulsions within these sterically crowded molecules. The Mo-Mo distances for these compounds are in the range 2.125(1) - 2.165(1) Å.

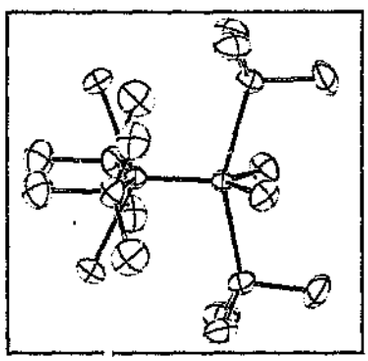


Figure 2.2 The molecular structure of the $Mo_2X_4(PR_3)_4$ complexes taken from the parameters for X=Br, R=Me.

2.1.2 Compounds with Bridging Ligands

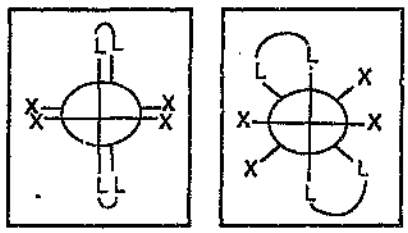
(a) Halide Complexes of the Type $Mo_2X_4(L\hat{}L)_2$

Thorough synthetic and structural studies by Cotton and coworkers [23, 24, 25, 26, 27] have been done on the $Mo_2X_4(L\hat{}L)_2$ compounds (where X = halide and L^L is a diphosphine spanning the M-M bond).

Similar atoms are disposed trans to each other and the two trans-$Mo_2X_2P_2$ units are rotated relative to each

other about the Mo-Mo bond, so that the Mo-L bonds in one such unit do not eclipse any of the Mo-L bonds in the other.

Maximum δ overlap occurs in the eclipsed conformation ($\chi = 0°$), illustrated by **1a**, and zero δ overlap occurs in the staggered form ($\chi = 45°$), which is illustrated by **1b**.



(1a) **(1b)**

The fact that the strength of the δ bond is greatest for $\chi = 0°$ does not necessarily mean that this is the preferred angle when all factors are taken into account, however. With the bidentate ligands that span the two metal atoms, the conformational preferences of the resulting M_2-containing rings favour twist angles different from zero. The value of χ is determined by the balance that is struck between the steric requirements of the substituents on the P atom, which favour a staggered arrangement, and the δ bond, which is a maximum at 0°.

Table 2.1 is a listing of such molecules studied during the research of the thesis.

The central portion, $Mo_2X_4(P-C-P)$, of the molecule, $Mo_2I_4(dppm)_2$, viewed down the Mo··Mo bond, is shown in Figure 2.3.

Table 2.1 Structural data for the $Mo_2X_4(L^{\frown}L)_2$ compounds

Compound	χ (deg.) P-Mo-Mo-P	χ (deg.) X-Mo-Mo-X	r (Å) Mo-Mo
$Mo_2I_4(dppm)_4$	4.9 19.7	15.6 17.2	2.152(2)
$Mo_2(NCS)_4(dppm)_2$	9 18.7	12 13.6	2.167(3)
$Mo_2Cl_4(tdpm)_2$	10.7 27.4	21 20	2.148(1)
$Mo_2Br_4(S,S\text{-}dppb)_2$	-22 -23	-20 -21	2.147(6)
$Mo_2Cl_4(S,S\text{-}dppb)_2$	-24.8 -24.8	-21.1 -27.5	2.147(3)
$Mo_2I_4(dppe)_2$	-26.5 -26.5	-25.5 -24	2.179(3)
$Mo_2Br_4(dmpe)_2$	36 37	36 37	2.169(2)

Abbreviations used in table:

dppm :$Ph_2P\text{-}CH_2\text{-}PPh_2$
tdpm :$PPh_2\text{-}CH(PHPh)\text{-}PPh_2$
S,S-dppb :$PPh_2\text{-}CHMe\text{-}CHMe\text{-}PPh_2$
dppe :$PPh_2\text{-}CH_2\text{-}CH_2\text{-}PPh_2$
dmpe :$PMe_2\text{-}CH_2\text{-}CH_2\text{-}PMe_2$

The dppm and tdpm ligands form two envelope-type, five-membered rings including the dimolybdenum bond.

These bridging ligands are not symmetrically coordinated since one of the two Mo-P distances associated with each Mo is ca. 0.1 Å longer than the other. Also, the Mo-Mo-P angles differ by ca. 6° for the dppm species, while those of the tdpm species differ by only 2°. These appreciable

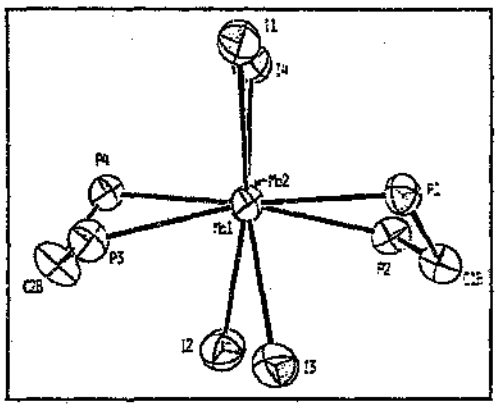


Figure 2.3 The rotational conformation of the dimolybdenum units Mo(1)-Mo(2) in $Mo_2I_4(dppm)_2$.

distortions are a result of internal crowding (evidence to exclude any electronic factor is clearly given by the studies done in this thesis - see Chapter 6).

From viewing the molecule down the Mo-Mo axis, it is immediately recognized that all four torsional angles are different, but in the same sense, and thus have the 'concerted' effect of an internal rotation. Each of the torsions results from the combined effects of a true internal rotation and other steric distortions.

The central portion, $Mo_2X_4(P\text{-}C\text{-}C\text{-}P)_2$, of the molecule $Mo_2I_4(dppe)_2$ is shown in Figure 2.4.
The two six-membered rings Mo-P-C-C-P-Mo, formed by the dppe and S,S-dppb ligands and the dimetal unit, have a conformation that can best be described as a distorted chair. In a simple chair conformation the C-C and Mo-Mo bonds would be parallel.
Because of the larger twist angles, the internal crowding is not as severe as in the above cases, and a more symmetrical structure is observed.

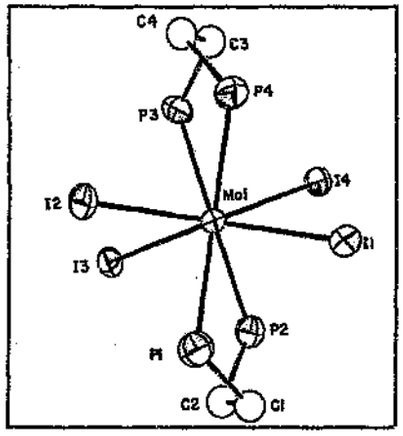


Figure 2.4 Central portion of $Mo_2I_4(dppe)_2$ viewed along the Mo(1)-Mo(2) axis.

In the case of $Mo_2Br_4(dmpe)_2$, the two six-membered rings formed by the dmpe ligands and the dimetal unit again take on chair conformations. Internal distortions are relieved by the large torsional twist of 36°, and symmetrical Mo-P bonds and Mo-Mo-P angles are seen. However, studies by molecular mechanics reveal an important difference from the previous molecules.

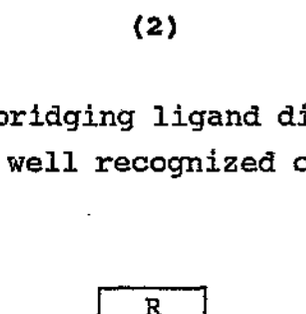
What angle of rotation can be tolerated without loss of the δ bond?
This is one of the questions that has an illuminating answer discussed in Chapter 6.

(b) The $Mo_2(X\text{-}Z\text{-}Y)_4$ and $Mo_2(X\text{-}Z\text{-}Y)_4L_2$ Compounds

These complexes might well be considered the single most important class of compounds to contain a Mo-Mo quadruple bond because they have traditionally been the starting point for the synthesis of almost all other derivatives of the quadruply bonded Mo_2^{4+} core.

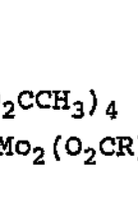
These molecular systems can be described by the general structural formula shown in **2**, or some simple variant of

it. In this type of compound there are two kinds of ligands. The bridging ligands X-Z-Y, all four of which are usually the same, form M-X and M-Y bonds called equatorial bonds; the X-Z-Y ligands may be called equatorial ligands. The M-L_{ax} bonds are called axial bonds and the L_{ax} ligands, axial ligands. The axial ligands, L_{ax} and L_{ax}', may be the same or different; one, or both may be absent. The bridging ligands, XZY, are usually unidentate groups in which a single atom, Z, connects the donor atoms X and Y.



(2)

The first class of bridging ligand discovered in 1971 is a member of the now well recognized class of carboxylato anions $[RCO_2]^-$, 3.



(3)

The properties of the carboxylato ligand can be varied in many ways. Its basicity can be altered by changing R from $C(CH_3)_3$ at one extreme to CF_3 at the other. Its steric properties can be changed from those with R = H to those with R = 2-phenylphenyl.

The structure of $Mo_2(O_2CCH_3)_4$ (Figure 2.5) [28] is entirely typical of the $Mo_2(O_2CR)_4$ compounds.

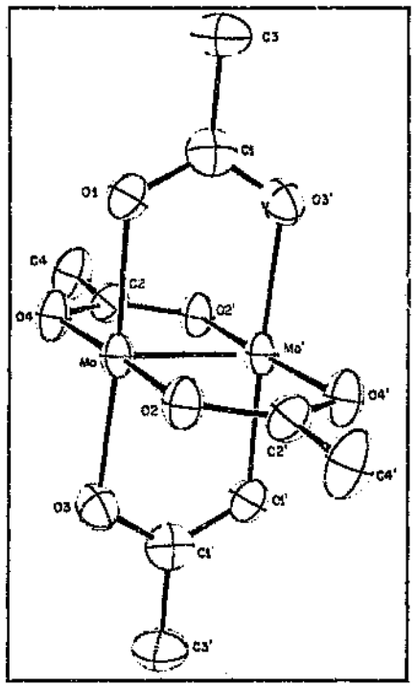


Figure 2.5 An ortep drawing of the $Mo_2(O_2CCH_3)_4$ structure.

The other compounds examined were the formate (R = H) [29], trifluoroacetate (R = CF_3) [30] and pivalate (R = $C(CH_3)_3$) [31].
These molecules are arranged to form infinite chains in which there is weak axial coordination of each molecule by oxygen atoms of its neighbours.

In the set of four unsolvated compounds with R = CMe_3, Me, H and CF_3, the Mo-Mo distances are invariant, suggesting insensitivity of the Mo_2 quadruple bond to the influence of changes in the inductive effect of the R groups as well as to variations in the location of the axial ligand. This is seen clearly from the data in Table 2.2.

Following the synthesis and structure determination of the trifluoroacetate $Mo_2(O_2CCF_3)_4$, its pyridine adduct was obtained upon dissolution in pyridine.

Table 2.2 Structural data for $Mo_2(O_2CR)_4L_2$, L_{ax} = intermolecular O donation

R	Mo--L_{ax} (Å)	Mo-Mo (Å)
CMe_3	2.90	2.088(1)
Me	2.65	2.093(1)
H	2.65	2.091(2)
CF_3	2.72	2.090(1)

Its structure [33], which is shown in Figure 2.6, reveals the expected axial coordination of the pyridine ligands. However, while the Mo-N distances (2.548(8) Å) are quite long, this interaction leads to a lengthening of the Mo-Mo bond by 0.039(6) Å relative to that in the parent molecule.

Does this lengthening mean there is an electronic weakening of the quadruple interaction; or is it simply steric in nature?

The axial donors share the same metal orbitals as those used to form the σ component of the Mo-Mo bond, and so weakening of the dimetal bond may be expected in the presence of axial donation. However, we must bear in mind that we are comparing observed Mo-Mo distances which are a result of both electronic and steric effects.

One would expect the presence of axial ligands to cause increased steric congestion within the molecule, resulting in a stretching of the dimolybdenum bond. Predictions of electronic weakening of the dimetal centre is possible only once steric factors are totally excluded.

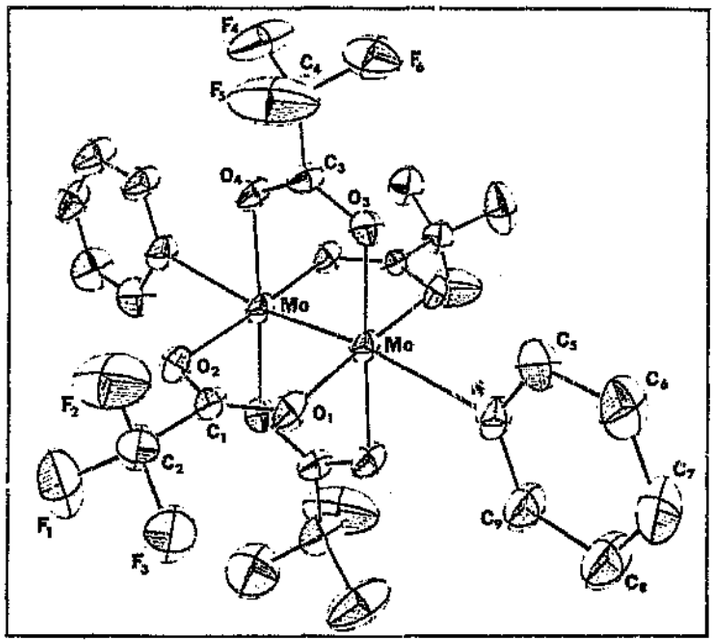


Figure 2.6 The structure of $Mo_2(O_2CCF_3)_4(py)_2$.

One has two alternatives in investigating the importance of axial coordination on the M-M bond length. One has to either construct a molecule with a very large R group that effectively enshrouds the molecule and prevents axial coordination, or one must study the free molecule in the gas phase.

The compound $Mo_2(O_2Cbiph)_4$, where $biphCO_2H$ is 2-phenylbenzoic acid, has been structurally characterized [34] by X-ray crystallography (Figure 2.7).
In this case the steric properties of the $[biphCO_2]^-$ ligands prevent intermolecular association, and the crystal structure consists of a simple van der Waals packing of the molecules with no axial ligation, intermolecular or otherwise. The Mo-Mo distance, 2.082(1) Å, is shorter than that for the structures with axial ligation.
This is expected on steric grounds, but one cannot exclude electronic factors.

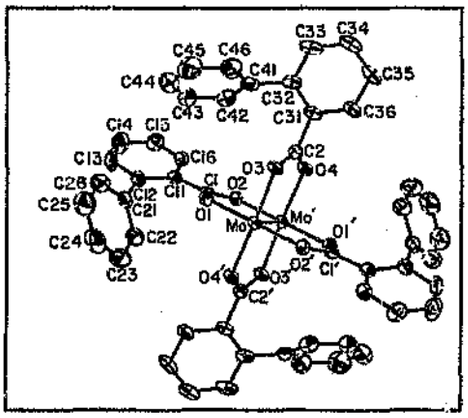
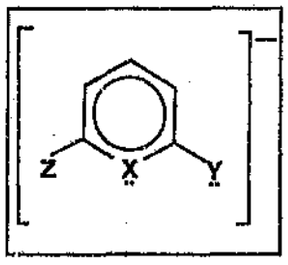


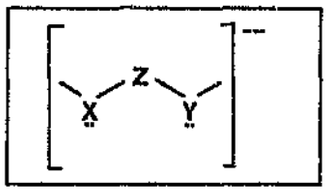
Figure 2.7 The structure of $Mo_2(O_2Cbiph)_4$.

The molecular structure of anhydrous tetraacetate, $Mo_2(O_2CCH_3)_4$ in the gas phase at 190°C, was determined by Kelley and Fink in 1982 [35]. The Mo-Mo distance (2.079(3) Å) is shorter by ca. 0.01 Å than that determined by X-ray crystallography, demonstrating the distorting effects on the quadruple bond of axial coordination. Interestingly, all other molecular dimensions are statistically indistinguishable between the gas and solid phases.

Extrapolations may be made from the $[RCO_2]^-$ group to isostructural and isoelectronic groups which also yield a large class of binuclear complexes. One such class is the group of monoanionic ligands which may be represented by **4a** and **4b**.

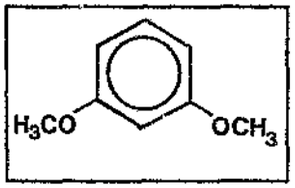


(4a)

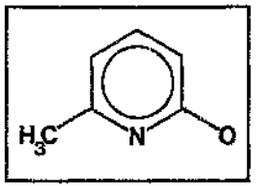


(4b)

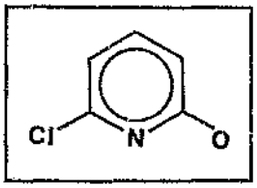
The ligand system **4a**, encompasses the following ligands:



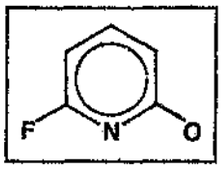
(i)



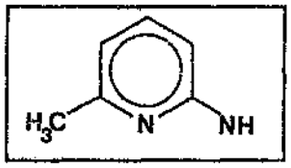
(ii)



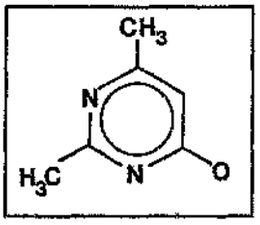
(iii)



(iv)



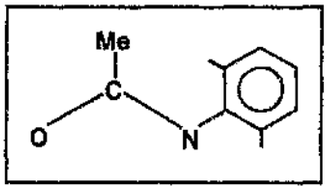
(v)



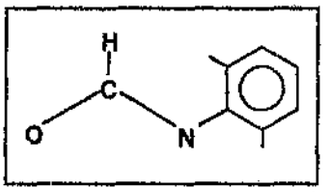
(vi)

i :2,6-dimethoxyphenyl anion, DMP [36]
ii :6-methyl-2-hydroxypyridine anion, MHP [37]
iii :6-chloro-2-hydroxypyridine anion, CHP [38]
iv :6-fluoro-2-hydroxypyridine anion, FHP [39]
v :6-methyl-2-aminopyridine anion, MAP [40]
vi :2,4-dimethyl-6-hydroxypyrimidine anion, DMHP [41]

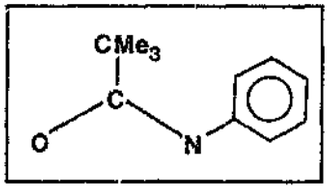
Ligands classified as class **4b** are shown below:



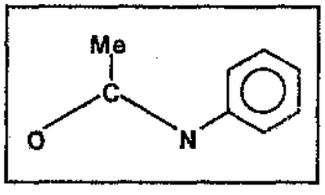
(i)



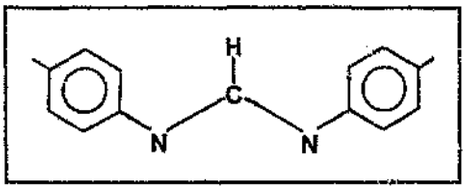
(ii)



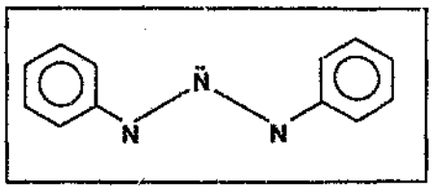
(iii)



(iv)



(v)



(vi)

i :N-(2,6-dimethylphenyl)acetamido anion; [(2,6-xylyl)N-C(Me)-O]$^-$ [42, 43, 44]

ii :N-(2,6-dimethylphenyl)formamido anion; [(2,6-xylyl)N-C(H)-O]$^-$ [45]

iii :N-phenylpivalamido anion; [PhN-C(CMe_3)-O]$^-$ [45]

iv :N-phenylacetamido anion; [PhN-C(Me)-O]$^-$ [46]

v :di-p-tolylformamide anion; [(tol)N-C(H)-N(tol)]$^-$, DFM, [47]

vi :1,3-diphenyltriazine anion; [PhN-N-NPh]$^-$ [48]

The structure of $Mo_2(MHP)_4$ is shown, as an example of the class **4a** ligands, in Figure 2.8.

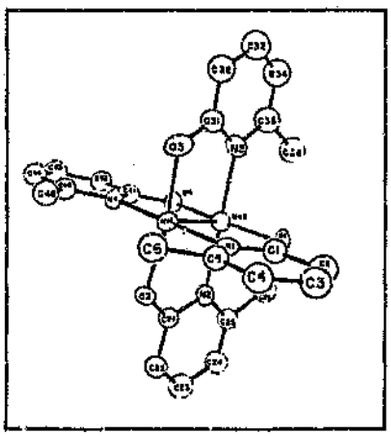


Figure 2.8 The structure of $Mo_2(MHP)_4$.

An example of class **4b** ligands is seen in Figure 2.9.

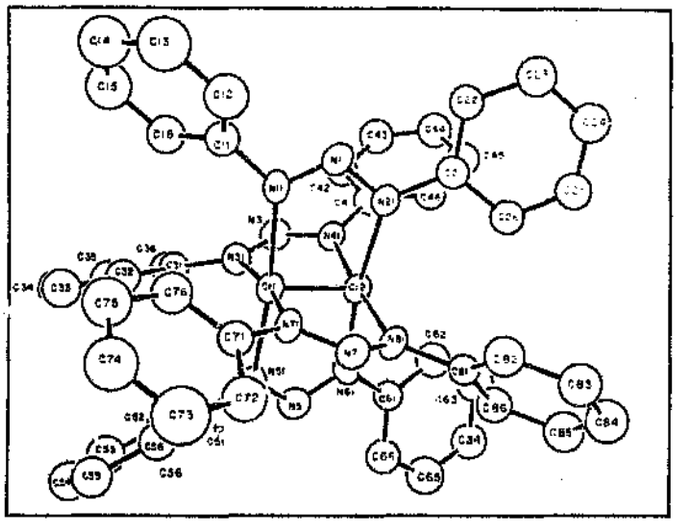


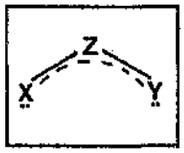
Figure 2.9 The structure of $Mo_2(PhN\text{-}N\text{-}NPh)_4$.

The Mo-Mo distances for these O^C-, N^N- and N^O-bridged compounds range from 2.064(1) to 2.085(4) Å in the absence of axial donation, and from 2.083(3) to 2.113(1)Å in the presence of axial ligation.

As in the carboxylato case, the presence of axial ligands causes a lengthening of the Mo-Mo distance. As mentioned earlier, we are not as yet in a position to attribute this bond lengthening specifically to steric or electronic factors, or both.

The axial ligation includes such neutral donors as pyridine, THF, 4-Me-pyridine, dichloromethane and dibromomethane.

Because of the delocalization of the negative charge over the XZY atoms in all the O^O, C^O, N^O and N^N ligands discussed above, 5, X and Y have their donor orbitals directed along approximately parallel lines. As a result, near-eclipsing of the X-Mo-Mo-Y unit is seen in all these molecules (besides the near-eclipsing enforced by δ bonding).



(5)

Another class of ligands, which are dianions, is the sulfates, $[SO_4]^{2-}$. The crystal structure [49, 50] of the dihydrate $K_4Mo_2(SO_4)_4.2H_2O$ (Figure 2.10) consists of the usual eclipsed conformation with four bridging sulfate ions and the axial positions of the dimer occupied by terminal oxygen atoms (Mo--O = 2.591(4) Å) from neighbouring sulfate ions. This bridging pattern leads to the infinite two-dimensional network as seen in the stereoscopic view of the unit cell (Figure 2.11)

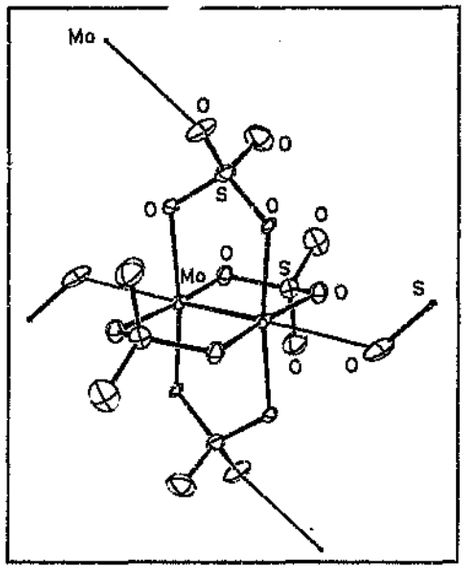


Figure 2.10 The structure of the $[Mo_2(SO_4)_4]^{4-}$ unit in $K_4Mo_2(SO_4)_4.2H_2O$.

Unlike the bridging ligands encountered above, here the Mo_2O_2S rings are non-planar, having an average dihedral bend of 20° across the O--O line. This is a result of the absence of electron delocalization over the O-S-O

bridging atoms.

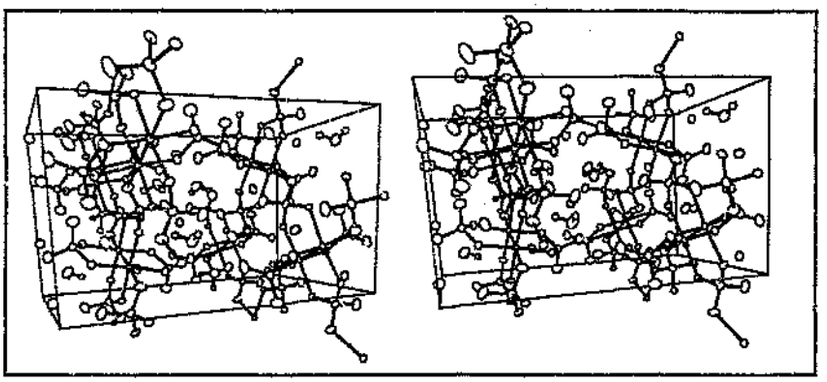


Figure 2.11 Stereoscopic view of the unit cell contents of $K_4Mo_2(SO_4)_4.2H_2O$.

The Mo-Mo distance, 2.111(1) Å, is longer (by ca. 0.11 Å) than that in the O^O-bridged compounds with similar intermolecular axial interaction.

A structural result that is true for all the dimolybdenum compounds with X-Z-Y bridging ligands is that, the structures involving axial donation have Mo-Mo distances longer than those lacking axial ligands. The significance of this bond lengthening upon introducing axial ligands is one of the aspects to be discussed in this thesis.

2.2 Bonds of Order 3.5

In the process of crystallizing pink $K_4Mo_2(SO_4)_4.2H_2O$ slowly so as to obtain useful crystals, it was found that lavender crystals also formed [50, 51]. X-ray crystallography showed that they have the composition $K_3Mo_2(SO_4)_4.3.5H_2O$ and contain the $[Mo_2(SO_4)_4]^{3-}$ ion, which has a structure very similar to that of $[Mo_2(SO_4)_4]^{4-}$, except for the presence of coaxial water molecules here, as opposed to sulfate O atoms in the 4- ion.

According to the accepted description of the quadruple bond, the electron lost from the 4- ion to give the 3- ion should come from the δ-bonding orbital, thereby giving the latter species a $\sigma^2\pi^4\delta^1$ configuration. The 3- ion is paramagnetic and e.s.r spectra show that the unpaired electron is evenly distributed over two magnetically equivalent Mo atoms.

There are two noteworthy quantitative changes on going from the 4- to the 3- ion. Firstly, loss of the δ electron causes a lengthening of the Mo-Mo bond, by ca. 0.054(6) Å. Secondly, the mean Mo-O(bridge) distance is ca. 0.07 Å shorter for the 3- ion. The direction of change accords with the fact that increasing the formal oxidation number of the metal atoms (by 0.5) should decrease their radius.

Each Mo-O-S-O-Mo ring is folded along the O--O line with a dihedral angle of 20°. Each Mo atom is approached by the O atom of a water molecule approximately along the extended Mo-Mo axis, but only at a considerable distance (2.55 Å).

Although there are two crystallographically distinct $[Mo_2(SO_4)_4]^{3-}$ ions in the structure, the bond distances and angles differ very little in the two complexes. The non-equivalence results from differences in the packing: Molecule 1 packs as isolated units with one H_2O molecule attached to each Mo atom (Mo-Mo = 2.167(1) Å); whereas molecule 2 forms an infinite chain parallel to the c-axis with water molecules being shared between sulfate molecules (Mo-Mo = 2.162(1) Å) i.e. H_2O molecules bridge the molybdenum dimers. The packing is shown in Figure 2.12, a stereoscopic view of the contents of the unit cell.

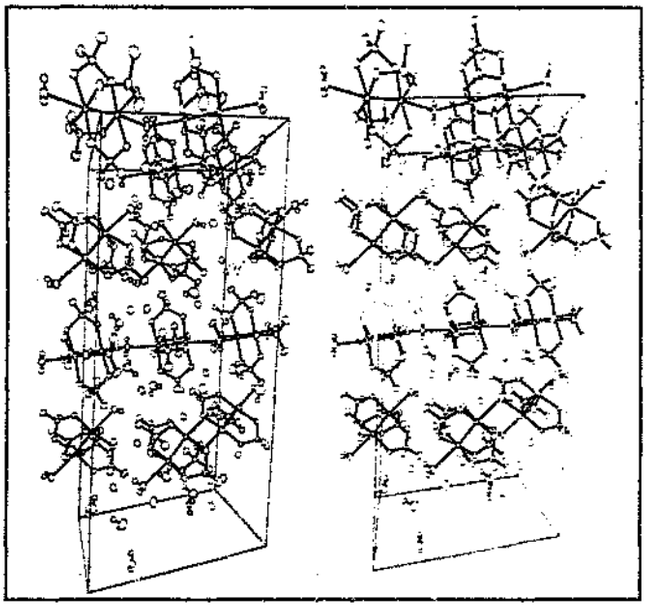


Figure 2.12 Stereoscopic view of the unit cell contents of $K_3Mo_2(SO_4)_4.3.5H_2O$.

The $[Mo_2(SO_4)_4]^{3-}$ anion has also been obtained in the form of compounds with formula $K_4[Mo_2(SO_4)]X.4H_2O$ (X = Cl, Br) [52, 53]. The Mo-Mo distances, 2.167(2) Å (Cl) and 2.169(2) Å (Br) are essentially identical. The molecules are structurally related to $K_3Mo_2(SO_4)_4.3.5H_2O$, but possess Mo--X axial interactions in place of Mo--H_2O. Continuous, linear (-Mo-Mo--X--Mo-Mo-) chains are formed.

The two anions $[Mo_2(SO_4)_4]^{4-}$ and $[Mo_2(SO_4)_4]^{3-}$ constituted the first pair of dinuclear, multiply bonded, isostructural complexes with electronic configurations differing by one electron. Another such pair is $Mo_2(DMF)_4$ and $[Mo_2(DMF)_4]^+$ [47]. The Mo-Mo distances in the molecule and the cation are 2.085(4) and 2.122(3) Å.

2.3. Mo(III)-Mo(III) Triple Bonds

The concept of a triple bond based on a $\sigma^2\pi^4$ configuration is, of course, a thoroughly familiar one

from main group and organic chemistry, where s and p atomic orbitals are used to form the necessary MO's.

The overwhelming majority of $\sigma^2\pi^4$ triply bonded systems have only three groups attached to each metal atom, arranged to give a staggered rotational conformation. There is no electronic barrier to rotation about the central M-M triple bond. These molecules are inorganic analogues of alkynes.

M_2X_6 compounds (X = NR_2 [54] and OR_2 [55]) adopt staggered ethane-like geometries; the central M_2E_6 skeleton (E = N or O) has virtual D_{3d} symmetry and the Mo-Mo-E angles are ca. 104°.

Figure 2.13 shows two views of the $Mo_2(NMe_2)_6$ molecule which is representative of this class of compounds. The first view emphasizes the staggered, ethane-like geometry, while the other view shows clearly the two types of methyl groups. Those lying more or less over the Mo≡Mo bond are called the proximal Me groups and the others are called the distal ones.

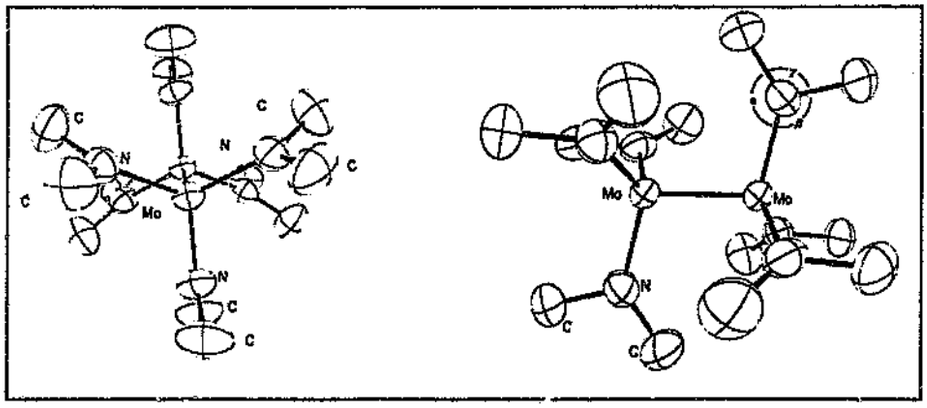


Figure 2.13 Two views of $Mo_2(NMe_2)_6$ showing the virtual D_{3d} symmetry of the $Mo_2(NC_2)_6$ moiety.

There is some ligand-ligand repulsion, as evidenced by the fact that the α angles defined in Fig. 2.13 are much greater (133°) than the β angles (116°) or the γ angles (110°). It is to be noted that the NMe_2 groups are essentially planar and that their planes are nearly parallel to the Mo-Mo axis, deviating by angles of only 0.3 to 3.6° from being parallel. Thus, the symmetry of the molecule is very close to that which would obtain if they were exactly parallel, namely D_{3d}.

The crystal contains two independent molecules virtually identical in structure, with Mo-Mo distances of 2.211(2) and 2.217(2) Å.

The structure of $Mo_2(OCH_2CMe_3)_6$ [55] has the same conformation as discussed above, with essentially the same Mo-Mo distance, 2.222(2) Å.

A number of closely related derivatives of general formula $Mo_2X_2(NR_2)_4$ where X = Cl [56] (Mo-Mo = 2.200(2)/ 2.202(2) Å); Me [57] (Mo-Mo = 2.201(1) Å); and Et [58] (Mo-Mo = 2.203(1) Å) are also of interest and adopt 1,2-disubstituted ethane-like geometries.

The structure of $Mo_2Cl_2(NMe_2)_4$ is representative of this class of compounds (Figure 2.14).

In all of the above compounds a simple analysis of the symmetry types of orbitals required to form M-M and M-L bonds and a consideration of the symmetry properties of the metal valence shell orbitals leads to a satisfactory qualitative formulation of bonding.

Defining the Mo-Mo axis as the z-axis, the triple bond is formed primarily by overlap of metal d_{z^2} orbitals to give a σ component and metal d_{xz}, d_{yz} orbitals to give the π components. For the M_2X_6 molecules the three Mo-L σ bonds

may use metal s, p_x and p_y orbitals.

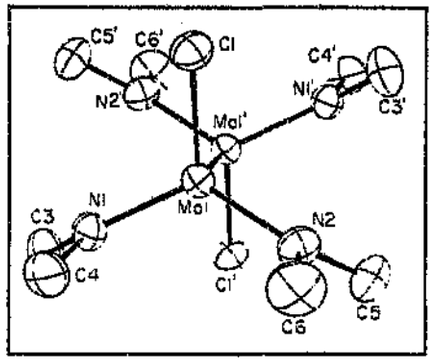


Figure 2.14 The structure of $Mo_2Cl_2(NMe_2)_4$ showing the central ethane-like structure and anti-rotational conformation.

When X = OR and NR_2 ligand-to-metal π bonding is also possible. The two pairs of Mo d_{xy} and $d_{x^2-y^2}$ atomic orbitals (usually involved in M-M δ bonding) may accommodate 8 electrons from the N(O) lone pairs i.e. there are 2 π bonds delocalized over 3 Mo-N(O) bonds. This allows the metal atoms to increase their number of valence shell electrons to sixteen (4 delocalized π electrons and 6 σ electrons make up the 3 M-L bonds; plus a total of 6 M-M bonding electrons). Two N(O) lone pairs will be in essentially non-bonding orbitals. In effect, each NR_2 and OR group is acting as a 4-electron donor ($\sigma^2\pi^2$). The formal Mo-N(O) bond order is therefore 1.6.

Structural evidence for ligand-to-metal π bonding is seen by the short M-N and M-O distances and, in the case of X = NR_2, by the planarity of the M-NC_2 units. The methylene carbons of the neopentoxy groups in $Mo_2(OCH_2CMe_3)_6$, also deviate little from the Mo-Mo-O planes.

In the 1,2-$Mo_2R_2(NMe_2)_4$ compounds the NC_2 blades are also aligned along the Mo-Mo axis. Substitution of NMe_2 by less π-donating Cl, Me and Et groups, would be expected

to increase N-to-Mo π bonding in the remaining Mo-NMe_2 groups. In fact, shorter Mo-N bond distances are seen (shorter by 0.01 to 0.03 Å). This may be indicative of Mo-N double bonds. Each Mo has one N lone pair occupying the d_{xy} orbital, the other the $d_{x^2-y^2}$ orbital.

The qualitative view that the valence electronic structure is composed of one σ and two π components has been verified through quantitative calculations by the SCF-Xα-SW method, and photoelectron spectra confirms the validity of the calculations [15]. Also, the extent to which N(O)-to-Mo π bonding actually occurs was shown by the calculations to be quite significant. The M-M bonding picture accounts for the observed diamagnetism of these compounds.

Verification of this qualitative picture of bonding, including the ligand-to-metal π bonding, is also provided by the molecular mechanics studies discussed later.

The structure of the $[Mo_2(HPO_4)_4(H_2O)_2]^{2-}$ unit is reminiscent of that found for $[Mo_2(SO_4)_4(H_2O)_2]^{3-}$ and also for $[Mo_2(SO_4)_4]^{4-}$, but there are significant differences in detail.

One of the most interesting differences is the long Mo-Mo distance, 2.223(2) Å, as compared to 2.164(2) Å in bond order (N) 3.5 and 2.111(1) Å in N = 4, which tells us quite clearly that we are dealing with a triple bond between the Mo atoms.

The structures of both $Cs_2[Mo_2(HPO_4)_4(H_2O)_2]$, which has axial water molecules (Mo-OH_2 = 2.46(1), 2.53(1) Å), and $(pyH)_3[Mo_2(HPO_4)_4]Cl$, in which there are infinite chains with shared Cl^- ions occupying axial positions (Mo-Mo = 2.232(1); Mo-Cl = 2.910(1) Å), have been determined [59, 60]. The structure of the latter is shown in Figure 2.15.

While the H atoms of the HPO_4 ligands were not observed, it is easy to tell where they are from the outer P-O distances. One on each ligand is about 1.48 Å (P=O) and the other is about 1.54 Å (P-OH).

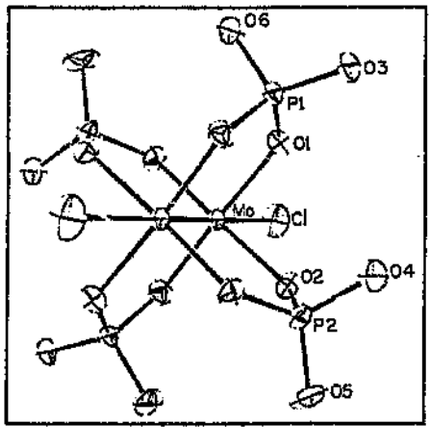


Figure 2.15 The structure of the $[Mo_2(HPO_4)_4(\mu\text{-}Cl)_2]$ unit.

The O=P-OH moieties are so arranged that the overall symmetry of the $[Mo_2(HPO_4)_4]^{2-}$ ion is C_{4h}; however, the inner Mo_2O_8 portion of the ion has effective D_{4h} symmetry, and the bonding can be understood as a $\sigma^2\pi^4$ configuration.

Since the existence of only a triple bond imposes no barrier to internal rotation, it is pertinent to examine the rotational conformation. The structure is essentially eclipsed, presumably because this conformation is favoured by the ligands.

A very interesting compound of formula $Mo_2(CH_2Bu^t)_2(O_2CMe)_4$ has a structure [61] closely related to that of the quadruply bonded $Mo_2(O_2CMe)_4$ molecule. The molecule retains the typical $Mo_2(O_2CMe)_4$ core supplemented by axially ligated neopentyl ligands (Figure 2.16). Remarkably, the Mo-Mo distance is 2.1302(6) Å,

only slightly longer than that in the parent molecule, 2.093(1) Å, and is the shortest yet seen for a d^3-d^3 Mo_2^{6+}-containing compound. It has been suggested that the valence MO configuration is $\pi^4\delta^2$.

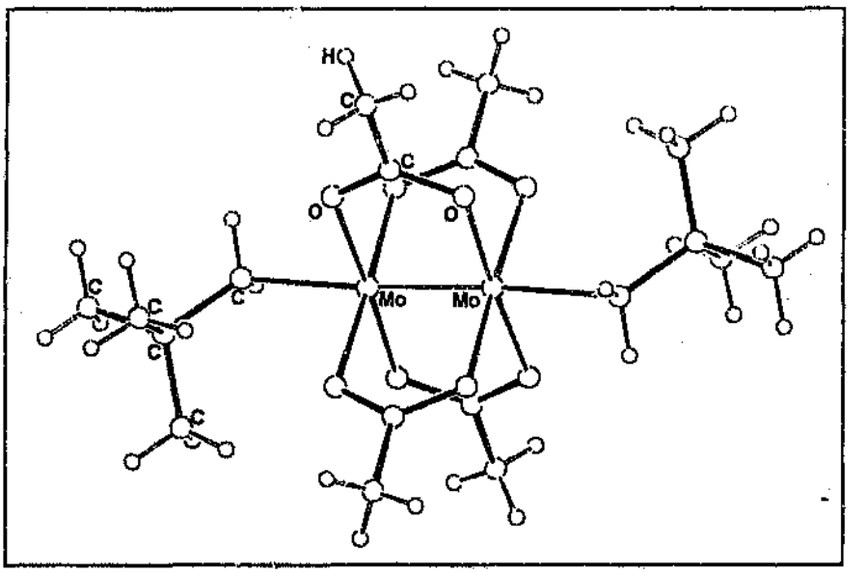


Figure 2.16 The structure of $Mo_2(CH_2Bu^t)_2(O_2CMe)_4$.

2.4 Double Bonds

There is as yet no proven well-defined example of a double bond between Mo atoms. Indeed no compounds are known which have M-M double bonds unbridged by ligand atoms, and thus there must be room for speculation about the M-M bond order. From the Mo-Mo distance alone it is not possible to distinguish unequivocally between the direct coupling of electron spins (double bond) and indirect coupling through the bridges.

The structure of the $Mo_2(OBu^t)_6(\mu\text{-}CO)$ molecule is shown in Figure 2.17.

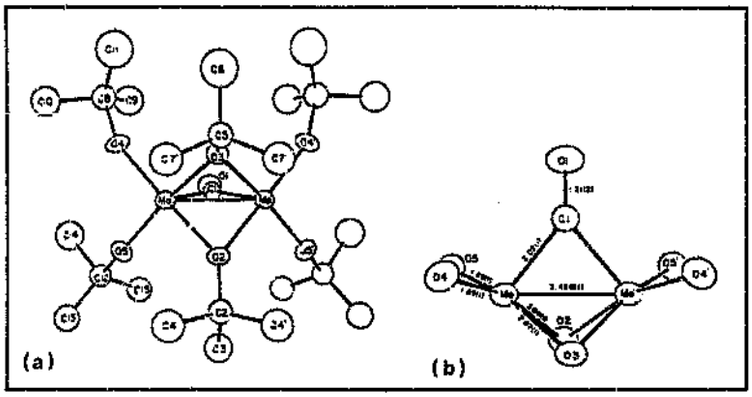


Figure 2.17 The structure of $Mo_2(OBu^t)_6(\mu\text{-}CO)$.
(a) The entire molecule; (b) Showing more clearly how the structure can be regarded as two square pyramids sharing one triangular face.

It can be thought of as consisting of two square pyramids fused on a common triangular face. The Mo-Mo distance is 2.498(1) Å which, together with the observed diamagnetism of this complex, is consistent with the existence of a double bond [62].

Qualitative electron counting for each Mo may be conducted as follows:
The neutral Mo atom has 6 d-electrons, each terminal OR (two of them) contributes one electron as does the bridging CO group, and the pair of bridging OR ligands contribute 3 electrons to each Mo atom. Hence 4 electrons from each Mo are involved in M-L bonding, leaving each Mo with 2 unpaired electrons. If there is a double bond, which is considered likely, it is perhaps best formulated in the following way.
Each Mo atom may be assumed to use atomic s, p_x, p_y, $d_{x^2-y^2}$ and d_{z^2} orbitals to form 5 σ bonds to the four O atoms and the carbonyl C atom which are disposed in a square pyramidal manner. (The z-axis is taken to be coincident with the Mo-C bond.)

In the C_{4v} symmetry of a regular square pyramid the d orbitals not used in M-L σ bonding fall into two sets: the d_{xy} orbital and the degenerate d_{xz}, d_{yz} pair. The d_{yz}-d_{yz} overlap results in a σ bond with maximum electron density along the Mo-Mo line. The d_{xz}-d_{xz} or d_{xy}-d_{xy} orbitals also can overlap to form a bent bond with maximum overlap density inside the flattened tetrahedron formed by the two Mo atoms and the two μ-O atoms.

$Mo_2(OPr^i)_8$ is an alkoxy-bridged dimer with a Mo-Mo distance of 2.523(1) Å [63]. The structural evidence in favour of Mo-Mo bond is cogently presented in Figure 2.18 where the $Mo_2(OPr^i)_8$ structure is contrasted directly with that of $Mo_2(OPr^i)_6(NO)_2$ in which there is no Mo-Mo bond and hence a net repulsive interaction between the two Mo atoms: Mo--Mo = 3.335(2) Å [64].

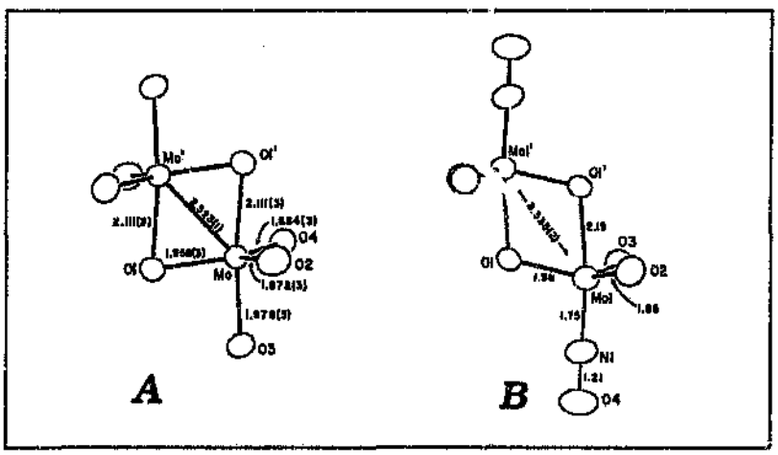


Figure 2.18 The central skeletons of the (a) $Mo_2(OPr^i)_8$ and (b) $Mo_2(OPr^i)_6(NO)_2$ molecules together with some pertinent bond distances. These views emphasize how each Mo atom is in a distorted trigonal bipyramidal environment.

In both compounds there is essentially trigonal bipyramidal coordination about each Mo atom and there is

a pair of bridging i-PrO ligands which form alternatively long (axial) and short (equatorial) Mo-O bonds. The most striking difference between the two structures are:

* the Mo-Mo distances and
* the angles of the planar $Mo_2(\mu\text{-}O)_2$ moieties.

The short Mo-Mo distance together with the acute angles (76.5(1)°) at the bridging O atoms and the obtuse angles (103.5(1)°) at the Mo atoms argues irrefutably for a direct bond between the Mo atoms in $Mo_2(OPr^i)_8$.

The double bond may be formulated in the following manner.
Let the z-axis be coincident with the axial O-Mo-O groups of each Mo. Then formation of five σ bonds to O may use s, p_x, p_y, p_z and d_{z^2} atomic orbitals. This leaves two doubly degenerate d orbitals, (d_{xz}, d_{yz}) and ($d_{x^2-y^2}$, d_{xy}), with the former lying lower in energy in a simple trigonal bipyramidal field.
If we then choose the y-axis to be coincident with the Mo-O(eq) bridging ligands, then the d_{yz} atomic orbitals can form Mo-Mo σ and σ^* orbitals; the d_{xz}-d_{xz} interaction will yield π and π^* orbitals.

These simple bonding pictures predict a Mo-Mo bonding configuration $\sigma^2\pi^4$ for a d^2-d^2 dimer.
The Mo-Mo distances fall between those of Mo≡Mo and those of single Mo-Mo, which, together with the observed diamagnetism (this requires a M-M bond of even order) suggests a Mo-Mo bond of order two.

2.5 Unbridged Single Bonds

The structure of bis-[cyclopentadienyl molybdenum tricarbonyl], $(\eta^5\text{-}C_5H_5)_2Mo_2(CO)_6$, was described by Cotton et al in 1974 [64]. The structure provides for a completed 18-shell for the Mo atom, in accord with the

observed diamagnetism of the compound. The molecule consists of an unsupported dimolydenum core, each Mo atom being bonded to three carbonyls and one cyclopentadienyl (Cp) ligand. The molecular shape, the rather long Mo-Mo bond (3.235(1) Å), and some rather short intramolecular nonbonded contacts suggest that the molecule is under considerable steric strain.

The structure of $(\eta^5\text{-}C_5H_5)_2Mo_2(CO)_5(CNCH_3)$ [65] is shown in Figures 2.19 and 2.20. The molecular structure is extremely similar to that of $(\eta^5\text{-}C_5H_5)_2Mo_2(CO)_6$. The replacement of one carbonyl group trans to the Mo-Mo bond by $CNCH_3$ causes essentially no change in the rest of the molecular structure. Even the Mo-Mo distance remains essentially identical with a value of 3.230(1) Å.

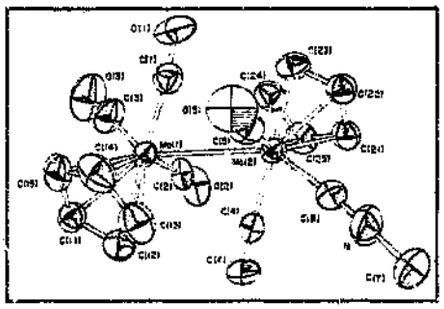


Figure 2.19 The structure of $(\eta^5\text{-}C_5H_5)_2Mo_2(CO)_5(CNCH_3)$.

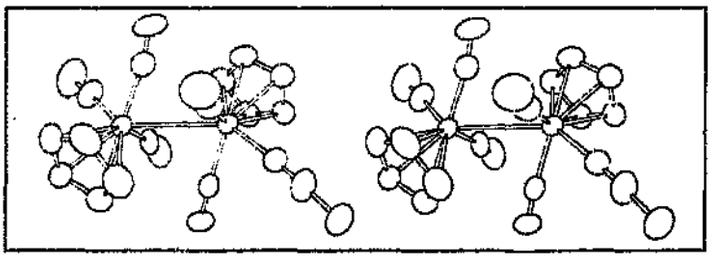


Figure 2.20 A stereo pair representation of the molecular structure.

Other structures derived from the parent molecule

are $(\eta^5\text{-}C_5Me_5)_2Mo_2(CO)_6$ (Mo-Mo = 3.281(1) Å) [66] (Figure 2.21) and $(\eta^5\text{-}C_5H_4\text{-}(CH_2)_3\text{-}OH)_2Mo_2(CO)_6$ (Mo-Mo = 3.213 Å) [67], and all have the same pseudo-square pyramidal configuration.

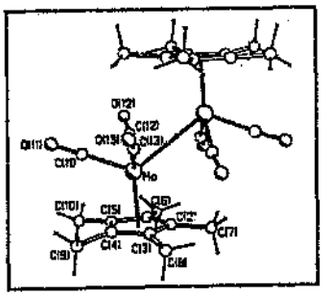


Figure 2.21 The molecular structure of $(\eta^5\text{-}C_5Me_5)_2Mo_2(CO)_6$.

Chapter 3

BONDS BETWEEN Cr ATOMS: THE LARGE RANGE OF Cr-Cr DISTANCES

3.1 Cr(II)-Cr(II) Quadruple Bonds

The Cr-Cr quadruple bonds have a curious history, beginning with the correct structure determination of $Cr_2(O_2CCH_3)_4(H_2O)_2$ in 1970, and the structure of $[Cr_2(CH_3)_8]^{4-}$. However, it was only for the former molecule that attention was explicitly directed to the nature of the M-M bonding. For carboxylato species of this type the lengths of the Cr-Cr bonds have been a source of considerable difficulty, and that is still true today.

However, with the discovery in 1977 of the first 'supershort' Cr-Cr bond (<1.9 Å), a new chapter of extensive, systematic chemistry of what are, indisputably, quadruple Cr-Cr bonds was begun.

One of the most challenging problems in the field of multiple bonds between metal atoms has been to identify and order the factors that influence the strength of the quadruple bond interaction between metal atoms in compounds containing the Cr_2^{4+} unit.

3.1.1 The Unbridged Chromium Dimer

The crystal and molecular structure of the only Cr(II)-Cr(II) dimer unsupported by bridging ligands, $Li_4Cr_2(CH_3)_8.4C_4H_8O$ was determined in 1970 [68]. The

Chapter 3

BONDS BETWEEN Cr ATOMS: THE LARGE RANGE OF Cr-Cr DISTANCES

3.1 Cr(II)-Cr(II) Quadruple Bonds

The Cr-Cr quadruple bonds have a curious history, beginning with the correct structure determination of $Cr_2(O_2CCH_3)_4(H_2O)_2$ in 1970, and the structure of $[Cr_2(CH_3)_8]^{4-}$. However, it was only for the former molecule that attention was explicitly directed to the nature of the M-M bonding. For carboxylato species of this type the lengths of the Cr-Cr bonds have been a source of considerable difficulty, and that is still true today.

However, with the discovery in 1977 of the first 'supershort' Cr-Cr bond (<1.9 Å), a new chapter of extensive, systematic chemistry of what are, indisputably, quadruple Cr-Cr bonds was begun.

One of the most challenging problems in the field of multiple bonds between metal atoms has been to identify and order the factors that influence the strength of the quadruple bond interaction between metal atoms in compounds containing the Cr_2^{4+} unit.

3.1.1 The Unbridged Chromium Dimer

The crystal and molecular structure of the only Cr(II)-Cr(II) dimer unsupported by bridging ligands, $Li_4Cr_2(CH_3)_8.4C_4H_8O$ was determined in 1970 [68]. The

$[Cr_2(CH_3)_8]^{4-}$ ion has a Cr-Cr distance of 1.980(5) Å and is isostructural and isoelectronic with the $[Mo_2(CH_3)_8]^{4-}$ ion. The presence of the δ bond receives strong support from the eclipsed nature of the Me ligands.

3.1.2 Bridged Dichromium Compounds

(a) Dichromium Tetracarboxylates

We begin with the $Cr_2(O_2CR)_4$ compounds since they are the earliest known Cr_2 molecules. It is convenient to keep in mind from the outset that virtually all of these $Cr_2(O_2CR)_4L_2$ and $Cr_2(O_2CR)_4$ compounds have the types of structure shown in Figure 3.1. The axial positions are filled either by separate ligands L_{ax} or by the oxygen atoms of other $Cr_2(O_2CR)_4$ molecules. In the latter case infinite chains are built up. Since the Cr-L_{ax} bonding uses, to some extent, the same Cr d_{z^2} orbital that is the principal contributor to the Cr-Cr σ bond, the presence of axial ligands may tend to weaken the Cr-Cr bond.

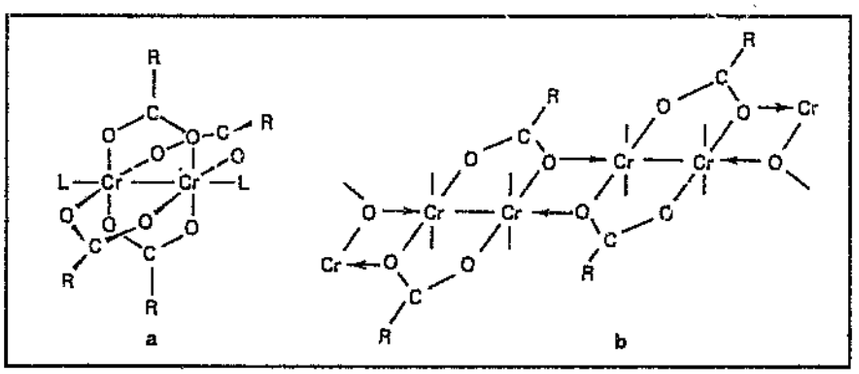


Figure 3.1 (a) The general structure of a $Cr_2(O_2CR)_4L_2$ molecule. (b) The formation of infinite chains of $Cr_2(O_2CR)_4$ molecules. Above and below each Cr_2 unit are two more RCO_2 groups not fully shown.

The dichromium carboxylates became integrated into the

main stream of research on M-M multiple bonds in late 1970, when an accurate measurement of the crystal structure of $Cr_2(O_2CCH_3)_4(H_2O)_2$ was carried out [69, 70]. This showed that the Cr-Cr distance is actually 2.362(1) Å, which made it reasonable to speak of "the quadruple M-M interaction as a strong one".

Crystals of unsolvated compounds were obtained by vacuum sublimation for $Cr_2(O_2CCH_3)_4$ [73] and $Cr_2(O_2CCMe_3)_4$ [74]. In each case, the X-ray studies revealed an infinite chain structure of the type shown in Fig. 3.1(b). The Cr-Cr distances are 2.288(2) Å and 2.388(4) Å, respectively.

Replacement of the water molecule by the bridging oxygens leads to a decrease in the Cr-Cr distance for R = Me. The bulky CMe_3 groups seem to cause the Cr-Cr distance to lengthen and the axial intermolecular contacts to be longer (2.44(1) Å) than those in the acetate (2.327(4)Å).

Formation of a 4-membered ring containing two Cr atoms and two bridging oxygens forces the axial oxygen off the Cr-Cr axis as seen in the packing diagram (Figure 3.2). Both the increase in the distance of the axial O atom in $Cr_2(O_2CR)_4$ and its displacement from the Cr-Cr axis should work to strengthen the σ contribution to the Cr-Cr bond.

Although it may be argued that the difference in the Cr-Cr distances in the hydrate and intermolecular cases is small from a chemical viewpoint, it is greater than the change in Mo-Mo distance which accompanies a much greater change in the axial ligand, when $Mo_2(O_2CCF_3)_4$ and $Mo_2(O_2CCF_3)_4(py)_2$ are compared.

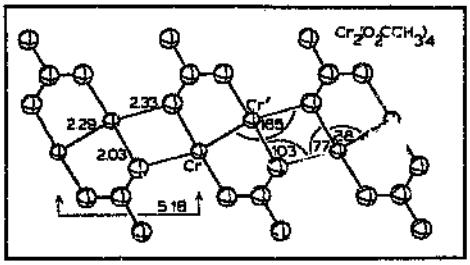


Figure 3.2 Packing diagram of anhydrous dichromium acetate along the short cell axis.

From the data for the formate compound, the more closely bound water molecules have a longer Cr-Cr distance, implying an inverse relationship between Cr-Cr and Cr-L_{ax} distances, and it was argued that such an inverse correlation should be more general.

Several other $Cr_2(O_2CR)_4L_2$ compounds have been structurally studied to determine the response of the Cr-Cr 'quadruple' bond, as that response is evidenced in the bond length, to the nature and proximity of axial ligand atoms, and the inductive character of the R group in the carboxylate ligand $[RCO_2]^-$. The only two structural parameters which vary significantly are the Cr-Cr and Cr-L_{ax} distances. Structural results are given in Table 3.1.

The most striking fact about these data is the enormous range covered by the Cr-Cr distances, from a low value of 2.214(1) Å in $[Cr_2(CO_3)_4(H_2O)_2]^{4-}$ to the highest one, 2.541(1) Å, in $Cr_2(O_2CCF_3)_4(Et_2O)_2$. Although there is significant variation in Mo-Mo quadruple bond lengths, the range covered for all kinds of diverse ligands is much smaller, viz., 0.13 Å.

It seemed natural for experimental chemists to search for possible empirical correlations. A plausible strategy in seeking empirical relationships was to focus on the

Table 3.1 Structures of Dichromium Tetracarboxylates, $Cr_2(O_2CR)_4L_2$

R	L_{ax}	Cr-Cr (Å)	Cr-L_{ax} (Å)	Ref.
Me	H_2O	2.362(1)	2.272(3)	6., 70, 71, 72
Me	inter[a]	2.288(2)	2.327(4)	73
H	py[b]	2.408(1)	2.308(3)	74
CMe_3	inter[a]	2.388(4)	2.44(1)	74
CF_3	Et_2O	2.541(1)	2.244(3)	74
O[d]	H_2O	2.214(1)	2.300(3)	75
Me	py[b]	2.369(2)	2.335(5)	76
Me	pyrazine	2.295(5)	2.31(1)	76
biphenyl	inter[c]	2.348(2)	2.309(5)	77
biphenyl	THF	2.316(3)	2.275(6)	77
CF_2H	Et_2O	2.490(3)	2.233(6)	78
CMe_3	2-CN-py	2.327(1)	2.388(4)	78
CMe_3	4-CN-py	2.335(1)	2.334(2)	78
CMe_3	py	2.359(3)	2.325(8)	78
CMe_3	4-NH_2-py	2.379(1)	2.282(2)	78
Me	4-CN-py	2.315(2)	2.327(4)	78
Me	4-NMe_2-py	2.411(1)	2.279(4)	78
H	4-CN-py	2.385(3)	2.34(1)	78
H	4-NMe_2-py	2.443(1)	2.270(4)	78
Me/$CClH_2$	py	2.367(2)	2.336(6)	78
$CClH_2$	4-CN-py	2.408(4)	2.23(2)	78
CF_2H	4-NMe_2-py	2.500(1)	2.246(9)	78
CF_2H	4-CMe_3-py	2.514(1)	2.277(9)	78

a :intermolecular oxygen donation
b :pyridine
c :dimer of dimers (see text for further information)
d :carbonate $(O-C(O)-O)^{2-}$

influence of axial coordination. It was supposed that the strength of the Cr-Cr bond would be inversely related to the strength of the axial ligand bonding. The principal basis for such a relationship would presumably be the competition between the Cr-Cr σ-bonding and the Cr-L_{ax} bonding for the metal d_{z^2} orbitals necessary to both.

Experimental chemists tried to establish systematic empirical relationships between the composition of $Cr_2(O_2CR)_4L_2$ compounds (i.e. the identities of R and L) and the Cr-Cr bond lengths, and in particular to see how the character and strength of the Cr-L_{ax} bonds would affect the Cr-Cr bond. A very coarse inverse relationship between the Cr-L_{ax} and Cr-Cr bond lengths was observed [74, 75] and there was some tenuous evidence for a dependence of the Cr-Cr distance on the inductive strength of R.

In these studies the variations in R and L were fairly random; it was hoped that the correlations would be so well defined that they would be evident even when strict control of all variables was not maintained.
Since that turned out not to be the case, Cotton and Wang [78] prepared and structurally characterized several series of compounds in which (a) a given L is retained throughout while R is varied over the maximum possible range of inductive effect (CMe_3 to CF_2H), and (b) R is maintained the same while employing a series of axial ligands that are as nearly as possible sterically identical, except for differences in basicity (4-substituted pyridines). With the data a systematic search was made for correlations between (a) the Cr-Cr and Cr-N bond lengths, (b) each of these bond lengths with the pK_a values of the carboxylic acids and (c) each of these bond lengths with the pK_a values of the pyridine ligands. With

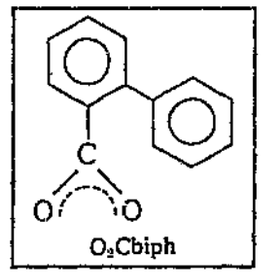
the exception of some compounds, the correlations sought were found. The Cr-Cr and Cr-N bond lengths are inversely related, though it is impossible to say whether this relationship is linear. The Cr-Cr bond lengths vary directly with the pK_a of L_{ax} and inversely with the pK_a of RCO_2H, while the Cr-N bond lengths show the opposite correlations with the pK_a values.

The results seemed to bear out the generally accepted concept that increased strength of axial ligation (as evidenced by a higher value of pK_a for the protonated base) and decreased donation by the bridging ligands leads to decreased strength of the M-M bond. However, as mentioned before one can expect irregularities in simple relationships to exist as long as the electronic and steric factors have not been separated.

The question of how long the Cr-Cr bond would be in an isolated $Cr_2(O_2CR)_4$ molecule, that is, when axial coordination is entirely nonexistent, provoked several efforts to isolate such a species. Logically there are only two approaches, given the fact, that even when no independent ligands are present, $Cr_2(O_2CR)_4$ molecules tend to associate with themselves. One approach is to use a gaseous sample, the other is to employ an R group of such size and shape as to prevent association.

In an attempt [77] to find the right sort of R group, the following approach was taken. It was recognized that to prevent association of $Cr_2(O_2CR)_4$ it is necessary to block access to the axial positions, but only to screen the carboxyl oxygen atoms so that they cannot use their lone pairs to reach the metal atom of an adjacent molecule. The R group chosen was 2-phenylphenyl, giving the carboxyl group 1, and it was hoped that the tendency of the pendant phenyl group to be nearly perpendicular to the $C_6H_5CO_2$ plane would lead to a situation in which two

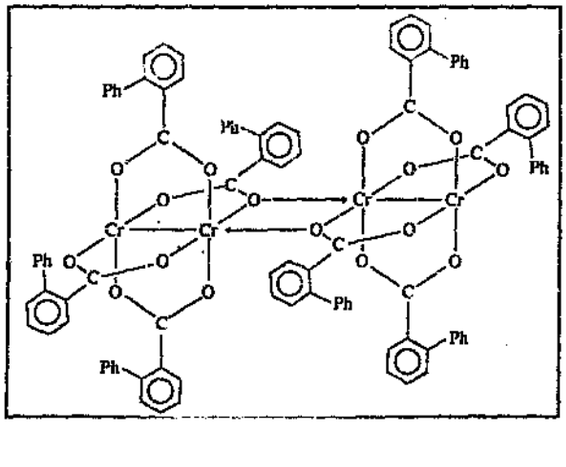
pendant phenyl groups would be directed toward each end of the $Cr_2(O_2Cbiph)_4$ molecule, thus preventing chain growth at either end.



(1)

When this compound was prepared in THF the results were exactly as anticipated, with the two pendant phenyl groups directed each way and not interfering with axial coordination of the two THF molecules. The compound was next prepared in a non-coordinating solvent, toluene, with the object of obtaining unassociated and uncoordinated molecules. However, an unanticipated result was obtained, as shown schematically in **2**. In each of two $Cr_2(O_2Cbiph)_4$ molecules, all pendant phenyl groups have oriented themselves to one end, thus preventing the use of oxygen atoms on that end for association. The unencumbered ends of the two $Cr_2(O_2Cbiph)_4$ molecules have then united, as in **2**, to produce a dimer.

The final comments required on the structural data for dichromium carboxylato compounds concern the fact that all the Cr-Cr bonds, even the shortest ones, are far longer than might have been expected from the Mo-Mo bond lengths in comparable compounds. In $Mo_2(O_2CCH_3)_4$, for example, the Mo-Mo distance is 2.093(1) Å. Since accepted bond radii of whatever specific form or origin are always at least a little smaller for chromium than for molybdenum, the Mo-Mo bond length might well have been



(2)

considered an upper limit for the Cr-Cr bond in a homologous compound.

It was concluded that the Cr-Cr quadruple bond interaction, within the tetra-μ-carboxylato environment, must be described by a very broad, relatively shallow potential function so that the Cr-Cr distance is easily varied over a broad range by a variety of factors.

(b) Other Bridged Dichromium Compounds

While it is generally accepted that the nature of both the axial and bridging ligands affects the Cr-Cr bond distance, views differ as to which influence is predominant. From studies on molecules where the $[RCO_2]^-$ groups are replaced by other bridging groups such as the amidato type ligands, with N-C-O units, the most critical factor appears to be whether axial coordination occurs or not, in that, for all such compounds the Cr-Cr distances are $\leq$1.95 Å when axial ligands are absent, whereas introduction of axial ligands causes increases in the Cr-Cr distance to as much as 2.246(2) Å in a $[di(THF)]_{ax}$ compound.

(i) The Supershort Bonds

A distinct dichotomy was created with the discovery of a series of compounds that contain ligands that are sterically and electronically similar to the carboxylato group, and yet have vastly shorter Cr-Cr bonds i.e. in a range ≤1.95 Å.

It was the preparation and characterization of $Cr_2(DMP)_4$, (DMP = 2,6-dimethoxyphenyl anion) whose structure is shown in Figure 3.3, that initiated the development of a broad, systematic chemistry of dichromium compounds with very short, unmistakably quadruple bonds.

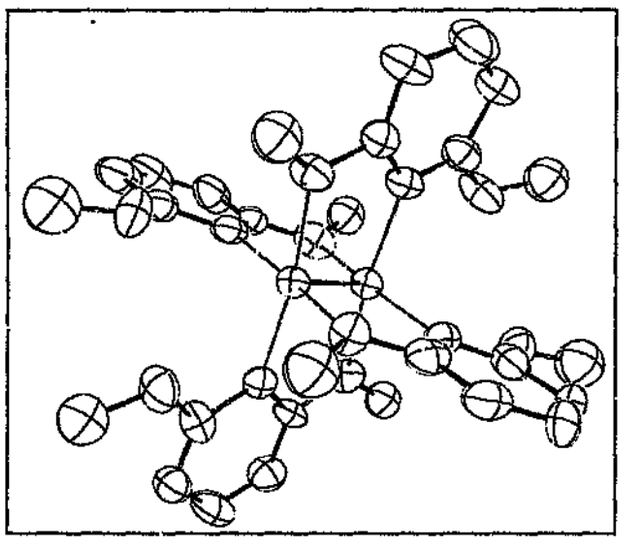


Figure 3.3 The molecular structure of $Cr_2(DMP)_4$.

At the time it was discovered (1977) [79, 80], the Cr-Cr bond distance of 1.847(1) Å was considered so surprisingly short as to raise the question of whether there might, somehow, be an error in the structure determination. This was recognized to be exceedingly unlikely, since every phase of the crystallographic structure determination had proceeded routinely, there had been no indication of twinning, disorder, and the

like, and the other bond lengths and angles were all normal. Nonetheless, to be fully certain that no subtle, unrecognized error had crept in, the structure of the chemically almost identical compound, $Cr_2(TMP)_4$ (TMP = 2,4,6-trimethoxyphenyl anion) was determined [80, 81]. The result was 1.849(2) Å, which is statistically indistinguishable from that for $Cr_2(DMP)_4$.

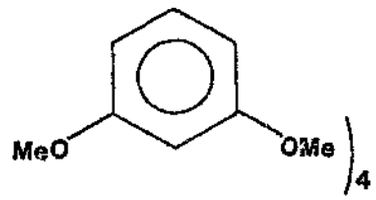
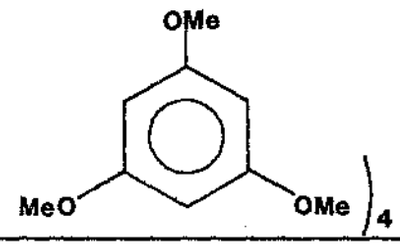
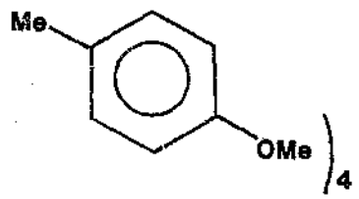
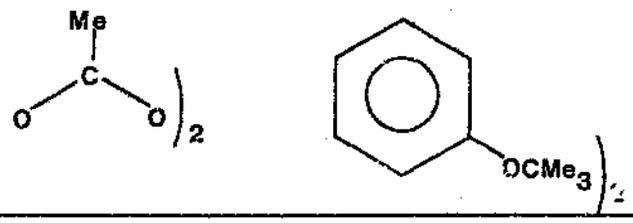
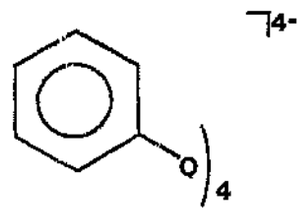
Other 'supershort' dichromium compounds bridged by the O^C unit are shown in Table 3.2.
The adjective 'supershort' has been defined to mean Cr-Cr ≤ 1.95 Å in length. This is, of course, an arbitrary definition, but it does correspond to a practical point of reference in dealing with the compounds of interest.

The $Cr_2(2\text{-}MeO\text{-}5\text{-}MeC_6H_3)_4$ compound has the shortest known Cr-Cr distance, 1.828(2) Å [82].

The fact that the Cr-Cr bonds are enormously shorter when four oxophenyl-type ligands are present than when there are four carboxyl groups posed the interesting question as to what the Cr-Cr distance would be if the ligand set consisted of two of each type.

By using the ligand, $2\text{-}Bu^tOC_6H_4$, where the t-butyl groups are so large as to inhibit the simultaneous attachment of four such ligands, it proved possible to obtain a product in which only two of the four acetate groups of $Cr_2(O_2CCH_3)_4$ are replaced. The crystal structure [83] of the resulting compound, shown in Figure 3.4, has the hoped-for ligand arrangement, and the Cr-Cr distance is 1.862(1) Å. The general features of the $(2\text{-}Bu^tOC_6H_4)_2Cr_2$ portion of the structure are the same as those previously observed.

Table 3.2 $Cr_2(L_{eq})_4$ structures, L_{eq} = O^C bridge, with supershort Cr-Cr bonds

$(L_{eq})_n$	Cr-Cr (Å)	Ref.
	1.847(1)	79, 80
	1.849(2)	80, 81
	1.828(2)	82
	1.862(1)	83
	1.830(4)	84

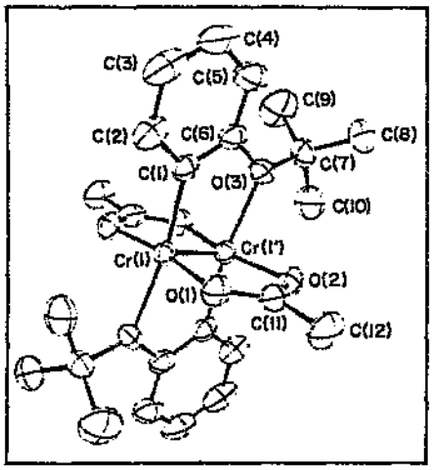


Figure 3.4 The molecular structure of $Cr_2(O_2CMe)_2(2\text{-}Bu^tOC_6H_4)_2$.

Finally, in this same period of time, and still using oxophenyl-type ligands, one more important compound was reported with the rather complex formula $Li_6Cr_2(C_6H_4O)_4Br_2.6Et_2O$. The crystal structure [84] is complex, but the unit of interest is shown in Figure 3.5. The Cr--Br distances are very long (3.266(2) Å) and there can be but little, if any, direct bonding.

Following the discovery of these compounds, the next development was the study of Cr_2L_4 compounds where L = MAP, MHP, DMHP and CHP. Isostructural compounds have already been encountered for dimolybdenum. Again supershort Cr-Cr distances are found: 1.870(3) Å for $Cr_2(MAP)_4.2THF$ [85], 1.889(1) Å for $Cr_2(MHP)_4.CH_2Cl_2$ [86], 1.907(3) Å for $Cr_2(DMHP)_4.O_3C_5H_{14}$ [87] and 1.955(2)Å for $Cr_2(CHP)_4$ [88].

The obvious question raised by these Cr_2L_4 compounds with supershort bonds was why some ligands (L) are conducive to the formation of such bonds and others not. Ligands like DMP, MHP, and MAP were originally selected because their stereoelectronic similarity to the carboxyl ions, $[RCO_2]^-$, was expected to allow the formation of Cr_2L_4

compounds having qualitatively similar structures. This qualitative similarity was found, but quantitatively there was also a major difference, namely, the very much shorter Cr-Cr bonds.

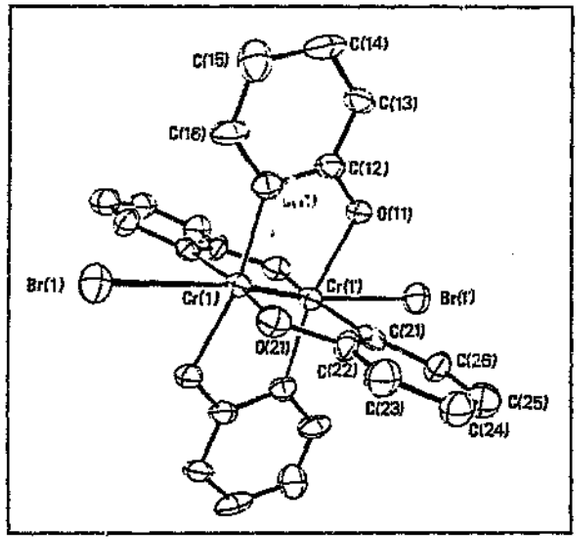
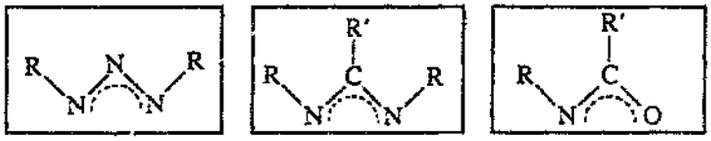


Figure 3.5 The structure of the $Cr_2(2\text{-oxophenyl})_4Br_2$ moiety in $Li_6Cr_2(OC_6H_4)_4Br_2.6Et_2O$.

In seeking an understanding of this phenomenon, one might first consider whether the identity of the ligating atoms is critical. In the supershort cases, we have seen the ligands C^O (DMP), N^O (MHP), N^N (MAP), and a combination of O^O/C^O. Since these variations have little effect on the Cr-Cr distance, it seems unlikely that simply going to the O^O combination could make such an enormous difference.

Another aspect of the ligands in the compounds with supershort bonds is that in all of them one of the ligating atoms is a member of an aromatic ring. This raised the possibility that the π and/or π^* orbitals of such a ring could exercise a decisive influence on the Cr-Cr distance. There are, however, now numerous counter examples, that is, Cr_2L_4 compounds with supershort bonds

in which the ligands do not contain donor atoms that form part of an aromatic ring. In pursuit of this goal the ligand types **3 a,b,c** (triazinates, amidinates and amidates, respectively) were employed.



3 **(a)** **(b)** **(c)**

Molecules containing these bridging ligands, **3**, are listed in Table 3.3.

Table 3.3 Supershort Cr_2L_4 compounds without incorporation of donor atoms into an aromatic ring

L_{eq}	Cr-Cr (Å)	Ref.
PhN-N-NPh	1.858(1)	89
PhN-C(Me)-O	1.873(1)	90, 91
(2,6xylyl)N-C(Me)-O	1.937(2)	92
DMF	1.930(2)	93

The data now available point to only one reasonable conclusion. All of the molecules with supershort Cr-Cr bonds have no axial ligands and no intermolecular association.

It therefore seemed very probable that a crucial feature controlling Cr-Cr bond lengths must be the presence or absence of axial bonds, while the electronic character of the bridging ligands is of much less importance.

Unfortunately, this correlation does not unambiguously

resolve the question, because the only molecules falling in the long-bond category are the carboxylato species. The import of this correlation would be a lot clearer if

* we had something besides carboxylates in the long-bond category, and
* we could examine at least one $Cr_2(O_2CR)_4$ molecule that is totally lacking in axial bonding.

(ii) The Effect of Axial Ligands on Supersnort Bonds

There has been the suggestion that, for an equatorial ligand set consisting of (4N+4O) or another combination not consisting exclusively of O atoms, there would be a pronounced tendency to develop strong and short Cr-Cr bonding even in the presence of axial ligands.

However, X-ray crystallography has shown that if there is good axial coordination a long Cr-Cr distance will be obtained whether the four bridging ligands are of the amidato ion $(N-C-O)^-$ type or the carboxylato group. The structural data for 'supershort' compounds with axial ligands is shown in Table 3.4.

With axial donation other than $L_{ax} = CH_2X_2$, the Cr-Cr distances are brought very close to the range typical of carboxyl compounds in general. In fact, the Cr-Cr distance is longer than the Mo-Mo distance in comparable compounds, which further illustrates the extreme sensitivity of the Cr-Cr 'quadruply' bonded systems to axial coordination.

The structural results show that the overwhelmingly most critical factor is whether axial coordination occurs or not, in the sense that, whatever the nature of the X-Z-Y ligands, the Cr-Cr distance will be short (<1.95 Å) when there is no axial coordination and long (>1.95 Å) when axial bonds are formed.

Table 3.4 Key bond distances for the N^O-bridged dichromium compounds with axial coordination

L_{eq}	$(L_{ax})_n$	Cr-Cr (Å)	Cr-L_{ax}	Ref.
PhN-C(NHPh)-O	$(THF)_2$	2.246(2)	2.350(5)	94
(2,6xylyl)N-C(Me)-O	$(CH_2Cl_2)_2$	1.949(2)	3.354(3) 3.58(1)	95
(2,6xylyl)N-C(Me)-O	$(CH_2Br_2)_2$	1.961(2)	3.335(4) 3.554(5)	92
(2,6xylyl)N-C(Me)-O	$(THF)_2$	2.221(3)	2.318(9) 2.321(8)	96
(2,6xylyl)N-C(Me)-O	$(THF)_1$	2.023(1)	2.315(4)	96
$(4NMe_2$-Ph)N-C(Me)-O	$(THF)_1$	2.006(2)	2.350(6)	96
FHP	$(THF)_1$	2.150(2)	2.266(6)	97

The conclusion that a $Cr_2(O_2CR)_4$ molecule having absolutely no coordination in the axial positions would have a Cr-Cr distance less than 2.00 Å is not logically demanded by these results, but is indicated as a distinct possibility.

As was the case for Mo_2, all the $Cr_2(XZY)_4$ and $Cr_2(XZY)_4L_2$ compounds have near eclipsing of the X^Y ligands about the M-M bond. This is not only favoured by the presence of any δ bonding, but also by the delocalization of the negative charge of the $(XZY)^-$ groups as discussed before.

(c) The Isolated $Cr_2(O_2CCH_3)_4$ Molecule

It has been asserted by some that these long Cr-Cr distances in $Cr_2(O_2CR)_4$ compounds are mainly a consequence of the electronic properties of the $[RCO_2]^-$

ligands and only secondarily traceable to the axial bonds. However, finally in 1985, the experimental demonstration (by electron-diffraction) [98] that isolated molecules of $Cr_2(O_2CMe)_4$ in the gas phase have a Cr-Cr bond length of 1.96(1) Å (substantially shorter than either of the X-ray values for $Cr_2(O_2CCH_3)_4L_2$, L = H_2O, intermolecular), refuted this idea and showed the primacy of the axial ligands in determining the strength of the Cr-Cr bond.

Besides having a shorter Cr-Cr distance, the Cr-Cr-O angles are obtuse, whereas in the presence of axial coordination these angles are slightly acute. The difference in Cr-Cr-O angles is probably a result of the 'bite' requirements of the O^O bridging ligand.

3.2 An Unbridged Single Bond

The only unsupported dichromium compound of formal bond order less than four, is $(\eta^5\text{-}C_5H_5)_2Cr_2(CO)_6$ [99]. The molecule is isostructural with $(\eta^5\text{-}C_5H_5)_2Mo_2(CO)_6$. The Cr-Cr distance, 3.281(1) Å, is far longer than would be expected for an unstrained single bond; it is actually ca. 0.06 Å longer than the Mo-Mo bond. The explanation for the unexpected result is to be found in the presence of substantial nonbonded repulsions.

Chapter 4
UNDERSTANDING THE NATURE OF DIMETAL BONDING

With the structural data discussed, accounting for the observed trends is the next step to understanding dimetal bonding.

4.1 The Effect of Axial Ligands

We have had the occasion to note the influence of axial ligands on M-M bond lengths in the previous chapters. The length of a M-M multiple bond is increased by the introduction of axial ligands. However, the magnitude of the effect varies markedly from one metal to another.

There are some very interesting contrasts between dichromium and dimolybdenum species. The $Mo_2(XZY)_4$ molecules appear to show real resistance to accepting axial ligands, and even when such ligands are present, the Mo-Mo bond distances are affected by only a few hundredths of an Angstrom (ca. 0.065 Å). The $Cr_2(XZY)_4$ units, however, seem to have a powerful attraction for axial ligands, and the Cr-Cr bond lengths are markedly affected, though not in an accurately predictable way, by the presence of such ligands. The Cr-Cr distance is increased from ≤ 1.96 Å in the absence of axial ligands to 2.541(1) Å in $Cr_2(O_2CCF_3)_4(Et_2O)_2$. There may well be a synergic effect with poorly donating bridging ligands enhancing the axial donation, or axial donation enhancing the Cr-Cr sensitivity towards the bridging ligand character.

The peculiarity is that, in spite of being highly multiple (at least formally), the observed dichromium bond distances vary over a range of ca. 0.7 Å. The existence of Cr-Cr bonds of order 4 is universally accepted for the species in the lower range (≤1.96 Å), but controversy has arisen concerning those in the upper range.

4.2 Formal vs. Effective Bond Order

Based on bond length, conformation, electronic and vibrational absorption spectroscopy, theoretical considerations employing sophisticated calculations and, above all, internal consistency, the evidence for a multiple bond in certain compounds is overwhelming. Such is the case for the quadruple $[Mo_2Cl_8]^{4-}$ anion.

However, not all cases are so clear cut since there may be extensive mixing of M-M and M-ligand bonding such that the significance and validity of a M-M bond order or its assignment is questionable.

So far, we have used the term M-M bond order only to indicate how many electron pairs are believed, on the basis of essentially qualitative considerations, to play a significant part in holding the pair of metal atoms together. This is defined as the formal bond order and depends purely on a qualitative electron count deduced from the formal oxidation state of the metal atoms in a particular ligand environment.

This formal definition overlooks such possibilities as the mixing of M-M and M-ligand (axial and/or equatorial) bonding; or the effect of torsional twist about the M-M bond on the δ component of the quadruple bond.

The dichromium (II) compounds are all formally quadruple

in order. However, the large variation in Cr-Cr distance raises the question whether these bonds can reasonably be considered to be of the same order. Such large differences indicate that behind the formal concept of quadruple bonding the real bonding situation may be quite different. Surely the axial and equatorial ligands have a decisive influence on the electron density at the dimetal centre? It has already been mentioned that there may be competition between the Cr-Cr σ bonding and the Cr-L_{ax} σ bonding for the metal d_{z^2} orbitals necessary to both.
Although the trends clearly depend on electronic factors, steric contributions to the observed effects are by no means excluded.

Likewise, the dimolybdenum(II) bonds are all formally quadruple. However, δ overlap is, of course, angle sensitive. The minimization of nonbonded repulsions, occurring between the sets of ligands at the two ends of a $X_4M_2(L,L)_4$ unit, usually (not always) favours a rotation away from the eclipsed conformation. The question is how much of a twist can occur without loss of the δ component to the quadruple bond. Also, the δ bonding depends upon the lateral overlap of the dδ orbitals, a type of overlap that diminishes rapidly as the internuclear distance increases. It is therefore necessary to examine how big a twist about the Mo-Mo bond, or Mo-Mo stretch is tolerable before the formal quadruple bond is effectively reduced to a lower order.

In short, the 'effective' or 'true' bond order of a dimetal centre may not depend only on the number of electrons formally available for M-M bond formation (which depends on the position of the metal in the periodic table and its oxidation state), but also on the nature (electronic and steric) of the ligand environment.

As chemists, we like to think of multiple bonds most simply as derived from the overlap of atomic orbitals of σ, π and δ symmetry. A major problem is that such descriptions, although attractive and simple, are oversimplifications. Simple electron counting and M-M d-orbital overlap are insufficient for the understanding of the true nature of dimetal bonding.

4.3 Theoretical Attempts at Resolving the Dichromium Controversy

Dichromium species have proved the most difficult to handle theoretically and much effort has been devoted to them.

The first calculation to be reported [100] was a HF-SCF calculation on $Cr_2(O_2CH)_4(H_2O)_2$ at a Cr-Cr distance of 2.362(1) Å, from which a nonbonded $\sigma^2\delta^2\delta^{*2}\sigma^{*2}$ configuration was assigned to the ground state. This result raised an important query as to whether this compound has a quadruple bond. It was not recognized that this result is erroneous, because electron correlation effects in this system are so great that a CI-level calculation is absolutely mandatory.

This controversy was settled rather quickly about a year later with the first calculations [101, 102] including CI and the first SCF-Xα-SW calculation [103].
With the inclusion of a limited amount of CI, the results shown in Figure 4.1 are obtained. The configuration corresponding to a full quadruple bond, $\sigma^2\pi^4\delta^2$, is the lowest energy configuration only at distances less than ca. 1.8 Å. Beyond that distance, the nonbonded $\sigma^2\delta^2\delta^{*2}\sigma^{*2}$ configuration has a lower energy. However, when a particular set of key excited configurations is used to introduce what should be a large fraction of the

necessary correction for electron correlation effects, a multiconfigurational ground state, in which the leading (i.e. most heavily weighted) configuration is $\sigma^2\pi^4\delta^2$, is obtained. It can be seen that this ground state potential energy curve has a minimum at ca. 2.45 Å, implying that the Cr-Cr separation in a truly isolated $Cr_2(O_2CR)_4$ molecule will not be in the 'supershort' range. Moreover, the minimum is very shallow, suggesting that the Cr-Cr bond length might easily vary, depending on details of the ligand properties.

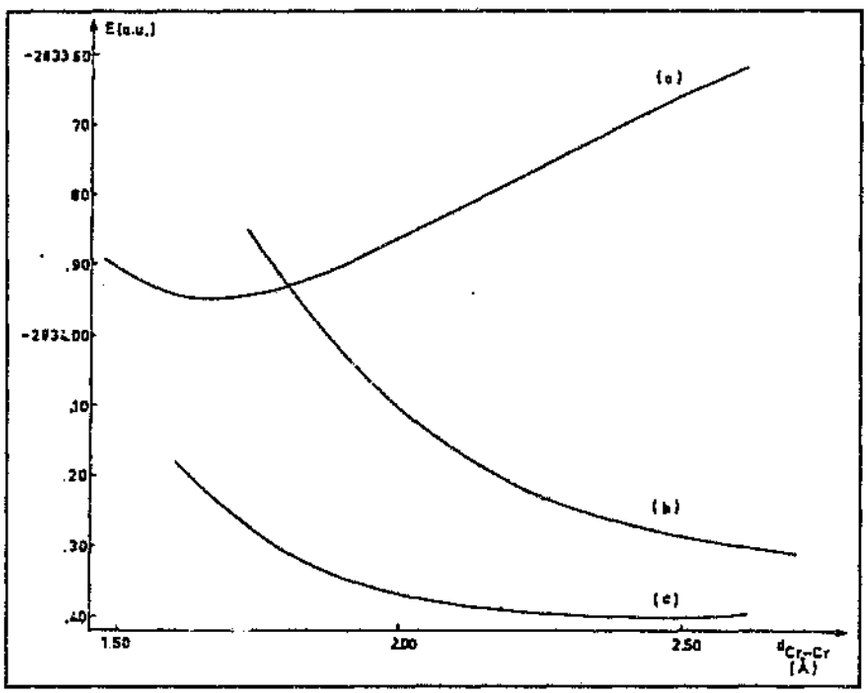


Figure 4.1 Potential energy curves for $Cr_2(O_2CH)_4$. (a) SCF-HF energy for the $\sigma^2\pi^4\delta^2$ configuration; (b) SCF-HF energy for the $\sigma^2\delta^2\delta^{*2}\sigma^{*2}$ configuration; (c) Ground state energy at the CI level.

It is interesting to examine in more detail the results of the SCF-HF-CI calculation for $Cr_2(O_2CH)_4$ and compare them with the results for $Mo_2(O_2CH)_4$, taking each one at its own lowest-energy internuclear distance. Actually, at

that time the distance for an isolated $Cr_2(O_2CR)_4$ molecule with no axial donors was unknown, so calculations covering a range of Cr-Cr bond lengths from 2.16 to 2.56 Å were carried out.

The results for two calculations [104], done in the same way for $Mo_2(O_2CH)_4$ and $Cr_2(O_2CH)_4$ gives the $\sigma^2\pi^4\delta^2$ configuration making up such a large fraction (67%) of the ground state for $Mo_2(O_2CH)_4$, that this configuration alone can give a reasonably good account of the properties of the bond. The insensitivity of the Mo-Mo distance to R and L_{ax} is in agreement with the calculations since the potential curve found at the SCF level is relatively deep.

For $Cr_2(O_2CH)_4$ the situation is quite different, with the quadruple-bond configuration making only a 16% contribution.

Orbital occupancies are determined from summations over all configurations in the wavefunction. From natural-orbital analysis $Mo_2(O_2CH)_4$ has a calculated bond order of 3.2 at 2.09 Å, and $Cr_2(O_2CH)_4$ a bond order of 1.5 at 2.20 Å.

Because the quadruply-bonded configuration represented such a small part of the wavefunction, a semantic argument, about whether or not these systems have a quadruple bond, ensued.

On the other hand, an SCF-Xα-SW calculation [103] for $Cr_2(O_2CH)_4$ at Cr-Cr = 2.20 and 2.36 Å gives an unambiguous result, showing that the ground state of the molecule does correspond to a $\sigma^2\pi^4\delta^2$ quadruple bond. However, as shown in Figure 4.2, this is a considerably weaker quadruple bond than that in the molybdenum compound.

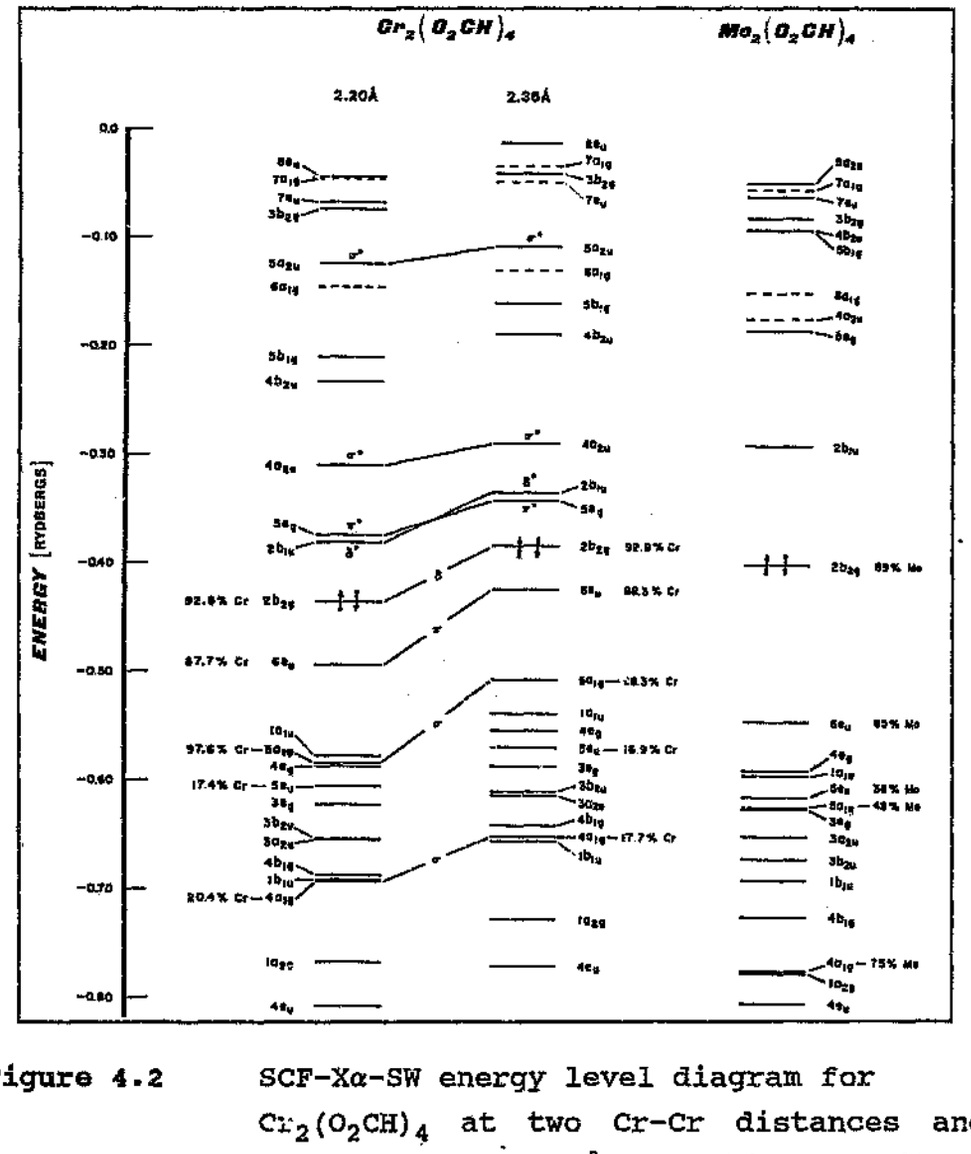


Figure 4.2 SCF-Xα-SW energy level diagram for $Cr_2(O_2CH)_4$ at two Cr-Cr distances and $Mo_2(O_2CH)_4$ at 2.09Å. The highest filled MO is indicated by two arrows. Percent characters are given for orbitals that have appreciable M-M bonding roles.

The δ component contributes little to the bond strength in either case. For $Mo_2(O_2CH)_4$ the π-bonding ($6e_u$) orbital is much more stable than the δ orbital.

Moreover, of the two a_{1g} orbitals that contribute to σ bonding, in $Mo_2(O_2CH)_4$ it is the very stable 4_{a1g} orbital

(75% Mo) that contributes most, whereas for $Cr_2(O_2CH)_4$ the σ-bonding orbital is almost entirely accomplished by the rather high-lying 5_{a1g} orbital (97.6% Cr). Thus the σ component of the quadruple bond is considerably weaker for Cr-Cr than for Mo-Mo.

The SCF-HF-CI and SCF-Xα-SW calculations seem to be in reasonably good agreement that there is a quadruple bond in the $Cr_2(O_2CR)_4$ molecules, but a far weaker one than in the $Mo_2(O_2CR)_4$ analogues.

It also appears that the SCF-Xα-SW calculations provide an explanation for the ease with which the $Cr_2(O_2CR)_4$ molecules bind axial donors, in contrast to their molybdenum analogues. For the chromium system the weakness of the σ bond means that there is a very low-lying empty σ^* orbital ($4a_{2u}$) into which these axial ligands may donate, whereas this is not the case for the molybdenum compound. Thus the axial ligands can be more firmly bonded to the Cr atoms and, in so doing, they populate a Cr-Cr σ^* orbital and weaken the Cr-Cr bond.

From ab initio calculations on anhydrous and dihydrated dichromium tetraformate [105] it was concluded that the axially situated water molecules had no major influence on the strength of the Cr-Cr bond. On the other hand, correlations have been established experimentally between the strength of the $Cr-L_{ax}$ interaction and the Cr-Cr bond [96].

Three independent studies have attempted to determine how the "inductive effect of the bridging ligands" affects the equilibrium Cr-Cr bond length, all employing some form of SCF-HF-CI calculation.

One of them [106] ventured no specific bond length predictions, but concluded that "variation in the

electrostatic potential at the metal centre, due to the different ligands...leads to large variations in the Cr-Cr separation", and, further that "these separations are mainly determined by the electrostatic potential at the metal centre...".

Another of these studies [107] implied that for amidato-bridged species a short distance would be expected (this, of course, was already known to be true), but predicted "an equilibrium bond distance of 2.4 Å for tetrakis(formato) dichromium", and emphasized that "the nature of the bridging ligand strongly affects the strength of the quadruple bond". The number of electrons in the bonding orbitals increases upon going from the formato species to the formamidato species, especially in the π orbital: $Cr_2(O_2CH)_4$ (Cr-Cr = 2.10 Å) $\sigma^{1.6}\pi^{2.8}\delta^{1.3}\delta^{*0.7}\pi^{*1.2}\sigma^{*0.4}$; $Cr_2(NH(O)CH)_4$ (2.10 Å) $\sigma^{1.7}\pi^{3.5}\delta^{1.5}\delta^{*0.5}\pi^{*0.5}\sigma^{*0.3}$.

Naturally, this difference between a formal bond order of four and a much smaller calculated bond order, led to some disagreement over whether these systems should be properly termed as having a quadruple bond. These calculations also predict that a dichromium tetrakis(carboxylato) species without axial ligands might have a shorter Cr-Cr distance than in their presence, but is not shortened enough to move it into the 'supershort' group.

Finally, the third paper [108] flatly predicted that the Cr-Cr distances in $Cr_2[N(H)C(H)O]_4$ and $Cr_2(O_2CH)_4$ should be 1.92 Å and 2.53 Å and stated that this large difference "shows that the effect of bridging ligands is at least as important as the observed influence of axial coordination in monitoring the length of the Cr-Cr quadruple bond". These authors went on to attribute to axial water molecules a capacity to further lengthen the

bond in $Cr_2(O_2CH)_4$ by "0.05 Å only".

The implication of these calculations is that one must have ligands more basic than carboxylates to have 'supershort' Cr-Cr bonds and that removal of the axial ligands from a tetracarboxylate will not result in a 'supershort' Cr-Cr bond. The electron diffraction study of $Cr_2(O_2CCH_3)_4$ with a dichromium distance of 1.96(1) Å is in accord with what might have been expected empirically from experimental data on related compounds, but completely at variance with the predictions from ab initio calculations.

Some of the SCF-HF-CI calculations carried out with principal emphasis on the $Cr_2(O_2CH)_4$ problem have also dealt with the $[Cr_2(CH_3)_8]^{4-}$ ion. An SCF calculation [101] yielded the $\sigma^2\delta^2\delta'^2\sigma^{*2}$ to be the lowest in energy, the quadruple bond configuration being 6eV higher in energy. Such a description of the Cr-Cr bonding is obviously incomplete, as this complex has no bridging ligands, and the quite short Cr-Cr distance and eclipsed configuration indicate a quadruple bond. Upon inclusion of a limited amount of CI [105], the quadruple bond configuration is found to contribute 42% to the CI wavefunction at 1.98 Å. However the ground state potential energy curve has a minimum at 2.16 Å, whereas the experimental bond length is 1.98 Å. The Cr-Cr bond is calculated to be only a double bond.

Although the more rigorous, quantitative forms of molecular electronic structure theory are becoming steadily more powerful, and have certainly reached the point where they can provide valuable guidance to those doing experimental work on multiple bonds between metal atoms, things have not yet reached the point where the results can be taken uncritically. All such calculations are subject to error.

$Cr_2[(R')NC(R)O]_4$ species with axial ligands behave enough like the $Cr_2(O_2CR)_4$ species with axial ligands, that it is reasonable to expect considerable similarity when the two kinds of molecules are compared without axial ligands. Thus the experimental Cr-Cr bond length in $Cr_2(O_2CCH_3)_4(g)$ is not in the least surprising from an empirical, common sense point of view.

Instead, we need to understand better how to handle ab initio calculations on such molecules.

No neat, unambiguous relationships have yet been found and consequently efforts have continued toward gaining a better understanding of the electronic structure and bonding in these compounds.

4.4 Another Theoretical Approach via Molecular Mechanics

Bond order can be defined in a purely electronic way, namely as the number of bonding electrons, and therefore independent of steric factors. Bond length depends, in the first instance, on bond order, but steric factors can have a powerful modulating influence thereon. This is illustrated in Figure 4.3.

It shows a family of potential energy curves representing different orders of chemical bonding between a given pair of atoms. The broken curve connecting the minima of the different bonding curves represents bond length as a function of electronic bond order only, i.e. in the absence of any steric effects. Calculations [109] of bond energy as a function of bond length are often assumed to follow relationships of this type, but they actually fail to do so because they ignore steric factors. The actual relationship cannot be described by a single curve. A given amount of steric strain deforms any of the bonds by an amount consistent with the shape of the bonding curve.

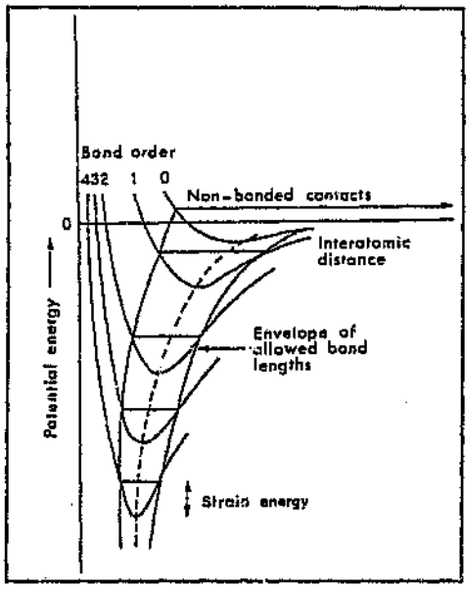


Figure 4.3 Qualitative representation of the relationship between bond order, bond length, and bond energy in metal-metal bonded compounds.

The resulting envelope defines a field of possible bond lengths and bond strengths for the system, which is designated in Figure 4.3 as the envelope of allowed bond lengths.

The experimental [74, 75, 78] attempts at correlating Cr-Cr bond strength with the nature of the bridging ligands, or the nature and proximity of axial donation, has been hindered by the effects of steric factors on the electronic bond distance. One can but only speculate about the relative importance of these two effects, since the true weakening or strengthening of the Cr-Cr bond by changes in the inductive nature of R and L_{ax}, as deduced from the Cr-Cr bond distance, is obscured by the added structural deformations caused by steric factors. How much of the Mo-Mo and Cr-Cr bond length distortion upon introducing axial ligands is genuine bond weakening, will only be recognized by separating out the steric element

also favouring bond deformation.

The use of experimentally observed M-M distances in the above calculations is perhaps not appropriate, since this distance is the outcome of a balance between electronic and steric components. More reliable, quantitative results may be obtained on using the 'true' electronic bond distance.

When considering the effect of torsional twists about the Mo-Mo bond, separation of the steric factors from the electronic element will enable one to determine how the δ component of the quadruple bond reacts to rotation about the M-M bond.

Therefore, rationalization of the observed trends would be greatly facilitated by separating steric from electronic factors. This can be achieved by the method of molecular mechanics.

To resolve the dichromium controversy, a dimetal system with definite bond orders is needed as a model. Since the formally quadruple Mo-Mo unit appears to be structurally rigid with relatively slight variations in the M-M distance due to the influences of the ligand environment, and because of the available range of bond orders structurally characterized, this system is used as our model of dimetal bonding to explain the bond length variation in Cr_2.

Chapter 5

THE METHOD OF MOLECULAR MECHANICS

"Chemical phenomena must be treated as if they were problems in mechanics."

Lothar Meyer (1868)

Chemical interaction between neighbouring transition-metal atoms in molecules is remarkably diverse and variable, ranging from simple van der Waals interaction to quadruple bonding. This variation from 0 to 4 in bond order is not necessarily matched by a parallel variation in observed structural properties.

It is proposed to analyze the interpretational problems discussed before by the methods of molecular mechanics. This will provide a direct quantitative estimate of all intramolecular steric interactions and by implication a means of identifying electronic effects.

5.1 Introduction

The basic idea is that bonds have 'natural' lengths and angles, and molecules will adjust their geometries so as to take up these values in simple cases. In addition, steric interactions are included using van der Waals potential functions. In more strained systems, the molecules will deform in predictable ways with 'strain' energies that can be accurately calculated.

The Born-Oppenheimer approximation [110], which is

commonly used in quantum mechanics, states that the Schrödinger equation for the molecule can be separated into a part describing the motions of the electrons and a part describing the motions of the nuclei; and that these two sets of motions can be studied independently.

It is a good approximation in general for studies involving molecules, and is usually used without comment in two different ways [111, 112]. First, with respect to electronic structure, it is common practice to establish the positions of the nuclei of the system by some method, and then to study the electronic structure using fixed nuclear positions. In molecular mechanics the opposite approach is taken. Namely, the motions of the nuclei are studied, and the electrons are not explicitly examined at all. They are simply assumed to find an optimum distribution about the nuclei.

The energy of the molecule in the ground electronic state is a function of the nuclear positions. The Born-Oppenheimer surface is the multidimensional 'surface' that describes the energy of the molecule in terms of the nuclear positions. In molecular mechanics it is usually just called the potential energy surface.

Molecular mechanics calculations employ an empirically derived set of equations for the Born-Oppenheimer surface whose mathematical form is familiar from classical mechanics [111].
This set of potential functions, called the force field, contains adjustable parameters that are optimized to obtain the best fit of calculated and experimental geometries.

In terms of molecular mechanics, a molecule is described as an interacting set of atoms. The equilibrium configuration is considered to correspond to a minimum in

the molecular potential energy function, which takes into account interactions between all possible atomic pairs in the molecule. The zero point of the potential function is defined to correspond to an arrangement in which each chemical bond, valence angle, bend or torsion has an ideal value determined by electronic factors only.

5.2 Potential Functions of Molecular Mechanics Force Fields

Simple molecular mechanics force fields express the total potential energy as the sum of bond stretching, angle bending, out-of-plane bending, torsional, and nonbonded terms (equation 5.1), where the sum extends over all such interactions.

$$V = \sum V_{\text{bond stretch}} + \sum V_{\text{angle bend}} + \sum V_{\text{torsion}} + \sum V_{\text{out-of-plane bend}} + \sum V_{\text{nonbonded}} \qquad 5.1$$

The sum of all these terms is called the steric energy of the molecule.

A multitude of expressions to represent the total strain energy have been developed all of which are based on the concept of additivity of atomic interactions.

5.2.1 Bond Stretching and Angle Bending

In most applications, the method only treats small distortions away from the electronic values; and to calculate the strain so introduced, harmonic restoring forces are assumed.

In the molecular mechanics model the atoms of a molecule may be thought of as joined together by mutually independent springs, restoring 'natural' values of bond

lengths and angles. One can then assume a harmonic potential with Hooke's Law functions (eqns 5.2 and 5.3), to model the strain induced by bond stretching and bending.

The amount of strain generated by bond length deformation, V_r, is thus:

$$V_r = \tfrac{1}{2}k_r(r-r_o)^2 \qquad 5.2$$

where k_r (mdyne/Å) is the force constant specific to the particular bond, and r_o (Å) the ideal bond length which will be distorted to an observed length, r (Å), by steric forces.

The strain induced in deforming angles, V_θ, is:

$$V_\theta = \tfrac{1}{2}k_\theta(\theta-\theta_o)^2 \qquad 5.3$$

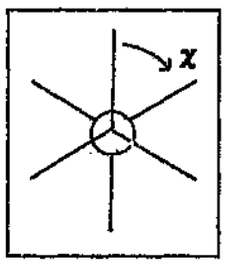
where k_θ (mdyne.Å) is the force constant specific to the particular angle, θ is the observed bond angle, and θ_o is the ideal bond angle. The ideal bond angles are usually taken as those pertaining to the particular geometry involved, i.e. 1.911 radian for tetrahedral coordination, 1.571 radian for octahedral or square planar, etc..

In general, the force constants for bond length deformation are larger than those for bond angle deformations, i.e. it is much easier to deform angles than bond lengths.

5.2.2 Torsional Strain

The physical significance of torsional strain is that it models the repulsion or attraction of the electron density in chemical bonds rather than atoms. Values of

χ between 180° and 360° are assigned negative values. Looking down the bond being twisted, a clockwise rotation of the far bond away from the near bond is considered positive χ, 1.



(1)

The 'twist' subroutine in the program presently employed for molecular mechanics calculations by our research group, is not really appropriate to the study of M_2 dimers and delocalized systems. For this reason, the torsional potential, which describes the interaction between bonding electron groups adjacent to the reference bond, was adjusted to provide an improved description of these systems. The incompleteness of the original potential is discussed further in Appendix A.

(a) Attractive Torsional Interactions

(i) L_4M-ML_4 Dimers of Order 4.0 and 3.5

As mentioned several times before, the δ component of the $\sigma^2\pi^4\delta^2$ and $\sigma^2\pi^4\delta^1$ configurations is sensitive to rotation (χ) about the M-M axis. This means that a torsional potential with a minimum at $\chi = 0°$ is needed to render the eclipsed conformation energetically favoured.

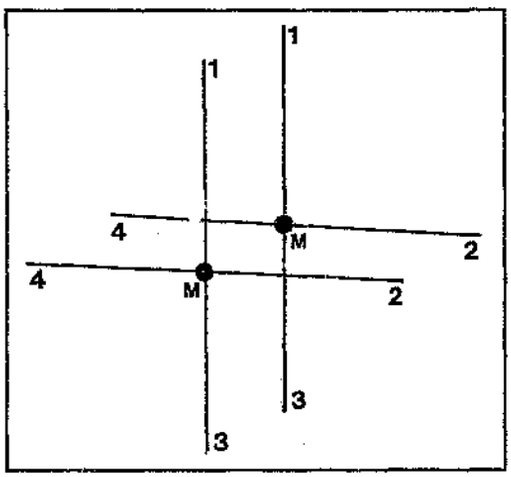
For the molecule represented in 2, it is clear that the total attractive potential can be separated into four

individual components; 1,1, 2,2, 3,3 and 4,4; each contributing equally to the attraction of electron density between adjacent M-L bonds demanded by the δ bond.

For these torsions treated individually, the torsional strain, $U_{\chi=0°}$, resulting from twists away from the eclipsed arrangement, is given by the expression:

$$U_{\chi=0°} = (V_{\chi=0°})/2[1+\cos(|\chi|-b)] \qquad 5.4$$

where the phase shift $b = \chi_0-180° = 0°-180° = -180°$, and $V_{\chi=0°}$ is the torsional potential (kcal/mol) for pairwise attraction of electron clouds.



(2)

(ii) Delocalized Interactions

In the case of a delocalized interaction, the torsion, as in a double bond, is described by a potential function of the same form, but now there are only two individual attractive components, each given by the expression:

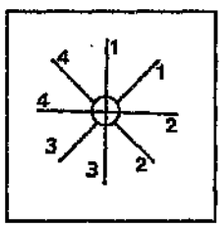
$$U_{\chi=0°} = (V_{\chi=0°})/2[1+\cos(|\chi|+180°)] \qquad 5.5$$

where $V_{\chi=0°}$ is the torsional potential (kcal/mol) for pairwise attraction of electron clouds, appropriate to the delocalized system involved.

(b) Repulsive Torsional Potentials

(i) L_4M-ML_4 Dimers of Order Three and Less

Here the $\sigma^2\pi^4$, π^4 and σ^2 configurations impose no constraint on rotation about the M-M bond axis. The repulsion between the electron clouds adjacent to the M-M bond leads to the preferred conformation adopting a staggered (χ=45°) arrangement as shown in the Newman projection, 3.



(3)

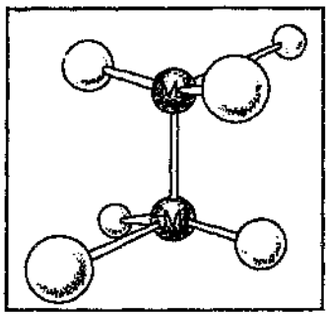
The four interactions, 1,1; 2,2; 3,3 and 4,4, contributing to the repulsion are each given by equation 5.6. which has minima at $|\chi|$ = 45°:

$$U_{\chi=45°} = (V_{\chi=45°})/2[1+\cos(|\chi|-b)] \quad 5.6$$

where the phase shift $b = \chi_0-180° = 45°-180° = -135°$, and $V_{\chi=45°}$ is the torsional potential (kcal/mol) for pairwise repulsion of electron clouds.
It is also stipulated that for $|\chi| > 45°$, $U_{\chi=45°} = 0$.

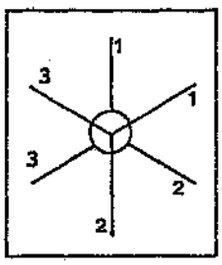
(ii) $L_3M\text{-}ML_3$ Dimers of Order Three and Less

For such dimers the compounds have a trigonal structure shown in 4.



(4)

Again there is no electronic factor opposing rotation about the M-M bond, so repulsion of electron clouds adjacent to the M-M bond favours a staggered arrangement ($\chi = 60°$) as shown in the Newman projection, 5.



(5)

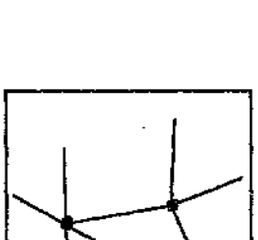
It makes physical sense that there be no repulsion at $|\chi| > 60°$. Since no more than three of the nine individual interactions can have $|\chi| < 60°$ simultaneously, it means that really only three interactions contribute to the total repulsion, 1,1; 2,2; and 3,3. Thus we have for each of the three torsions a torsional potential with minima at $|\chi| = 60°$:

$$U_{\chi=60^\circ} = (V_{\chi=60^\circ})/2[1+\cos(|\chi|-b)] \quad 5.7$$

where the phase shift $b = \chi_o - 180^\circ = 60^\circ - 180^\circ = -120^\circ$ and $V_{\chi=60^\circ}$ is the torsional potential (kcal/mol) for pairwise repulsion of electron clouds.
Also, for $|\chi| > 60^\circ$, $U_{\chi=60^\circ} = 0$.

(iii) Torsions About Other X-Y Bonds

The above torsional interactions are implemented when encountering the specific geometries discussed. For all other situations, such as that in 6, we simply employ equation 5.7.



(6)

5.2.3 Out-of-Plane Bending

Constraints are placed on the angular movement (δ) of atoms bound to cyclopentane and phenyl rings out of the plane of the ring. Out-of-plane distortion at a trigonal planar centre (eg. out-of-plane bending of bond C_1-X from the plane of atoms C_1=C_2-H) also requires the restraint of the potential function of the form:

$$U_\delta = \tfrac{1}{2}k_\delta(\delta-\delta_o)^2 \quad 5.8$$

where k_δ is the force constant (mdyne.Å) for such

deformations, δ is the calculated or observed angle and δ_o is, obviously, zero.

5.2.4 Nonbonded Interactions

Nonbonded interactions comprise van der Waals and electrostatic interactions.

(a) Coulombic Potential

It is common practice to apportion electric charges (q) at the atoms in the molecule and estimate the intramolecular electrostatic energy as a pairwise sum of interactions.

The electrostatic term is based upon partial atomic charges at the atom centres q_i, q_j, separated by a distance, r_{ij} (Å), with the energy being calculated according to:

$$V_q = c\ (q_i.q_j)/r_{ij} \qquad 5.9$$

where c = 2.30722 mdyne.Å^2.

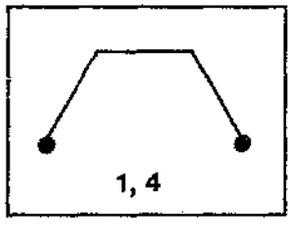
(b) Van der Waals Interactions

A further contribution to strain energy, which is probably the most important, are the forces between atoms that are not bonded to each other.

By normal convention, the calculation of nonbonded terms is not performed for atoms connected through one or two bonds (1,2- and 1,3-interactions) because there, contributions are assumed to be implicit in the bond-stretch and bond-bend force constants, respectively.

Interactions between atoms separated by more than two bonds (≥ 1,4-interactions, 7) are described in terms of potentials to represent van der Waals interaction.

A variety of potentials are used, but all of them correspond to a repulsive force at short distances, and an attractive component at longer distances - both of which asymptotically go to zero at still longer distances.



(7)

The curve is characterized mainly by the minimum energy distance (related to the van der Waals radii), the depth of the potential well (related to the polarizabilities), and the steepness of the repulsive part (the hardness): $V_{nonbonded} = R-A$.

The attractive component as a dispersive interaction between induced dipoles is formulated [113] as:

$$A = c/(r_{ij})^6 \qquad 5.10$$

The repulsive component is less well defined, and the different formulae in use seem to depend on personal taste as much as anything. The ready parameterization of the Buckingham function for a variety of atoms [114, 115] is no doubt responsible for its wide application.

$$\text{Buckingham Potential: } R = a\exp(-br_{ij}) \qquad 5.11$$

Hence,

$$V_{nonbonded} = a\exp(-br_{ij}) - c/(r_{ij})^6 \qquad 5.12$$

One must be aware of the fact that the potential becomes strongly attractive at short interatomic distances as shown in Figure 5.1.

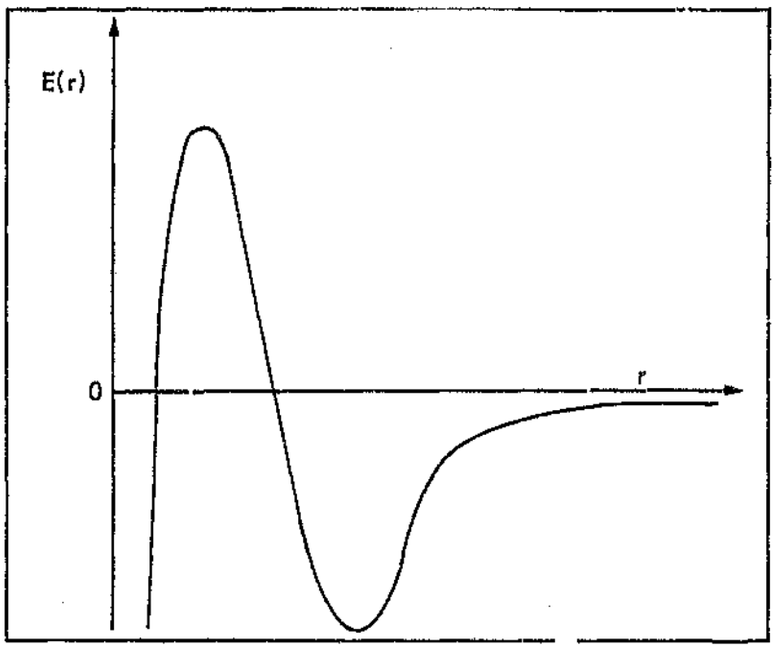


Figure 5.1 Interatomic potential energy curve according to the Buckingham potential, which fails at short interatomic distances.

Long range nonbonded interactions which are greater than the user defined limit of 7 Å are avoided so as to prevent unnecessary calculation of strain energies which are effectively zero.

The constants b and c needed for each atom pair were

estimated by the method of Scott and Scheraga [115].

The constant c is a function of the polarizabilities, α (a_0^3), and valence electron densities, N, of the atom pair [115, 116, 117]:

$$c = (3/2\ \alpha_1\alpha_2)/[(\alpha_1/N_1)^{1/2}+(\alpha_2/N_2)^{1/2}] \quad 5.13$$

The units of c is (10^{-11} ergs.Å^6/molecule).

The constant b is a shielding function. Values of b (Å^{-1}) as a function of atomic number are plotted in [115], and for atoms i and j:

$$b_{ij} = \sqrt{(b_{ii}.b_{jj})} \quad 5.14$$

The constant a (10^{-11}erg/molecule) is obtained by minimizing equation 5.12 at $r = r_1+r_2$, where r_1 and r_2 are the van der Waals radii of the two atoms:

$$a = [6ce^{xp}(br)]/(br^7) \quad 5.15$$

Energies, $V_{nonbonded}$, are thus expressed in units of 10^{-11} erg/molecule ≡ kcal mol^{-1}/144.

The peculiar units above are required by the molecular mechanics program [118].

The ability of the forces involved in the molecule to dominate other forces where clashes arise in terms of steric requirements are generally: nonbonded repulsive forces > bond length deformation forces > bond angle deformation forces ≥ torsional forces > nonbonded attractive forces.

5.3 Parameterization

The quality of a molecular mechanics force field, that is, the accuracy of its predictions and their reliability, is critically dependent on the potential functions and on the parameters used. Parameter optimization has to be done with the same care that is used in the selection of the potential functions.

Molecular mechanics calculations of metal complex structures are often not straightforward because of uncertainties concerning the appropriate force field parameters for structural elements involving the metal.

Also, current force field formulations are not generalized readily to the varieties of molecular shapes exhibited by many inorganic (both main group and transition metal) complexes.

Since the introduction of the molecular mechanics procedure for organic molecules, there has been continuing development of the method toward the modelling of other types of compounds such as transition metal complexes. Although many of these studies have been quite informative they nevertheless tend to be somewhat fragmentary with, for example, a single structure (or small number of similar structures) being modelled with little indication that the force field used has general applicability.

It has been our experience that a single structure may be fitted equally well with several different parameter sets; it is only by testing the parameters over a considerable number (and range) of structures that it is possible to decide between alternative sets.

Also, because different force fields usually differ not

only in their parameters, but also in the mathematical form of one or more of the potential functions, it is usually hazardous to try to transfer the parameters from one force field to the other.

In short, most of the force constants currently used in molecular mechanics are not too well adapted to the study of dimetal compounds.

In view of the extreme variability of observed stretching frequency of dimetal bonds, it is almost impossible to obtain transferable force constants for metal-metal bonds from spectroscopic measurements not supported by full normal-coordinate analyses [123].

Since it is impractical to restrict the use of molecular mechanics to compounds for which adequate force fields are available from vibrational analyses, approximate force fields based on totally different criteria inevitably come into being. Crystallographic results are one fertile source of force constants derived by trial-and-error methods aimed at a computational match of the observed molecular structure.

5.4 Generating Unique, Transferable (k_r,r_0) Values for the Dimetal Centre

For most of the structures studied in this thesis, obtaining transferable force field parameters for all interactions, but the metal-metal bond, was not too troublesome. Once the ligand backbone of the dimetal compound is correctly modelled, suitable values of force constant, k_r, and characteristic bond length, r_0, for the metal-metal bond can be obtained [123]. This, too, is a trial-and-error issue.
A likely value for k_r, e.g., is assumed and r_0 is adjusted

until a combination (k_r, r_o) is found to reproduce the observed structure after energy minimization. This is repeated for a range of values of k_r to define a solution set $\{k_r, r_o\}$. In order to obtain unique transferable values, one looks for different solution sets pertaining to the same bond order and intersecting at a single point [123]. This procedure will become clearer in the chapters covering the results of such calculations.

5.5 Energy Minimization

It is assumed that with all force constants and potential functions correctly specified in terms of the electronic configuration of the molecule, the nuclear arrangement that minimizes the steric strain corresponds to the observed molecular structure. Any discrepancies between calculated and observed structure parameters must be ascribed to an inappropriate force field or to experimental errors in the observed structure [122]. As mentioned earlier, to avoid the latter possiblity, no disordered structures or structures suspected of disorder were researched.

The object of the exercise is to minimize the intramolecular potential energy, or steric strain, as a function of the nuclear coordinates. The most popular procedure is by a computerized Newton-Raphson method, described adequately by Boyd [118].

The energy minimization is an iterative geometry optimization, so unless there is only one potential well for a molecule, the minimum energy geometry obtained will depend on the starting geometry of the optimization, i.e. in which potential well we begin our input structure. False minima do not generally occur when using the coordinates from the crystal structure of the molecule itself.

Chapter 6

Mo_2: OUR MODEL OF DIMETAL BONDING FOR GROUP VIA METALS

6.1 Introduction

To resolve the dichromium dichotomy, a dimetal system in which the formal bond orders are the 'true' bond orders is essential; that is, the dimetal bond order must be a function only of the position of the metal in the periodic table and its oxidation state. Effects due to the nature of the ligand environment must be absent, or insignificant.

The dimolybdenum system is periodically related to Cr_2 and the Mo-Mo bonding is insensitive to its environment- Mo_2 serves as a model of dimetal bonding for period VIA metals.

By the method of molecular mechanics, we will obtain unique, transferable $(k_r, r_o)_{Mo\text{-}Mo}$ values for bonds of order four through to one. Knowing the unique force constant, k_r, and unique electronic bond distance, r_o, for the dimolybdenum bond of each order, N_{Mo}, we can formulate relationships between k_r and r_o, and between N_{Mo} and k_r, or N_{Mo} and r_o.

Since molybdenum and chromium are periodically related, we can transfer these relationships to the chromium system and investigate the large variation in observed Cr-Cr distances.

Simultaneously, we will have the opportunity to examine the effect of torsional twists about a quadruple Mo-Mo bond, which has been the subject-matter of numerous structural studies performed by Cotton.

6.2 Molecular Mechanics Calculations of Quadruple Dimolydenum Compounds

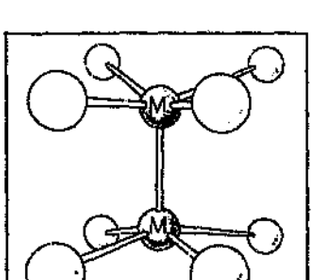
In all these compounds the formal oxidation state of molydenum is (II), implying a formal Mo-Mo quadruple bond.
It is perhaps best to discuss the force field used in the calculations and the results pertaining to each structural type separately.

Hydrogen coordinates not given in the crystal structure data, together with sterically important lone pairs (L_p), were placed in geometrically calculated positions using the program SHELX [119].

The maximum standard deviations of the calculated structure parameters are: bond distances 0.1 Å; angles, 3° and; out-of-plane bends and torsions, 5° (these values apply to all calculations performed).

6.2.1 The Unbridged $[Mo_2X_8]^{4-}$ and $Mo_2X_4(PR_3)_4$ Compounds

These structures are characterized by their essentially eclipsed D_{4h} (for the $[Mo_2X_8]^{4-}$ ions) and D_{2d} (for $Mo_2X_4(PR_3)_4$) idealized geometries. Both have the general tetragonal structure shown in **1**. The observed Mo-Mo-X angles are 105°-116°, the observed Mo-Mo-P angles are 98°-105°, the X-Mo-X angles are 85°-87°, and the X-Mo-P angles are 82°-89°. We therefore model these structures as two square planar MoL_4 units held together by Mo-Mo bonding.



(1)

(a) Force Field Parameters

The force field adopted for these unbridged Mo_2 compounds is summarized in Tables 6.1 - 6.3.

Table 6.1 Details of the bond-deformation parameters

Bond	k_r (mdyne/Å)	r_o (Å)
Mo-Cl	0.70	2.35
Mo-Br	0.70	2.52
Mo-C	1.98	2.27
Mo-P	0.70	2.50
Mo-C	2.00	2.20
Mo-Cl	0.70	2.39
Mo-Br	0.70	2.53
Mo-I	0.70	2.70
C-C	5.00	1.54
C-H	5.00	1.08
P-C	3.5	1.80
C_{ar}-C_{ar}	7.65	1.39
C_{ar}-C_{ar}(para)	0.05	2.78
C_{ar}-H_{ar}	5.00	1.08
P-H	5.00	1.25

It is noted that we have a -0.5 charge on the Cl, Br and Me ligands for the $[Mo_2X_8]^{4-}$ ions. The overall 4- charge of the ion is apportioned at the atoms situated furthest apart. It was necessary to include the coulombic interaction between these -0.5 charges, to obtain an acceptable match of the observed structure parameters. This is a result of the charge being localized or atoms bonded directly to the dimetal centre.

Planarity of the phenyl ring is ensured by excluding 1,4-(C_{ar}--C_{ar}) nonbonded interactions, and treating para(C_{ar}-C_{ar}) as a bonded interaction.

Table 6.2 The angle-bending parameters

Angle	k_θ (mdyne.Å)	θ_o (rad.)
Mo-Mo-$Cl^{-\frac{1}{2}}$	0.60	1.571
$Cl^{-\frac{1}{2}}$-Mo-$Cl^{-\frac{1}{2}}$	0.50	1.571
Mo-Mo-$Br^{-\frac{1}{2}}$	0.70	1.571
$Br^{-\frac{1}{2}}$-Mo-$Br^{-\frac{1}{2}}$	0.50	1.571
Mo-Mo-$C^{-\frac{1}{2}}$	0.70	1.571
$C^{-\frac{1}{2}}$-Mo-$C^{-\frac{1}{2}}$	0.60	1.571
Mo-Mo-P	0.30	1.571
Mo-Mo-C	0.10	1.571
P-Mo-C	0.10	1.571
Mo-Mo-X^a	0.10	1.571
X^a-Mo-P	0.10	1.571
H-C-H	0.52	1.911
C-P-C	0.10	1.911
P-C_{ar}-C_{ar}	0.65	2.094
C_{ar}-C_{ar}-C_{ar}	1.00	2.094
C_{ar}-C_{ar}-H_{ar}	0.65	2.094
P-C-H	0.65	1.911
C_{ar}-P-H	0.65	1.911
C_{ar}-P-C	0.10	1.911

a: X = Cl, Br, I

Constraints were placed on the angular movement (δ) of the hydrogen atoms bound to C_{ar} out of the plane of the phenyl ring: k_δ = 0.29 mdyne.Å.

Table 6.3 Parameters of nonbonded interactions (Buckingham potential)

Interaction	a (u)[a]	b ($Å^{-1}$)	c (u.$Å^6$)
Mo--Mo	110.3	2.60	6.60
Mo--Cl	520.7	3.12	10.2
Mo--Br	176.5	2.69	14.6
Mo--C	769.1	3.46	3.80
Mo--H	153.0	3.44	1.28
Mo--P	723.8	3.2	8.04
Mo--I	188.2	2.55	22.7
H--H	175.3	4.55	0.343
H--C	881.9	4.57	0.912
H--P	898.8	4.24	1.83
C--C	5037.0	4.60	2.53
C--P	4766.0	4.26	5.16
C_{ar}--C_{ar}[b]	5037.0	4.60	2.53
P--P	4664.0	3.95	10.60
Cl--Cl	2166.0	3.75	17.4
Br--Br	332.3	2.79	36.0
Cl--P	3110.0	3.85	13.6
Cl--C	3020.0	4.15	6.61
Cl--H	601.7	4.13	2.35
Br--P	1082.0	3.32	19.6
Br--C	1036.0	3.58	9.53
Br--H	229.6	3.56	3.40
I--I	405.4	2.51	86.6
I--P	1205.0	3.15	30.3
I--C	1181.0	3.40	14.8
I--H	265.5	3.38	5.26

a :u = 10^{-11} erg/molecule

b :for >1,4-interactions; for 1,4-(C_{ar}--C_{ar}) a=b=c=0

Torsional contributions to steric strain arise from

* the attractive interactions C_{ar}-C_{ar}-C_{ar}-C_{ar} and H_{ar}-C_{ar}-C_{ar}-H_{ar}, for which $V_{\chi=0°}$ = 0.05 kcal/mol and,
* the remaining torsions being repulsive interactions with $V_{\chi=60°}$ = 0.0049 kcal/mol.

(b) The Delta Contribution to the Quadruple Bond Strength

The torsional interactions about the Mo-Mo bond are interesting. The molecular mechanics program [118] offers the constraint option of 'driving' atoms about a specified torsion, while refining the structure at each angle step.

Once all the calculated parameters are of the correct order of magnitude, one can calculate barriers to rotation about the Mo-Mo bond. The torsional parameter used to render the eclipsed conformation energetically favoured is replaced by an artificial incremental parameter [118] to drive the rotation around the Mo-Mo bond, sampling the equilibrium steric strain at each position.

For the $Mo_2X_4(PR_3)_4$ molecules (Figure 6.2), the calculated strain as a function of rotation about Mo-Mo has a minimum at χ=0°. It leaves no doubt that there is a steric contribution to the observed conformation, and explains the successful modelling of the structures without the need for a torsional parameter rendering the eclipsed arrangement energetically favoured.

For $[Mo_2X_8]^{4-}$, the δ bonding is crucial to the stereochemistry; it alone is responsible for the eclipsed conformation. Steric factors clearly favour a staggered arrangement of the ligands about the Mo-Mo bond. In each case the potential energy has a maximum at χ=0°, viz. the eclipsed conformation (Figure 6.1). This shows

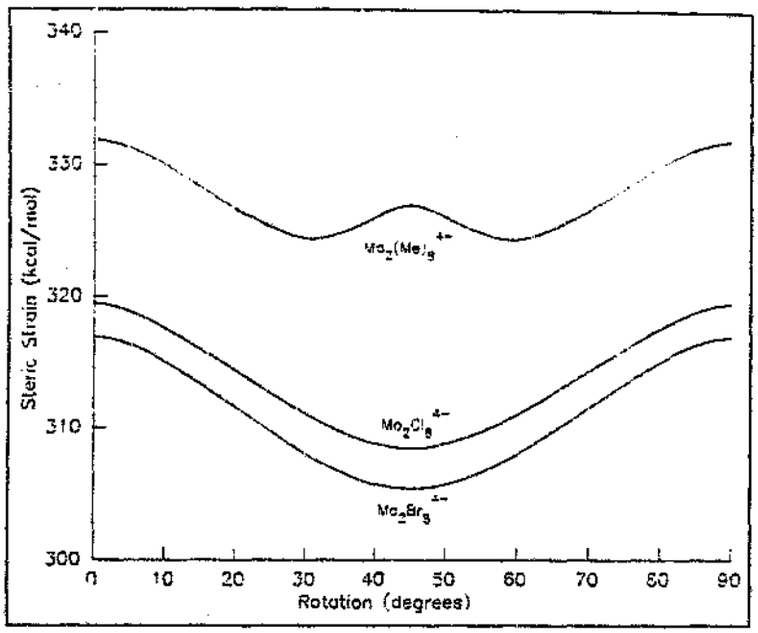


Figure 6.1 Angular variation of steric strain in quadruply bonded $[Mo_2X_8]^{4-}$ ions.

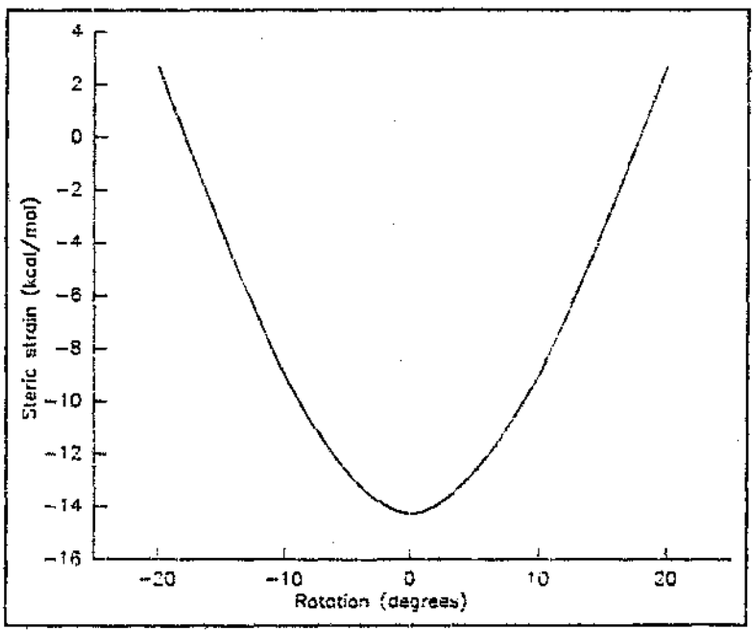


Figure 6.2 Steric strain in $Mo_2Cl_4(PMe_3)_4$ as a function of twist angle.

conclusively that an electronic factor, i.e. δ bonding, is responsible for the stabilization of the observed conformation.

For $[Mo_2Me_8]^{4-}$, potential minima are observed at χ=30° and 60°, and not at 45°. The explanation for this lies in the fact that the potential energy curve essentially reflects interaction between hydrogen atoms on methyl groups. These have local threefold symmetry, which is superimposed on the fourfold symmetry of the anion. The compromise is a local submaximum at 45°.

The difference in potential energy between the maximum and minimum, ΔU = 7.5, 11, 11.5 kcal/mol for X = Me, Cl, and Br, respectively, defines a lower limit for the δ contribution to the quadruple-bond strength.

Other attempts at estimating the δ-electronic barrier give 15 kcal/mol [120] and 9.9 kcal/mol [121], in close accord with the molecular mechanics results.

(c) $\{k_r, r_o\}$ Solution Curves for the Mo_2 Centre

The major aim of the molecular mechanics calculations is the generation of $\{k_r, r_o\}_{Mo\text{-}Mo}$ solution curves for the dimolybdenum centre and ultimately the creation of unique $(k_r, r_o)_{Mo\text{-}Mo}$ couples for each Mo_2 bond order.

One can be confident that the force field summarized above affords a suitable match between calculated and observed structural parameters and hence is suitable for the analysis of data for the dimolybdenum centre.

The results of the trial-and-error procedure are shown in Figure 6.3.

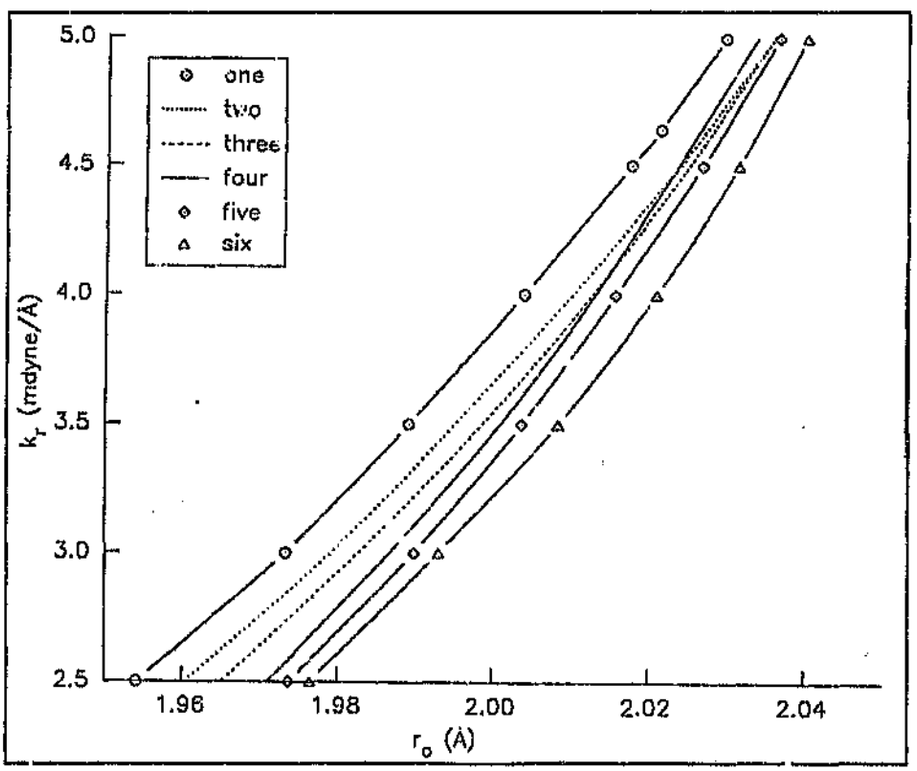


Figure 6.3 Molecular mechanics solution curves $\{k_r, r_o\}$ for the unbridged dimolybdenum centre of order four.

The observed Mo-Mo distance is reproduced to within 0.001 Å as shown in Table 6.4.

The curves are all of positive slope implying stretching of the Mo-Mo bond by steric factors. Added evidence for Mo-Mo stretching by steric elements, is the lengthening of the Mo-Mo bond on rotation from the sterically favoured staggered arrangement to the electronically demanded eclipsed conformation (driver calculations).

Very interestingly there are only six $\{k_r, r_o\}_{Mo\text{-}Mo}$ solution curves for the ten structures studied. Some

compounds have coinciding curves. It is perhaps not surprising to find compounds with similar observed Mo-Mo distances being stretched from the electronic separation by the same magnitude and in the same manner by steric forces.

Table 6.4 Calculated and observed Mo-Mo distances

Molecule	Obs. (Å)	Calc. (Å)	Figure Label
$[Mo_2Me_8]^{4-}$	2.148(2)	2.148	three
$Mo_2Me_4(PMe_3)_4$	2.1489(4)	2.149	one
$Mo_2Cl_4(PHPh_2)_4$	2.1474(9)	2.149	one
$[Mo_2Cl_8]^{4-}$	2.138(4)	2.136	six
$[Mo_2Br_8]^{4-}$	2.135(2)	2.135	six
$Mo_2Br_4(PMe_3)_4$	2.125(1)	2.126	four
$Mo_2I_4(PMe_3)_4$	2.127(1)	2.126	four
$Mo_2Cl_4(PMe_2Ph)_4$	2.1288(8)	2.129	five
$Mo_2Cl_4(PMe_3)_4$	2.130(1)	2.130	five
$Mo_2Me_4(PMe_2Ph)_4$	2.164(1)	2.164	two

Boeyens [123] found the solution curves for the quadruple $W_2(O_2CEt)_4$ and triple $W_2(O_2CEt)_4.2CH_2Ph$ to coincide. Both have identical structures apart from the benzyl group.

The curves do not intersect at a single point to yield a unique $(k_r,r_o)_{Mo-Mo}$ couple for the quadruple bond. To achieve this, "it is necessary to identify bonds of the same order in sterically different environments" [123]. In the present case, compounds with bridging ligands suggest themselves as appropriate classes for comparison.

Although there is no fixed point of intersection, the

$\{k_r, r_o\}_{Mo-Mo}$ solution curves are sufficiently clustered together over a r_o range of only 0.02 Å, to assume quadruple Mo-Mo bonding in all these compounds. This small range may be expected since the observed Mo-Mo distances cover a range of only 0.04 Å.

(d) Steric Deformations

As already mentioned the Mo-Mo bond in these unbridged complexes is being stretched from the electronic r_o characteristic of the quadruple bond to the observed separations. Steric repulsions are also partly overcome by Mo-Mo-X and Mo-X deformation.

In $[Mo_2X_8]^{4-}$, structural accommodation of the increased X^---X^- repulsion (Cl^-<Br^-) does not occur along the Mo-Mo bond. One would expect a more stretched Mo-Mo bond in the Br^- analogue on the basis of the size of the X^- group. Instead, the Mo-Br^- bond is longer and the Mo-Mo-Br^- angle more obtuse. Hence, in $[Mo_2Br_8]^{4-}$, the Br^---Br^- repulsions are less than the Cl^---Cl^-, resulting in a slightly longer Mo-Mo bond in the chloro analogue. $[Mo_2Me_8]^{4-}$ has the same magnitude Mo-Mo-C^- angle as Mo-Mo-Cl^-, but the Mo-C^- distance is shorter than Mo-Cl^-. The shorter Mo-C^- distance means greater Me--Me repulsion; consequently the longer Mo_2 separation.

In the $Mo_2X_4(PMe_3)_4$ compounds, the Mo-Mo distance shows an obvious indifference to the nature of the halide ligand. Structural accommodation of the increasing interligand repulsion in the series Cl<Br<I does not occur along the Mo-Mo bond, instead being reflected solely in their M-X bonds and Mo-Mo-X angles.

$Mo_2Me_4(PMe_3)_4$ and $Mo_2Me_4(PMe_2Ph)_4$ have longer Mo-Mo distance than their halide analogues because of the shorter Mo-C distance.

Replacement of Me groups by Ph in the series $Mo_2Cl_4(PR_3)_4$, causes the sterically bulkier Ph groups to lengthen the Mo-Mo bond. The same occurs in the $Mo_2Me_4(PR_3)_4$ set of molecules.

In short, the observed deformations are purely of steric origin.

6.2.2 The Bridged $Mo_2(X\text{-}Z\text{-}Y)_4$ and $Mo_2(X\text{-}Z\text{-}Y)_4L_2$ Compounds

On separating the electronic from the steric elements, we are able to study the influence of varying the inductive nature of both the bridging XZY group and the axial ligand, L_{ax}. The structural data discussed in Chapter 2 demonstrated the distorting effects on the Mo-Mo quadruple bond of axial coordination. Is the effect steric or electronic, or both?

(a) Force Field Parameters

A central feature of these compounds is the familiar paddle-wheel type structures formed by the spanning bridging ligands: O^O, O^C, N^O and N^N. The $Mo_2(X\text{-}Z\text{-}Y)_4$ molecules are treated as two fused square planar $Mo(X_2Y_2)$ units; and the $Mo_2(X\text{-}Z\text{-}Y)_4L_2$ molecules as having an octahedral disposition of the Mo_2, $(L_{eq})_4$ and L_{ax} atoms about a central Mo_1 atom. This is reasonable considering the near-orthogonal Mo-Mo-L_{eq}, L_{eq}-Mo-L_{eq}, and L_{ax}-Mo-L_{eq} angles.

Within a given class of bridging ligands all molecular dimensions, besides the Mo-Mo bond, are statistically indistinguishable, i.e. the supporting framework is comparatively insensitive to changes in the dimetal bond length. This enables the supporting framework for a given X-Z-Y set of compounds to be simulated by a virtually

transferable force field.

Lone pairs have been treated as hydrogen atoms in nonbonded interactions. Their behaviour in all other situations is defined in the tables.

Force field parameters not defined before, are summarized in Tables 6.5 - 6.7.

Table 6.5 Force field parameters for interacting pairs of atoms

Bond	k_r (mdyne/Å)	r_o (Å)
O_{br}-C_{br}[a]	3.00	1.26
O-L_p	6.00	1.00
O=S	3.50	1.44
N_{ar}-C_{ar}	7.65	1.34
C_{ar}-N_{ar} (para)	0.05	2.78
C-F	2.00	1.30
O-C	3.00	1.42
N_{br}-N_{br}	3.00	1.25
N-L_p	6.00	1.00
N-H	5.00	1.00
N-C	3.00	1.44
N_{br}-C_{br}	3.00	1.30
C-Cl	2.00	1.70
C-Br	2.00	1.80
O-S	3.00	1.50
Mo-O_{br}	0.84	2.07
Mo-O_{br} (sulfate)	0.90	2.10
Mo-C_{br}	1.96	2.14
Mo-N_{br}	0.84	2.10
Mo-O_{ax}[b] (intermolecular)	0.40	2.65
Mo-N_{ax}	0.80	2.54
Mo-O_{ax} (THF)	0.60	2.50
Mo-Cl_{ax}	0.20	3.30
Mo-Br_{ax}	0.30	3.40
Mo-O_{ax} (sulfate) (intermolecular)	0.50	2.57

a :br = bridging atom

b :ax = atom bonded axially to Mo

Table 6.6 Bond bending parameters for $Mo_2(X\text{-}Z\text{-}Y)_4$ and $Mo_2(X\text{-}Z\text{-}Y)_4L_2$

Angle	k_θ (mdyne/Å)	θ_o (rad.)
$Mo\text{-}Mo\text{-}L_{ax}$	0.30	3.1416
$Mo\text{-}Mo\text{-}L_{br}$	0.20	1.571
$L_{ax}\text{-}Mo\text{-}L_{br}$	0.80	1.571
$X_{br}\text{-}Mo\text{-}Y_{br}$	0.8	1.571
$Z_{br}\text{-}(Y/X)_{br}\text{-}H(L_p)$	0.60	2.094
$(Y/X)_{br}\text{-}Z_{br}\text{-}L_p$	0.60	2.094
$X_{br}\text{-}Z_{br}\text{-}Y_{br}$	1.50	2.094
$(X/Y)_{br}\text{-}Z_{br}\text{-}C(H)$	1.00	2.094
C-C-C(O)	0.10	1.911
C-C-H(F)	0.65	1.911
F-C-F	0.52	1.911
$L_{ar}\text{-}L_{ar}\text{-}L_{ar}$	1.00	2.094
$L_{ar}\text{-}L_{ar}\text{-}L$	0.65	2.094
$Z_{br}\text{-}(Y/X)_{br}\text{-}L$	0.20	2.094
X-C-H	0.65	1.911
$Y\text{-}O\text{-}L_p$	0.40	1.911
C-O-C	0.20	1.911
C-O-C	0.10	2.094
X-C-X	0.10	1.911
$O_{br}\text{-}S_{br}\text{=}O$	1.00	1.911
$O\text{=}S_{br}\text{=}O$	0.80	1.911
$Mo\text{-}O_{br}\text{-}L_p$	0.40	2.094
$Mo\text{-}(X/Y)_{br}\text{-}Z_{br}$	0.20	2.094
$Mo\text{-}O_{br}\text{-}C$	0.20	2.094
$Mo\text{-}N_{br}\text{-}H$	0.40	2.094
$Mo\text{-}N_{br}\text{-}C_{ar}$	0.20	2.094
$Mo\text{-}O_{ax}\text{-}C$	0.20	2.094
$Mo\text{-}X_{ax}\text{-}C$	0.20	1.911

Y_{br}, X_{br}, Z_{br} = C_{br}, N_{br}, O_{br}
L_{ar} = C_{ar}, N_{ar}
L = H_{ar}, O_{br}, C, N_{br}, F, Cl, C_{ar}, Mo
X = Cl, Br, O
Y = C, L_p, S_{br}

Table 6.7 Parameters of nonbonded interactions

Interaction	a (u)	b ($Å^{-1}$)	c (u.$Å^6$)
O--O	2519.0	4.62	2.53
O--H(L_p)	621.1	4.58	0.890
O--C	3528.0	4.61	2.52
O--F	1023.0	4.62	1.40
O--S	1680.0	4.18	4.60
F--H(L_p)	246.7	4.59	0.462
S--H(L_p)	380.0	3.94	2.18
C--F	1381.0	4.61	1.36
F--F	453.9	4.63	0.815
S--S	2950.0	3.80	14.0
Mo--N	538.1	3.46	3.82
Mo--S	637.0	3.16	9.06
Mo--O	629.3	3	3.93
Mo--F	294.2	3	2.32
N--N	3880.0	4.61	2.47
N--C	2983.0	4.60	2.49
N--H	553.7	4.58	0.89
N--O	2244.8	4.61	2.62
N--F	929.5	4.62	1.43
O--Cl	2278.2	4.16	6.63
N--Cl	2133.3	4.16	6.88
Br--O	807.0	3.58	9.54
Br--N	773.0	3.58	9.91
N_{ar}--C_{ar}[a]	2983.0	4.60	2.49

a :for >1,4-interactions; for 1,4-(C_{ar}--N_{ar}) interaction a=b=c=0

It should be noted that unlike the $[Mo_2X_8]^{4-}$ ions, the structure of $[Mo_2(SO_4)_4]^{4-}$ was successfully modelled without the inclusion of coulombic interactions. The -0.5 charge would be located on the outermost oxygen atoms, and would have no influence on the central Mo_2O_8 core.

Again constraints were placed on the angular movement (δ) of the atoms (H, O, C, Cl, Mo and F) bound to C_{ar} and N_{ar} out of the plane of the phenyl ring using
k_δ = 0.29 mdyne.Å.
Out-of-plane bending of atoms bound to the delocalized $(X/Y)_{br}$-Z_{br} bond also requires the restraint of this k_δ.

The torsional interactions about the ligand-ligand and metal-ligand bonds are of an attractive nature for C_{ar}-C_{ar}, C_{ar}-N_{ar}, and $(X/Y)_{br}$-Z_{br} ($Z_{br}\neq S$), with
$V_{\chi=0°}$ = 0.05 kcal/mol, and repulsive for twists about the other bonds with $V_{\chi=60°}$ = 0.0049 kcal/mol. (Recall from Chapter 2 that the Mo_2O_2S rings are non-planar, having an average dihedral bend of 20° across the O--O line.)

(b) The Delta Contribution to the Quadruple Bond Strength

Very interestingly, no torsional parameter was needed to render the eclipsed conformation energetically favoured.

In the case of the monoanionic bridging ligands, the delocalization of the negative charge over the XZY atoms forces the X and Y atoms to have their donor orbitals directed along approximately parallel lines. This, in turn, results in the near-eclipsing of the X-Mo-Mo-Y unit, suppressing the need for extra constraints from the δ bonding.

For the sulfate-bridged compound, such electronic delocalization is absent. Rather, steric preference for the eclipsed conformation excludes the need for a

torsional parameter to ensure the eclipsing of ligands about the Mo-Mo bond. Molecular mechanics calculations on the isostructural, but triply bonded, $Mo_2(HPO_4)_4(L_{ax})_2$ molecules shows the eclipsed conformation to be sterically favoured in the absence of any δ bonding.

This result clearly demonstrates that eclipsing does not imply the presence of δ bonding, yet δ bonding demands eclipsing. The need for the torsional potential in the calculations depends on the steric fancy for the electronically demanded conformation.

(c) $\{k_r, r_o\}$ Solution Curves for the Mo_2 Centre

Very rewardingly, the solution curves for the Mo_2 centre supported by bridging ligands intersect the curves of the unbridged complexes, thus permitting the identification of a unique $(k_r, r_o)_{Mo\text{-}Mo}$ couple for the quadruple Mo-Mo bond.

The $\{k_r, r_o\}_{Mo\text{-}Mo}$ solution curves are presented in Figure 6.4.

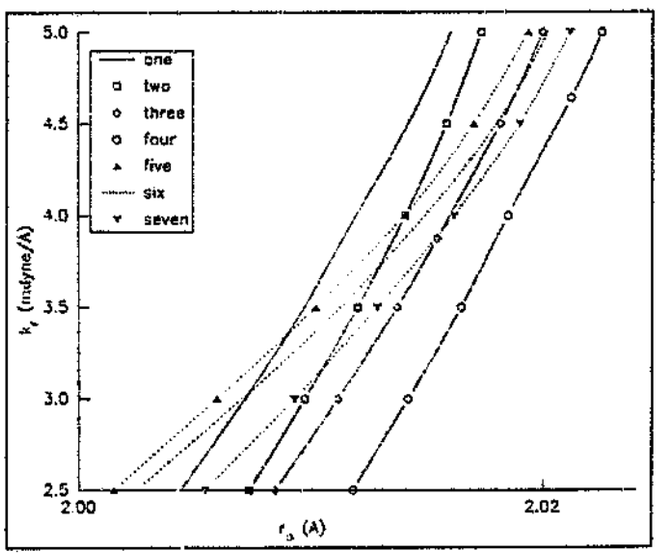


Figure 6.4 Molecular mechanics solution curves for the Mo_2 centre spanned by bridging ligands.

The calculated Mo-Mo distances match the observed values within 0.001 Å, as seen in Table 6.8.

Table 6.8 Calculated and observed Mo-Mo distances for $Mo_2(XZY)_4L_2$

(X-Z-Y)	$(L_{ax})_n$	Calc. (Å)	Obs. (Å)	Figure Label
O-C(Me)-O	-	2.079	2.079(3)	three
O-C(biph)-O	-	2.082	2.082(1)	four
DFM	-	2.082	2.085(4)	four
PhN-N-NPh	-	2.083	2.083(2)	four
CHP	-	2.083	2.085(1)	four
PhN-C(Me)-O	-	2.083	2.086(2)	four
DMP	-	2.064	2.064(1)	two
MHP	-	2.064	2.065(1)	two
DMHP	-	2.072	2.072(1)	one
PhN-C(CMe_3)-O	-	2.071	2.070(1)	one
MAP	-	2.071	2.070(1)	one
(2,6xylyl)N-C(Me)-O	$(CH_2Cl_2)_2$	2.083	2.083(3)	four
(2,6xylyl)N-C(Me)-O	$(CH_2Br_2)_2$	2.083	2.085(2)	four
(2,6xylyl)N-C(Me)-O	$(py)_1$	2.100	2.101(1)	five
(2,6xylyl)N-C(Me)-O	$(4\text{-Mepy})_2$	2.100	2.102(1)	five
(2,6xylyl)N-C(Me)-O	$(THF)_2$	2.091	2.093(2)	six
O-C(H)-O	$(inter.)_2$	2.090	2.091(2)	six
O-C(Me)-O	$(inter.)_2$	2.091	2.093(1)	six
O-C(CMe_3)-O	$(inter.)_2$	2.089	2.088(1)	six
O-C(CF_3)-O	$(inter.)_2$	2.090	2.090(1)	six
FHP	$(THF)_1$	2.090	2.092(1)	six
O-S(O_2)-O	$(inter.)_2$	2.112	2.111(1)	seven
(2,6xylyl)N-C(H)-O	$(THF)_2$	2.112	2.113(1)	seven
O-C(CF_3)-O	$(py)_2$	2.126	2.129(2)	seven

There are clearly two sets of curves with different, but both positive, slopes. The solid lines correspond to the $Mo_2(XZY)_4$ compounds lacking axial ligands, and to the $Mo_2(XZY)_4L_2$ molecules with very weakly, if at all, donating CH_2Cl_2 and CH_2Br_2 axial ligands. The dashed curves are for the compounds having one or two more closely bound neutral ligands donating at the metal axial positions. The positive slopes are indicative of the Mo-Mo bond being stretched by steric forces from the electronic separation to the observed distance.

The $\{k_r, r_o\}_{Mo\text{-}Mo}$ solution curves are sufficiently clustered to be classed together as quadruple bonds. This demonstrates the steric origin of the distorting effects on the quadruple bond of axial coordination, which was earlier speculated as perhaps demonstrating weakening of the Mo-Mo bonding.

Also noteworthy, is the fact that (k_r, r_o) for $Mo\text{-}L_{br}$ is independent of the inductive nature of the bridging group.

(d) Steric Deformations

Within a given XZY bridging group, structural accommodation of steric factors occurs mainly along the Mo-Mo bond since all other molecular dimensions are statistically indistinguishable.

The bridging framework, X-Z-Y, as noted before by Boeyens [122, 123], is sterically cohesive and the lowest energy configuration, in the absence of M-M interaction, occurs at an intermetal distance of ca. 2.2 Å. Thus the bridge stretches the Mo-Mo bond toward the 'bite' distance. Obviously, the presence of closely bound axial ligands introduces added steric interactions, which reinforce the effects of the bridging system. Hence, the less positive

slope in the presence of axial donation, and the longer observed Mo-Mo distances.

Incomplete distortion of the Mo-Mo electronic separation to the 'bite' distance is compensated for by the opening of the Mo-Mo-L_{br} angles. In the case of the N^O- and C^O-bridged molecules, the excessive 'bite' is compensated for almost entirely by the more obtuse Mo-Mo-O_{br} angles compared to the near-orthogonal Mo-Mo-$N_{br}(C_{br})$ angles. The larger 'bite' of the sulfate bridge is a contributing factor to the longer observed Mo-Mo separation than in the carboxylato ligands having the same axial intermolecular donation.

It is notable that, without exception, the bonds to the neutral axial ligands are relatively long, indicating that even at their strongest, these bonds are much weaker than those to the equatorial ligands [Mo-O_{ax}(intermolecular) = 2.59 - 2.93 Å; Mo-O_{ax}(THF) = 2.53 - 2.59 Å; Mo-N_{ax} = 2.55 - 2.59 Å; but Mo-O_{br} = 2.10Å and Mo-N_{br} = 2.14 - 2.20 Å]. The remote Mo-X_{ax} (X = CH_2Cl_2, CH_2Br_2) distances of ca. 3.5 Å could be dismissed as mere nonbonded 'packing' contacts.

Supplementary evidence for the steric origin of Mo-Mo lengthening in the presence of axial ligands is seen on comparing the (k_r,r_o) parameters for the Mo-O_{br} [(0.84, 2.07); $(0.90, 2.10)_{sulfate}$] and Mo-O_{ax} bonds [$(0.40, 2.65)_{inter.}$; $(0.60, 2.50)_{THF}$; $(0.50, 2.57)_{sulfate}$]; as well as the Mo-N_{br} [(0.84, 2.10)] and Mo-N_{ax} [(0.80, 2.54)] bonds.

Clearly, for Mo-L_{ax}, k_r is smaller and r_o longer by ca. 0.5 Å, indicative of weaker interaction, too weak to affect the Mo-Mo bonding interaction.
The Mo-X_{ax} (X = Cl, Br) interaction is even weaker as demonstrated by the still smaller k_r and extremely long

r_o values.

In summary, the molecular mechanics results demonstrate the insensitivity of the Mo-Mo electronic interaction to the presence of axial ligands or the nature of the bridging group. The Mo-Mo bond remains quadruple regardless of its environment. This result substantiates the deep potential energy curve found for $Mo_2(O_2CH)_4$, at the SCF level by Benard [105].

Of particular importance is the intersection, or at least overlap region, of the Mo_2-bridged and -unbridged $\{k_r, r_o\}$ solution curves. However, since we have as yet not fully covered all the quadruple compounds, it is best first to discuss the results of calculations of the equally interesting $Mo_2X_4(L\hat{}L)_2$ compounds.

6.2.3 The 'Twisted' $Mo_2X_4(L\hat{}L)_2$ Molecules

(a) Introduction

It is well known that compounds containing a M-M quadruple bond have a preference for an eclipsed rotational conformation about the M-M bond because of the angular dependence of the δ bond. In simple, unbridged compounds of the type $X_4Mo\text{-}MoX_4$, this tendency dominates the repulsive forces between opposed ligand atoms and fully eclipsed structures are observed.

With bidentate phosphine ligands, $R_2P\text{-}C_n\text{-}PR_2$, that span the two metal atoms, the conformational preferences of the resulting M_2-containing rings often favour twist angles about the Mo-Mo bond different from zero. It is therefore necessary to examine and discuss the twist angles that are found in molecules containing Mo-Mo multiple bonds. Minimizing the ring strain in these systems is apparently more important than maximizing δ

overlap in the Mo-Mo bond.

Several structures of these molecules have been crystallographically determine with the presence of disorder in the metal-metal bond. Naturally, these structures are excluded since the Mo-Mo distance is the prime structural parameter of our studies. Crystal structure solutions have revealed the presence of two conformations of the $Mo_2(P-C_n-P)$ ring in certain cases.

An example is the structure of $Mo_2I_4(dppm)_2.2C_7H_8$ studied by Cotton et al [124]. The dimer resides on the crystallographic special position, i. The rotational conformation around the Mo-Mo' bond is strictly eclipsed (+5.7°, -5.7°, +6.2°, -6.2°).
However, another crystal structure determination by Fanwick et al [125], showed two independent sets of molecules in the unit cell both of which possess the structure of the same molecule $Mo_2I_4(dppm)_4$. One molecule which resides on a crystallographic inversion centre is said to have an 'apparent' Mo-Mo distance of 2.178(3) Å and an eclipsed geometry, while the two symmetry related molecules in general positions have a Mo-Mo distance of 2.152 Å and twist angles of 4.9°, 19.7°, 15.6° and 17.2°.

This is an example of where two quite different rotational geometries are present in the solid state for a molecule of this general type. It was stated that "an important implication stemming from this is that crystal packing forces can apparently have a greater effect in determining the rotational geometry than may previously have been supposed" and "intermolecular packing forces can assume a decisive role in stabilizing each one at a different site". This, we feel, is desperation with poorly resolved crystal structures. The fact that identical molecules can reside on both a general and a special position causes immediate suspicion of disorder.

The molecule lying on the special position is most probably a crystallographically averaged electron density of two or more structures, causing virtual i symmetry to be imposed. In this spirit we have only considered molecules residing on general positions.

(b) Force Field Parameters

The bidentate phosphine structures are modelled using the same parameters as for the unidentate phosphines. Additional parameters needed are given in Tables 6.9 and 6.10.

Table 6.9 Details of additional parameters

Bond	k_r (mdyne/Å)	r_o (Å)
C-S	2.50	1.62
P-L_p	6.00	1.00
C≡N	3.00	1.15
Mo-NCS	0.70	2.00
Angle	k_θ (mdyne.Å)	θ_o (rad.)
Mo-P_{br}-C_{br}	0.10	1.911
Mo-N≡C	0.30	3.1416
Mo-Mo-N	0.10	1.571
P-Mo-N	0.10	1.571
P_{br}-C_{br}-P_{br}	0.60	1.911
N≡C-S	0.30	3.1416
C-P-L_p	0.40	1.911
C_{br}-C_{br}-P_{br}	0.60	1.911
P_{br}-C_{br}-P	0.20	1.911
P_{br}-C_{br}-C	0.10	1.911

Table 6.10 Nonbonded parameters

Interaction	a (u)	b ($Å^{-1}$)	c ($u.Å^6$)
P--L_p	898.8	4.24	1.83
P--N	3091.0	4.27	5.12
C--S	2180.0	4.05	5.38
S--P	3991.0	3.90	12.0
N-S	2586.0	4.21	5.79

(c) The Delta Contribution to the Quadruple Bond Strength

Of extreme importance is the magnitude of the torsional parameter needed to model the observed twists around the Mo-Mo centre. From viewing these molecules down the Mo-Mo axis, it is immediately recognized that all four torsional angles are non-zero. If they are not of the same magnitude, as is the case for the P-C_1-P set, they are in the same sense, and thus have the 'concerted' effect of an internal rotation. Each of the torsions results from the combined effect of a true internal rotation and other steric distorsions. The reaction of the δ component to such twists is readily studied by molecular mechanics.

Very interestingly, the triply bonded $Re_2Cl_4(dppm)_4$ and $Re_2Cl_4(dppe)_4$ molecules have totally staggered conformations. Not surprising, then, the envelope-type conformation in $Mo_2(P-C_1-P)$, and the distorted chair arrangement in $Mo_2(P-C_2-P)$, imply the presence of some degree of δ bonding favouring the eclipsed conformation. We therefore expect nonzero $V_{\chi=0°}$ torsional potentials. The values required, together with the calculated and observed χ values, are shown in Table 6.11. The torsions about the Mo-Mo bond are matched to within 2°.

Table 6.11 Torsional data and parameters

$X_4(P\text{-}C_n\text{-}P)_2$	χ (deg.) P-Mo-Mo-P		χ (deg.) X-Mo-Mo-X		$V_{\chi=0°}$ (kcal/mol)
	Obs.	Calc.	Obs.	Calc.	
$I_4(dppm)_2$	4.9 19.7	6 21	15.6 17.2	16 17	10.7/4
$(NCS)_4(dppm)_2$	9 18.7	11 16	12 13.6	10 14	10.7/4
$Cl_4(tdpm)_2$	10.7 27.4	10 26	21 20	19 20	9.9/4
$Br_4(S,S\text{-}dppb)_2$	-22 -23	-20 -21	-20 -21	-20 -20	8.5/4
$Cl_4(S,S\text{-}dppb)_2$	24.8 24.8	-23 -23	21.1 27.5	-20 -26	8.5/4
$I_4(dppe)_2$	26.5 26.5	-28 -26	25.5 -24	-25 -25	7.4/4
$Br_4(dmpe)_2$	36 37	38 37	36 37	36 36	0

The torsional potential values are given as x/4, since x, the total attractive potential, can be compared to the values obtained via driver calculations for the $[Mo_2X_8]^{4-}$ ions (7.5, 11, 11.5 kcal/mol for X = Me, Cl and Br resply.). If a $V_{\chi=0°}$ value greater than those shown is used, the calculated torsion angles are too small; a smaller value results in greater staggering.

The greater the observed twist, the smaller the parameter required to maintain eclipsing. Obviously the δ interaction is diminishing.

In fact, for $Mo_2Br_4(dmpe)_2$, no potential is required i.e. no δ interaction opposes the twist away from eclipsing.

Even though this molecule has the proper number of electrons to form a $\sigma^2\pi^4\delta^2$ quadruple bond, the sterically favoured twist of 36° has resulted in total destruction of the δ component.
This molecule does not have its $\{k_r, r_o\}$ solution curve positioned with the others - it has shifted down to the triply bonded molecules. Notwithstanding the different bond order, $Mo_2Br_4(dmpe)_2$ was modelled with the same bridging framework force field as the other diphosphine complexes. Only $(V_{\chi=0°})_{Mo\text{-}Mo}$ and $\{k_r, r_o\}_{Mo\text{-}Mo}$ are different.

If we take 11.5 kcal/mol as representing the δ contribution to quadruple bonding, then the smallest $V_{\chi=0°}$ value, 7.4 kcal/mol, means 64% of the δ bond is still present. Is this sufficient to stabilize a δ^2 electron configuration?

It should be noted that the dependence of the δ overlap [123] on the angle of internal rotation χ is given by $\cos 2\chi$. Therefore, considerable deviation from perfect eclipsing can occur without loss of δ bonding. Indeed a rotation of 30°, that is, two thirds of the way towards the fully staggered conformation, causes a loss of only half of the δ overlap.

(d) Molecular Mechanics Solution Curves

The answer to the above lies in the position of the $\{k_r, r_o\}_{Mo\text{-}Mo}$ solution curves relative to the other quadruply bonded compounds. The results are shown in Figure 6.5. The calculated Mo-Mo distance is within 0.001 Å of the observed value (Table 6.12).

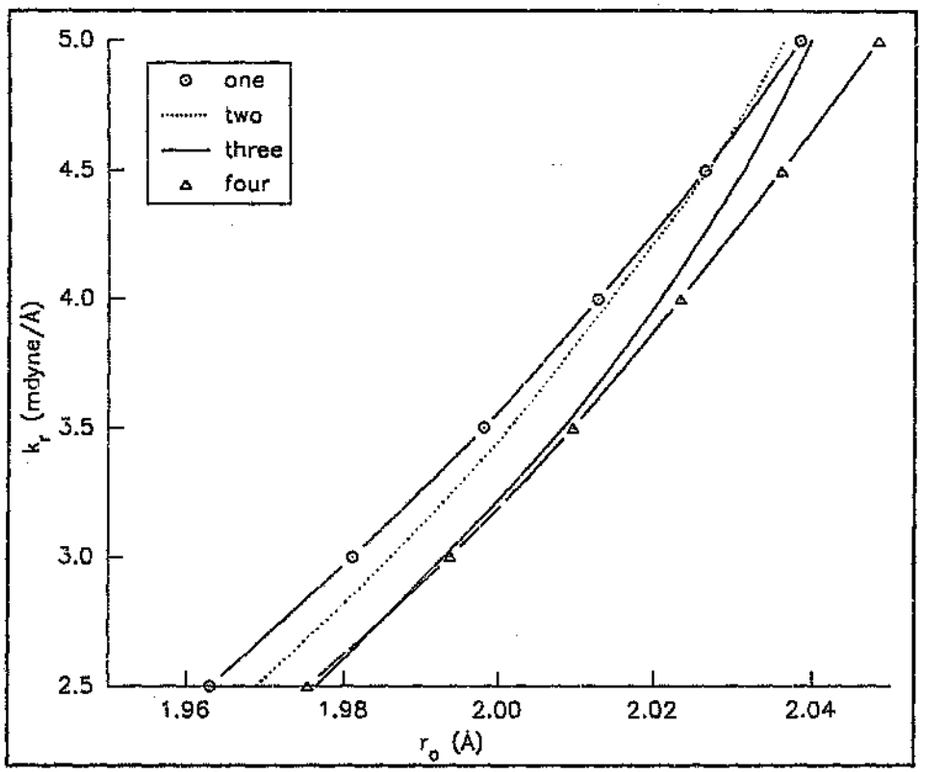


Figure 6.5 Molecular mechanics solution curves $\{k_r, r_o\}_{Mo-Mo}$ for the $Mo_2X_4(P\hat{}P)_2$ compounds.

Table 6.12 Calculated and observed Mo-Mo distances

Molecule	Calc. (Å)	Obs. (Å)	Figure Label
$Mo_2I_4(dppm)_2$	2.150	2.152(2)	two
$Mo_2(NCS)_4(dppm)_2$	2.165	2.167(3)	one
$Mo_2Cl_4(tdpm)_2$	2.150	2.148(1)	two
$Mo_2Br_4(S,S\text{-}dppb)_2$	2.144	2.147(6)	three
$Mo_2Cl_4(S,S\text{-}dppb)_4$	2.144	2.147(3)	three
$Mo_2I_4(dppe)_4$	2.180	2.179(3)	four

The fact that the solution curves are clustered amongst those of the unbridged-Mo_2 set, implies the persistence of the quadruple bond, even with rotations of ca. 25°.

The δ bond still retains much of its strength, and there is no resultant unpairing of the δ electrons.

It is satisfying that the observed differences in χ between analogous Mo and Re dimers can be explained by different bond multiplicities.

$Mo_2I_4(dppm)_4$ and $Mo_2Cl_4(tdpm)_2$ have identical solution curves despite their different $V_{\chi=0°}$ values. This means that regardless of different degrees of δ interaction, both are of the same bond order.

Just as steric forces can cause a certain stretch of the Mo-Mo bond away from r_o and hence decrease the lateral overlap of the δ interaction, so too can a certain degree of rotation occur without total destruction of the δ interaction.

(c) Steric Deformations

It is interesting to discuss how the degree of rotation χ is influenced by the number of atoms in the $R_2P\text{-}(CH_2)_n\text{-}PR_2$ bridge (where n = 1, 2).

These compounds are all formally quadruple. The equilibrium structure therefore depends on the balance struck between the δ bond favouring eclipsing, and the steric forces working against this inherent tendency favouring a staggered arrangement.

(i) The (P-C_1-P) Bridge

The dppm and tdpm ligands, for which n=1, form two envelope-type, five-membered rings including the Mo_2 bond. The torsion angles within each molecule are of different magnitude, but in the same sense. Also, these bridging ligands are not symmetrically coordinated since

one of the two Mo-P distances associated with each Mo is ca. 0.1 Å longer than the other (I: 2.58, 2.54 Å; NCS: 2.62, 2.55 Å; tdpm: 2.65, 2.55 Å). The Mo-Mo-P angles differ by ca. 6° for the dppm species, while those of the tdpm species differ by only 2°.

Since the same force field is applied to the bridging phosphine framework throughout the whole series of complexes (i.e. the electronic factors are constant), the unsymmetrical distorsions in these bonds and angles are a result of internal crowding (i.e. steric and not electronic in nature).

The true internal twist is rather small since the $V_{x=0}$ is decreased by only ca. 10% from that of the $[Mo_2X_8]^{4-}$ ions. The observed torsion angles are a result of a small internal twist with added distortion due to internal crowding. The presence of δ bonding opposes twisting around the Mo-Mo bond, and, fortunately, the energy of the system as a whole is minimized at a small internal rotation accompanied by unsymmetrical distortion of the molecule to relieve the strain, with little loss of δ interaction.

(ii) The (P-C_2-P) Bridge

Very differently, when n=2, a balance between the δ bonding demanding eclipsing and the steric factors favouring staggering is struck at larger twist angles of essentially equal magnitude, with symmetrically distorted Mo-P and Mo-Mo-P parameters. Consequently, the true internal twists are larger, as seen by the lower torsional parameters needed in the calculations.

The steric strain when n=2 can only be alleviated at the expense of 26-36% of the δ interaction. These molecules are not able to overcome steric forces by distorting

unsymmetrically at small internal rotations as was seen for n=1.

(f) General Conclusions

Fruitless attempts by Cotton et al. to obtain an empirical correlation between the observed Mo-Mo distance and cos 2χ are now understandable. Scatter in the data occurs. This is probably due to the incorporation of compounds containing disorder, including the erroneous assumption that the observed bond length will be linearly proportional to the strength of the δ bond. As mentioned earlier, the observed torsion angles differ in the $Mo_2(P-C_1-P)$ rings because each results from the combined effects of a true internal rotation and other steric distorsions. Cotton assumed that these steric distortions will tend to be random, so that averaging the four individual torsional angles will give a meaningful estimate of the true internal twist, χ.

Indeed, there are compounds with small twists having Mo-Mo distances longer than those with larger twists, contrary to Cotton's attempt at directly relating the Mo-Mo distance to the degree of rotation. In fact, the equilibrium structure, including the Mo-Mo distance, is the result of complex interplay of electronic and many nonbonded forces. It is therefore an oversimplification to expect the observed Mo-Mo distance to be a function simply of the δ bond strength.

It is safer only to consider electronic distances without steric complications. The electronic Mo-Mo distance, r_o, is fixed at the quadruple-bond value for twists from 0° to ca. 26°; and reduces to that characteristic of a triple bond for a twist of 36°.

6.2.4 The Unique (k_r, r_o) Couple for Mo-4-Mo

It is very intriguing to consider the combined set of solution curves for the formally quadruple compounds. The overlap region of the $\{k_r, r_o\}_{Mo-Mo}$ solution sets is seen in Figure 6.6. Only the curves needed to define the boundaries of this region are shown; all others obviously occur within the envelopes shown.

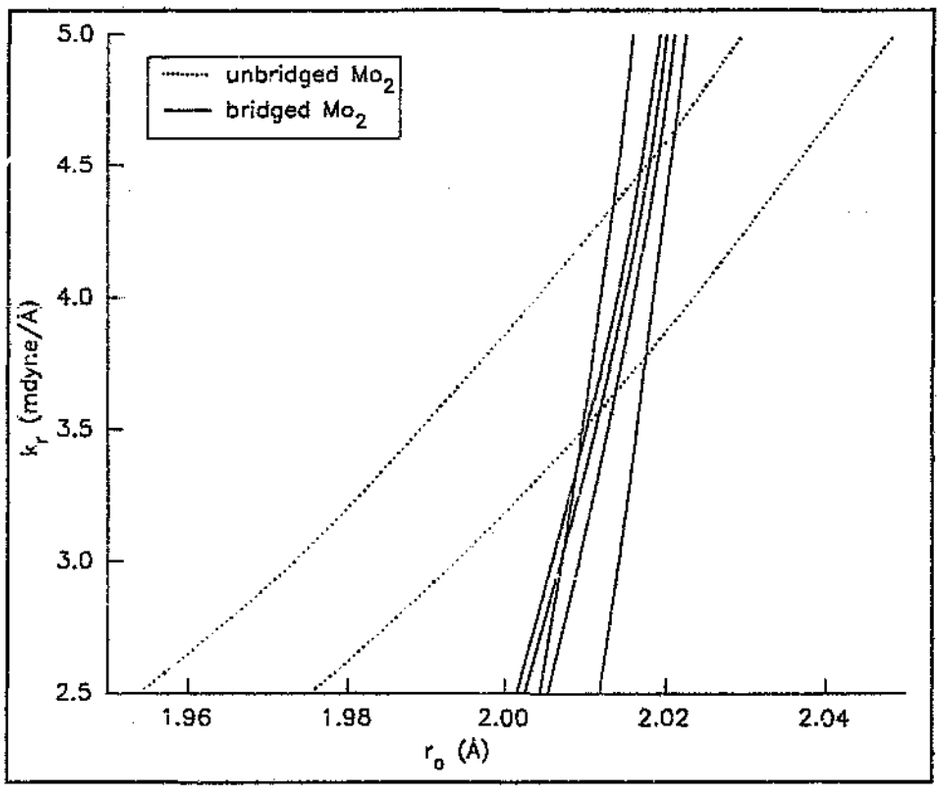


Figure 6.6 Combined molecular mechanics $\{k_r, r_o\}$ solution curves for the set of quadruply bonded Mo_2 compounds.

The narrow overlap region, k_r:4.64 - 3.5 mdyne/Å and r_o:2.02 - 2.01 Å, is very rewarding considering the number of compounds investigated. The average, $(k_r, r_o)_{Mo-Mo}$ = **(4.07 mdyne/Å, 2.02 Å)**, is accepted as the most likely couple, for the quadruple bond.

Thus, for any given bond order between a given pair of metal atoms, there is a range (0.1 Å for Mo-(4)-Mo) of observed internuclear distances , but only one electronic separation, r_o.

4.2.5 Experimental ν_{Mo-Mo} and the Molecular Mechanics 4.07 mdyne/Å.

The molecular mechanics value for k_r(Mo-Mo) is the result of assuming harmonic distortion of the Mo-Mo bond. The values of the harmonic force constant that would yield the experimentally observed frequencies for these quadruple Mo_2 compounds are given in Table 6.13.

Table 6.13 Experimental vibrational frequencies and corresponding diatomic force constants

Compound	ν (cm^{-1})[a]	$k_{diatomic}$ (mdyne/Å)	Ref.
$Mo_2(O_2CCF_3)_4$	398	4.45	127
$Mo_2(O_2CH)_4$	403	4.59	29
$Mo_2(O_2CCH_3)_4$	404	4.61	128
$Mo_2(O_2CCF_3)_4(py)_2$	368	3.83	127
$[Mo_2(SO_4)_4]^{4-}$	371	3.89	52
$Mo_2(MHP)_4$	425	5.11	129
$Mo_2(CH_2)_4$	405	4.64	129
$Mo_2(FHP)_4(THF)_1$	430[b]	5.23	39
$[Mo_2Cl_8]^{4-}$	350	3.46	130
$[Mo_2Br_8]^{4-}$	335	3.17	130
$[Mo_2Me_8]^{4-}$	336[c]	3.19	131
$Mo_2Cl_4(PMe_3)_4$	355	3.56	20
$Mo_2Br_4(PMe_3)_4$	352	3.50	20
$Mo_2I_4(PMe_3)_4$	43	3.33	20

a :solid-state Raman spectroscopy
b :solution study by infra-red spectroscopy
c :solution study by Raman spectroscopy

The ν_{Mo-Mo} values vary over a considerable range of 95 cm^{-1}, even though they are all of the quadruple order.

Raman spectroscopy supports a previously held view that the Mo-Mo bond is stronger in the $Mo_2(XZY)_4$ species where the ν_{Mo-Mo} frequencies are about 400(30) cm^{-1} as compared with about 345(10) cm^{-1} for the $[Mo_2X_8]^{4-}$ set and 371 cm^{-1} for the sulfate.

With respect to the evaluation of force constants there are the difficulties that frequency data can rarely be corrected for anharmonicity, and that they rarely refer to isolated modes of vibration. It is therefore problematic to calculate force constants from observed frequencies.

Except in the case of gaseous diatoms, M-M bonds are embedded in a polyatomic matrix and coupling with motions of neighbouring atoms must be considered in analyzing the vibrational spectrum. For most compounds of interest, the modes which mix substantially with M-M stretching may be characterized as M-ligand stretching and M-ligand deformation. Mixing is generally slight if the frequencies of these modes are far from the M-M frequencies or if the ligand atoms are much lighter than the metal atoms. As the frequencies approach one another, and as the ligand masses become comparable to the metal masses, the modes become strongly coupled, to the point where it may be misleading to speak of M-M frequencies at all, except as a crude approximation.

The amount by which these so-called ν_{Mo-Mo} modes are essentially limited to vibration of the Mo-Mo bond is somewhat uncertain and may well vary from case to case. Complete normal coordinate calculations from which a reliable potential energy distribution matrix (U matrix) could be derived would be informative, but the amount of

experimental and computational work required for this is formidable, and only very incomplete normal coordinate analyses have been published.

Although it is typical to denote the quadruple bond with the notation $\sigma^2\pi^4\delta^2$ this is an oversimplification. In the $[Mo_2X_8]^{4-}$ ions the M-M bonding comes close to the ideal qualitative picture, but the orbital characters become more complicated in other cases. In the carboxylato compounds, the Mo-Mo σ bonding is provided by two MO's. This is in contrast to $[Mo_2Cl_8]^{4-}$ where the highest filled a_{1g} orbital, with 83% metal character, is mainly responsible. So, in many cases the Mo-Mo bonding interactions are distributed over more than one MO of the appropriate symmetry - a more complex orbital mixing pattern emerges.

Ketteringham et al [132] concluded that the Mo-Mo stretch contains about 15% contribution from the $O_4M\text{-}MO_4$ deformation, whereas Cotton and coworkers assigned the Raman feature at 404 cm^{-1} as the symmetric Mo-Mo stretch, with no significant contribution from other stretching or bending modes. In the case of $Mo_2(O_2CCH_3)_4$ there is direct experimental evidence showing that the strong Raman band at 404 cm^{-1} is due to a motion that is virtually pure Mo-Mo stretching [128]. On comparing the Raman spectrum of the acetate having the natural distribution of Mo isotopes (effectively ^{96}Mo) with that of a sample containing 97.4% ^{92}Mo, a shift of 9±1 cm^{-1} was found, which agrees well with the value of 8.7 cm^{-1} calculated for a completely isolated Mo-Mo vibration.

Of course, this result cannot be considered general, since here the Mo-Mo-O_{br} angles are very close to 90° and the O atoms are very much lighter than the Mo atoms.

In $[Mo_2Cl_8]^{4-}$, the Mo-Mo-Cl angles are about 103° and the

ligand atoms heavier, both of which could lead to more coupling between the ν_{Mo-Mo}, ν_{Mo-Cl} and $\delta_{Mo-Mo-Cl}$ totally symmetric modes.
Since the Mo-Mo-X angles in the $Mo_2X_4(PMe_3)_4$ species are also significantly > 90° the diatomic approximation for extracting the Mo-Mo force constant is inaccurate for two reasons:

* the effective reduced mass of the Mo-Mo system changes because of contributions from the ligand masses and,
* G-matrix mixing of the M-M and M-X coordinates becomes appreciable.

Thus comparisons of simple diatomic force constants, from observed frequencies, among complexes containing different ligand sets, must be viewed with caution in seeking meaningful information regarding the relative M-M bonding in these systems.

Metal isotope shifts in the Raman spectrum of $[Mo_2(SO_4)_4]^{4-}$ also demonstrate a rather 'pure' Mo-Mo stretch for this compound, yet it has a lower observed ν_{Mo-Mo} frequency than the $Mo_2(O_2CCH_3)_4$ species.

The possibility of anharmonic deformation of the Mo-Mo bond as opposed to harmonic displacement, cannot be discounted.

In resonance Raman spectroscopy, the measured values of so many overtones of the ν_{Mo-Mo} mode allow an accurate assessment of the anharmonicity constant and this, in turn, can give us some idea of the validity of our molecular mechanics harmonic potential for bond deformation. To the extent that some ν_{Mo-Mo} is mixed in with ν_{Mo-L} and $\nu_{Mo-Mo-L}$, the latter may also experience some resonance enhancement.

The resonance Raman spectra of $[Mo_2X_8]^{4-}$ (X = Cl, Br), and $Mo_2Br_4(PMe_3)_4$, suggest that the Mo-Mo stretching fundamental is very close to being harmonic in these complexes. However, other progressions arising from the M-X stretching fundamental are seen; an outcome of mixing of different modes.

The existence of harmonic stretching of the Mo-Mo mode in these molecules, validates the use of harmonic potentials in the molecular mechanics force field.

Experimental force constants are molecule-specific quantities and therefore dependent on the environment of the respective molecules. The difference in observed frequencies is not due to a real difference in force constant for the Mo-Mo bond, but simply a consequence of coupling of the Mo-Mo stretch to Mo-ligand displacement coordinates. In most cases the mode responsible for the observed band is only roughly approximated by the description 'Mo-Mo stretching', though it undoubtedly incorporates a substantial proportion of the Mo-Mo symmetry coordinate. Possible anharmonic deformation of the Mo-Mo bond is an added complication.

The force constants obtained for Mo-Mo quadruple bonds in the normal coordinate analyses [131, 132] range over 3 - 5 mdyne/Å; the mean value being that obtained by molecular mechanics.

Perhaps it is best to consider the average diatomic k_r(Mo-Mo) calculated from these observed frequencies, namely 4.04 mdyne/Å. Very surprisingly, this is the exact value obtained by molecular mechanics inspection of these quadruple compounds.

6.3 Molecular Mechanics Calculations on the Mo-Mo Bond of Order 3.5.

6.3.1 Introduction

To improve our understanding of the bonding in dimolybdenum compounds, several attempts have been made to study the monopositive ions that can be derived from them and to compare the parent molecules and the daughter ions.

The $[Mo_2(SO_4)_4]^{3-}$ and $[Mo_2(DMF)_4]^{+}$ ions have structures very similar to that of their parents. The 3- ion is paramagnetic and e.s.r. spectra show that the unpaired electron is evenly distributed over two magnetically equivalent Mo atoms. The use of the same force field parameters for each $Mo^{2.5+}$ atom in these $\sigma^2\pi^4\delta^1$ compounds is in accord with the unpaired electron being evenly distributed between the two Mo nuclei. The parent molecules have authentic quadruple Mo_2 centres. Loss of one electron from these quadruple compounds means we are certainly dealing with Mo_2 centres of order 3.5.

As discussed in Chapter 2, there are quantitative changes on going from the parent molecules to the daughters. The Mo-Mo bond lengthens and the Mo-L distances shorten. The former is due to the lower bond order; the latter a result of the increased formal charge on the Mo atom.

6.3.2 Force Field Parameters

The bridging framework is modelled using the same parameters as for the quadruply bonded compounds. The only additional information pertains to the Mo-L_{ax}, Mo-L_{br} and Mo-Mo bonds. This is given in Tables 6.14 - 6.15.

Coulombic interactions are not necessary, and the lack of a torsional parameter for rotation about the Mo-Mo bond is expected on the basis of the previous explanations given for the quadruple compounds. The H positions were located in the crystal structure of the sulfate, and the axial water molecules have a tetrahedral arrangement about O.

Table 6.14 Force field parameters specific to $Mo^{2.5+}$

Bond	k_r (mdyne/Å)	r_o (Å)
$Mo-N_{br}$	0.84	2.08
$Mo-O_{br}$	0.90	2.05
$Mo-O_{ax}$	0.80	2.53
$Mo-Cl_{ax}$	0.50	2.86
$Mo-Br_{ax}$	0.50	2.90
O-H	5.00	0.96
Angle	**k_θ (mdyne.Å)**	**θ_o (rad.)**
H-O-H	0.40	1.911
$H-O-L_p$	0.40	1.911
$Mo-O_{ax}-H(L_p)$	0.40	1.911

Table 6.15 Nonbonded parameters

Interaction	a (u)	b ($Å^{-1}$)	c ($u.Å^6$)
Cl--S	2706.2	3.80	15.4
Br--S	950.4	3.27	22.1

As can be seen the $(Mo-O_{br})^{+2.5}$ and $(Mo-N_{br})^{+2.5}$ have shorter r_o values than the corresponding Mo^{+2} bonds, in accord with the smaller intrinsic size of the higher charged ion. Again, the $Mo-L_{ax}$ r_o values are long compared to the equatorial Mo-L bonds, implying weak

axial donation.

6.3.3 $\{k_r, r_o\}$ Solution Curves for the Mo_2 Centre

The force field for these compounds is well established from the quadruple set, and generation of the $\{k_r, r_o\}_{Mo-Mo}$ solution curves proceeded rather swiftly.

The solution curves for the Mo-Mo interaction are shown in Figure 6.7. Once again the Mo-Mo bond distance was reproduced to within 0.001 Å as seen in Table 6.16.

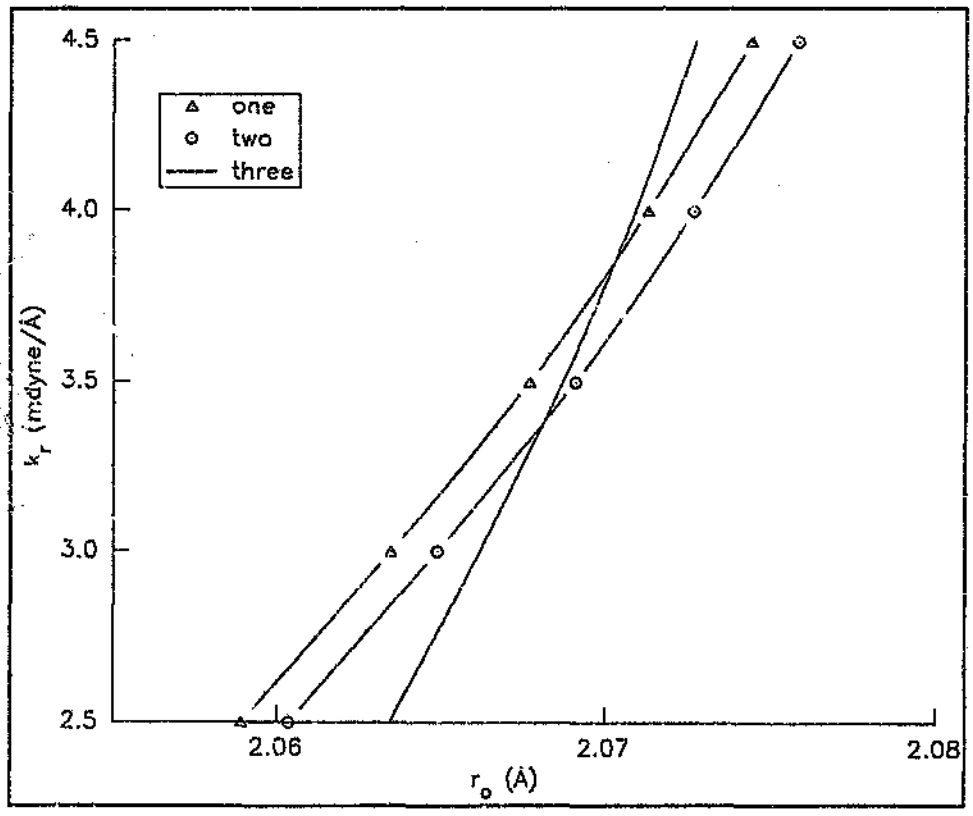


Figure 6.7 Molecular mechanics solution curves $\{k_r, r_o\}$ for the Mo-Mo bond of order 3.5.

Table 6.16 Calculated and observed Mo-Mo distances

Molecule	$(L_{ax})_2$	Calc. (Å)	Obs. (Å)	Figure Label
$[Mo_2(DMF)_4]^+$	-	2.120	2.122(3)	three
$[Mo_2(SO_4)_4]^{3-}$	H_2O (isolated)	2.166	2.167(1)	two
$[Mo_2(SO_4)_4]^{3-}$	H_2O (chains)	2.162	2.162(1)	one
$[Mo_2(SO_4)_4]^{3-}$	Cl (chains)	2.166	2.167(2)	two
$[Mo_2(SO_4)_4]^{3-}$	Br (chains)	2.166	2.169(3)	two

The crystal structure of $[Mo_2(SO_4)_4(H_2O)_2]^{3-}$, reveals the presence of two crystallographically independent molecules. Each is approached by the O atom of a water molecule approximately along the extended Mo-Mo axis, but only at a considerable distance (2.55 Å). The nonequivalence results from differences in the packing. One molecule packs as isolated units with one water molecule attached to each Mo atom, whereas the other molecule forms an infinite chain of ions linked together by water bridges. The same (k_r, r_o) value models the $Mo-O_{ax}$ bonding, but the molecules have different solution curves.

6.3.4 Discussion

In $[Mo_2(SO_4)_4X]^{4-}$ (X = Cl, Br) there are infinite chains of the type (-Mo-Mo···X··Mo-Mo-), with very long axial bonds: 2.881(1) Å for Mo··Cl and 2.926(1) Å for Mo··Br. The Mo-Mo distance is the same within experimental error, and so it is not surprising that their molecular mechanics solution curves coincide. In fact, the isolated

sulfate molecule has an identical Mo-Mo separation and the same solution curve.

The slopes of the solution curves are all positive indicative of the Mo-Mo bond being stretched, as was the case in the corresponding quadruple Mo_2 compounds. The slope of the solution curve for the $[Mo_2(DMF)_4]^+$ molecule is steeper than the sulfate molecules having axial ligands. This is the result of the axial ligands reinforcing the stretching of the Mo-Mo bond by the bridging group to the 'bite' distance.

The observed Mo-Mo distance is longer in the sulfate compounds than the DMF molecule because of the larger 'bite' of the sulfate ligand and the presence of axial ligands.

How the Mo-Mo electronic separation changes upon oxidizing a Mo_2^{4+} complex to a Mo_2^{5+} complex is quite interesting. The difference in electron population is expected to occur in the δ orbital. The role of the δ component of the quadruple bond in contributing to the extraordinary shortness of such bonds can therefore be assessed by observing the change in r_o(Mo-Mo) when the bond order changes from 4.0 to 3.5. Several attempts have been made to assign a value to the change upon loss of half of the δ bond, but all considered the observed Mo-Mo distances.

No one point of intersection occurs. However, the solution curves are closely packed together to be considered of the same order. The narrow overlap region permits the assumption that the average value, $(k_r, r_o)_{Mo-Mo}$ = (3.63 mdyne/Å, 2.07 Å), is characteristic of a Mo-Mo bond of order 3.5.

Loss of half of the δ^2 component to quadruple bonding

results in a 0.05 Å lengthening of the electronic Mo-Mo distance.

As was the result for the quadruple Mo-Mo bond, neither the inductive nature of the bridging group nor the presence of axial ligation alters the Mo-Mo bonding.

6.3.5 Experimental ν_{Mo-Mo} and the Molecular Mechanics 3.63 mdyne/Å.

The weakening of the Mo-Mo bond should manifest itself in other ways besides the increase in Mo Mo bond length. One of the more obvious additional effects of lowering the bond strength should be a decrease in the force constant of the Mo-Mo bond and this might be expected to reveal itself in the Raman spectra.

Solid-state Raman spectra have been recorded for the sulfate compounds [52, 53, 133].
For $[Mo_2(SO_4)_4(H_2O)_2]^{3-}$, the greater number of bands observed adds to the complexity of the spectrum. However, much of this complexity may be rationalized if most bands are considered to be split into two compounds. A straightforward interpretation of this splitting is possible by relating it to the existence of the two crystallographically distinct species in the solid of this substance. The Mo-Mo vibration is observed as a single Raman band at 371 cm^{-1} for Mo_2^{4+} and as a doublet at 373 cm^{-1} and 386 cm^{-1} in the spectrum of Mo_2^{5+}. The Mo-Mo vibration frequency is higher in the Mo_2^{5+} sulfate. A lower bond order would imply a lowering of the Mo-Mo frequency. Obviously the coupling of modes and anharmonic effects must be the cause of this discrepancy. Coupling between one sulfate ion and the next is also possible in the sulfates linked by common axial ligation.

Both $[Mo_2(SO_4)_4X]^{4-}$ ions display sharp, strong Raman bands

at essentially the same frequency, 370(1) cm^{-1}.
Metal isotope studies for X=Cl were done, to determine how much the modes ordinarily described as ν_{Mo-Mo} may in fact deviate from that character as a result of mixing with other a_{1g} modes. The observed shift in the Mo-Mo frequency, upon isotopic substitution, is equal to the calculated shift for pure Mo-Mo stretching (uncoupled with any other internal modes). This implies little mixing of other modes with the Mo-Mo stretch. The Mo_2^{4+} sulfate was also found to have a relatively 'pure' Mo-Mo frequency from isotopic studies. It was concluded that "in both $[Mo_2(SO_4)_4]^{n-}$ species, the Raman band at ca. 370 cm^{-1} is a virtually pure ν_{Mo-Mo} mode and that the explanation for the negligible difference from one of these species to the other is that very small variations in the dynamics of the two vibrating systems could easily obscure the inherent differences". This in itself tells us that the observed Mo-Mo frequencies are not a direct measure of the strength of the bond.

The average of the three frequencies, 377 cm^{-1}, gives a k_r(Mo-Mo) of 4.00 mdyne/Å, of the same order, but significantly higher than the derived value of 3.63 mdyne/Å.

One must also be aware that there is some uncertainty as to the assignment of the observed bands in the Raman spectra. In most cases it is simply assumed that the most intense band be assigned to the Mo-Mo stretching frequency.

6.4 The Triply-bonded Mo_2 Centre

Each of the structurally different Mo≡Mo compounds will be discussed separately.

6.4.1 The Mo_2L_6 Compounds

The simplest of complexes containing the $\sigma^2\pi^4$ Mo≡Mo bonding configuration are the unbridged, ethane-like, d^3-d^3 dinuclear compounds of Mo. The existence of these unbridged $X_3Mo{\equiv}MoX_3$ compounds emphasizes the importance of M-M bonding.

(a) Force Field Parameters

The essential trigonal symmetry on each end of the molecules (Mo-Mo-L= 98.3°-107.2°; L-Mo-L= 111°-121°) demands the geometry of each MoL_3 unit to be trigonal planar in the molecular mechanics force field.

In the $(Mo{\equiv}Mo)^{6+}$ compounds, either one or both of the in-plane Mo atomic orbitals ($d_{x^2-y^2}$, d_{xy}) are available for RN-to-Mo and RO-to-Mo π bond formation. Structural parameters suggest the presence of such an interaction. The Mo-NC_2 moieties are planar and deviate little from the Mo-Mo-N planes. Also, the methylene carbons of the neopentoxy groups deviate little from the Mo-Mo-O planes. Both these structural observations require the influence of an electronic element in the force field. Steric factors alone does not allow for a match of the calculated and observed structures.

The planar N in NMe_2, and planar O in OCH_2CMe_3, are modelled by trigonal planar (sp^2) geometries. All other atoms adopt the well-known tetrahedral arrangement.

Force field parameters not already defined, are given in

Table 6.17.

Table 6.17 Force field parameters for bond and angle deformations

Bond	k_r (mdyne/Å)	r_o (Å)
Mo-(1.6)-O	0.84	1.85
Mo-(1.6)-N	0.84	1.96
Mo=N	0.84	1.90
Mo-Cl	0.70	2.34
Mo-C	2.00	2.13
C-O	3.00	1.42
Angle	k_θ (mdyne.Å)	θ_o (rad.)
Mo-Mo-L	0.20	1.571
L-Mo-L	0.10	2.094
C-O-L_p	0.40	2.094
C-C-O	0.10	1.911
O-C-H	0.65	1.911
C-N-C	0.10	2.094
N-C-H	0.65	1.911
Mo-O-L_p	0.40	2.094
Mo-O-C	0.20	2.094
Mo-N-C	0.20	2.094
Mo-C-H	0.10	1.911
Mo-N-C	0.20	2.094
Mo-C-C	0.10	1.911

The Mo-L bonds have been modelled with the same force constants as in quadruple and 3.5 Mo_2, but now the r_o

values are shorter as a result of the increased oxidation state of the Mo atom to +3.

The qualitative proposal of the different modes of Mo-N bonding in the $Mo_2(NMe_2)_6$ and $Mo_2L_2(NMe_2)_4$ molecules (Chapter 2) is confirmed not only by the required modelling of trigonal planar geometries about N and O, but also by the different $(k_r, r_o)_{Mo-N}$ values needed to match the observed Mo-N bond distance in each molecule (Table 6.17). This bonding scheme probably extends to the Mo-O bonding in $Mo_2(OCH_2CMe_3)_6$.

The presence of multiple Mo-N and Mo-O bonding is also confirmed by the need for restriction of the angular movement (δ) of one of the Me groups from the plane of the remaining Mo-N-C unit in $MoNMe_2$; and of the lone pair from the plane of the Mo-O-C unit in $Mo_2(OCH_2CMe_3)_6$.

For $\sigma^2\pi^4$, the Mo-Mo triple bond is cylindrical and does not exhibit a preference for staggered or eclipsed geometries with respect to each end of the molecule. The observed conformations are determined by ligand interactions across the Mo-Mo bond. The staggered conformation is therefore the favoured arrangement. The three repulsive torsional potentials, $V_{\chi=60°}$, for rotation about the Mo-Mo bond is 0.0049 kcal/mol.

(b) Steric Accommodation of the Electronically Demanded Structure

All these molecules exhibit a 'propeller' arrangement of the $Mo-NC_2$ and $Mo-O(C)(L_p)$ planes about each $Mo(NMe_2)_3$ or $MoX(NMe_2)_2$ group, and $Mo(OCH_2CMe_3)_3$ group, respectively. This arrangement is clearly demanded by the electronic interaction between Mo and N/O, as seen by the force field parameters.

The orientations of each planar $MoNC_2$ unit leads to a proximal and a distal Me group with respect to the Mo≡Mo bond. This obviously introduces steric crowding within the molecule. The steric interaction between the planar NC_2 units, or between the planar NC_2 unit and Cl, Me or Et ligand, on adjacent Mo atoms, is minimized by the bending away of the NC_2 group(s), as recognized by the distortion of the Mo-N-C angles. The $(Mo\text{-}N\text{-}C)_{proximal}$ angles open to ca. 132°, while the $(Mo\text{-}N\text{-}C)_{distal}$ angles close to ca. 115°. Obviously the opening of the Mo-Mo-N and/or Mo-Mo-X (X=Cl, Me, Et) angles also alleviates the steric strain.

In the $Mo_2(OCH_2CMe_3)_6$ molecule, four of the methylene carbons are distal and two are proximal with respect to the Mo≡Mo bond. Also, the proximal carbon on one Mo atom is adjacent to the distal carbons on the other Mo. This obviously allows for minimum steric congestion. Steric repulsion causes the $[Mo\text{-}O\text{-}C(L_p)]_{proximal}$ angles to open to ca. 134° and the $[Mo\text{-}O\text{-}C(L_p)]_{distal}$ to close to 115°; and the Mo-Mo-C angles open up too, however, more so for the C with a distal Me group.

All of the equilibrium structures achieve a minimum strain energy at essentially the same Mo-Mo separation. Slight differences in internal steric congestion amongst these molecules is compensated for by other distortions.

Steric factors impede rotation about the Mo≡Mo bond, leading to the isolation of either anti- or gauche-rotamers. All structures, except $Mo_2Et_2(NMe_2)_4$, adopt the anti-conformation.
The steric bulkiness of the Et groups favour the gauche rotamer, with little effect on the distances and angles associated with the $Mo_2N_4C_2$ skeleton. The methyl groups of the Et ligands are distal from the Mo≡Mo bond, minimizing steric crowding within the molecule.

In short, steric congestion is successfully minimized within the electronically favoured arrangement of the NC_2 and OCH_2CMe_3 units.

The influence of packing forces in the crystal on the equilibrium structure, believed by some [55], is clearly refuted by matching the observed arrangement with an intramolecular molecular mechanics force field.

6.4.2 The $[Mo_2(HPO_4)_4]^{2-}$ Ion

The structure of the $[Mo_2(HPO_4)_4]^{2-}$ ions is reminiscent of that found for the $[Mo_2(SO_4)_4]^{n-}$ (n = 4, 3) ions of order 4 and 3.5, respectively, but there are significant differences in detail. The Mo-Mo bond has lengthened and the Mo-O_{br} distances have shortened, a consequence of the lower bond order and higher oxidation state of the Mo atom, respectively.

(a) Force Field Parameters

Because of the structural similarity to the sulfates, the force field used is much the same, except for the Mo-O_{br} bond and the presence of a P atom instead of sulfur.

The $[Mo_2(HPO_4)_4]^{2-}$ ion has the familiar paddle-wheel structure. There are axial ligands, but these are loosely bonded with terminal Mo-OH_2 distances of 2.46(1) and 2.53(1) Å, and infinite chains of Mo-Cl distances of 2.910(1) Å. The insensitivity of the Mo_2 bond to the ligand environment is expected to persist in these triple compounds. The geometry modelled about the Mo atom is again octahedral.
The hydrogen positions were not given in the structural data. The water molecule can have orientations consistent with either a planar (sp^2) or a tetrahedral (sp^3) fragment, donating either two or one lone pairs into

antibonding Mo orbitals. Hence, both geometries are modelled for the axial water molecule.

Additional force field parameters are given in Tables 6.18 - 6.19.

Table 6.18 Force field parameters specific to $[Mo_2(HPO_4)_4(L_{ax})_2]$ (L_{ax} = H_2O, Cl)

Bond	k_r (mdyne/Å)	r_o (Å)
Mo-O_{br}	0.90	2.00
Mo-O_{ax}	0.80	2.45
Mo-Cl_{ax}	0.50	2.86
P-O	3.50	1.52
P=O	3.50	1.46
Angle	**k_θ (mdyne.Å)**	**θ_o (rad.)**
H-O-H	0.40	2.094
P-O_{br}-I_{lp}	0.40	1.911
O_{br}-P-O_{br}	1.50	1.911
O_{br}-P-O	1.00	1.911
O-P=O	0.80	1.911
P-O-H	0.40	1.911
Mo-O_{br}-P	0.20	1.911
Mo-O_{ax}-H	0.40	2.094

The bond deformation parameters for the axial ligands once again demonstrate their weak donor properties.

Table 6.19 Nonbonded parameters

Interaction	a (u)	b ($Å^{-1}$)	c (u.$Å^6$)
P--O	3507.0	4.27	5.19

The Mo-O_{br} bond has the same force constant as the Mo_2 units of order 4.0 and 3.5, but the r_o distance is shorter. In fact, the r_o value decreases from 2.10 Å for Mo^{+2}, to 2.05 Å for $Mo^{+2.5}$, and finally to 2.00 Å for Mo^{+3}. The direction of change is in perfect accord with the decreased intrinsic size of the Mo^{n+} ion as n increases.

The same (k_r, r_o) value for the Mo-O_{ax} bond is used for the tetrahedral and planar geometries. In fact, both geometries have identical $\{k_r, r_o\}_{Mo\text{-}Mo}$ solution curves, illustrating the insensitivity of the Mo_2 unit to the extent of axial donation.

There is no barrier to internal rotation about a triple Mo-Mo bond. Consequently, a staggered conformation ($\chi = 45°$) would be favoured. The four repulsive torsional potentials used, $V_{\chi=45°}$, have a value of 0.0033 kcal/mol. However, the observed conformation is eclipsed. This is purely a steric preference of the four bulky bridging ligands bound to the central Mo_2 unit.

6.4.3 The $Mo_2(O_2CCH_3)_4(CH_2Bu^t)_2$ Molecule

This molecule retains the $Mo_2(O_2CMe)_4$ core supplemented by two mononegative neopentyl ligands, one bonded to each Mo along the Mo-Mo axis.
The Mo-C_{ax} distances, which fall in the range 2.17-2.21Å, are typical of those seen for alkyl ligands bonded to $(Mo{\equiv}Mo)^{6+}$ centres.

(a) Force Field Parameters

The carboxylato framework has the same force field used previously. Additional force field parameters are given in Table 6.20.

Table 6.20 Additional force field parameters

Bond	k_r (mdyne/Å)	r_o (Å)
Mo-O_{br}	0.95	2.05
Mo-C_{ax}	2.00	2.13
Angle	k_θ (mdyne.Å)	θ_o (rad.)
Mo-C_{ax}-H	0.40	1.911
Mo-C_{ax}-C	0.20	1.911

The (k_r, r_o) for the M-C_{ax} bond is identical to that used to model the Mo-C bond in the $Mo_2R_2(NMe_2)_4$ molecules. The axial bonding here is therefore of a different nature from that encountered previously. A typically strong Mo-C interaction is present.

It has been suggested [61] that this molecule has a $\pi^4\delta^2$ valence electron configuration. The lack of a formal Mo-Mo σ component to the triple bond is believed to result from the formal cancellation of the Mo-Mo σ and σ^* bonding components. Unfortunately, the molecular mechanics calculations cannot reinforce nor refute this idea, since the eclipsed conformation persists despite the presence or absence of an electronic contribution to this arrangement. If a torsional potential were demanded in the quadruple carboxylato compounds to render the eclipsed conformation energetically favoured, the presence of such an electronic element in the triply bonded carboxylate would have substantiated the $\pi^4\delta^2$ configuration.

Whatever the electronic configuration, the $Mo_2(O_2CCH_3)_4(CH_2Bu^t)_2$ molecule has a triple Mo-Mo bond. We have already seen that assignment of the bonding to specific orbitals is an oversimplification, anyway.

6.4.4 The $\{k_r, r_o\}_{Mo-Mo}$ Solution Curves

As before, the Mo-Mo distances match the observed values to within 0.001 Å. Certain crystals contain two independent molecules virtually identical in structure. The two $Mo_2(NMe_2)_6$ molecules have identical solution curves. Unnecessary calculation was avoided by matching the calculated structure to the average Mo-Mo distance for $Mo_2Cl_2(NMe_2)_4$.

The $\{k_r, r_o\}_{Mo-Mo}$ solution curves for these formally triple-bond compounds is seen in Figure 6.8. The compounds corresponding to the solution curves are listed in Table 6.21.

Table 6.21 Calculated and observed Mo-Mo distances

Molecule	$(L_{ax})_2$	Calc. (Å)	Obs. (Å)	Figure Label
$Mo_2(NMe_2)_6$	-	2.214 2.218	2.211(2) 2.217(2)	two
$Mo_2(OCH_2CMe_3)_6$	-	2.219	2.222(2)	two
$Mo_2Cl_2(NMe_2)_4$	-	2.200	2.201(2)	one
$Mo_2Me_2(NMe_2)_4$	-	2.200	2.201(1)	one
$Mo_2Et_2(NMe_2)_4$	-	2.201	2.203(1)	one
$[Mo_2(HPO_4)_4]^{2-}$	H_2O	2.226	2.223(2)	four
$[Mo_2(HPO_4)_4]^{2-}$	Cl	2.230	2.232(1)	four
$Mo_2(O_2CMe)_4$	CH_2Bu^t	2.130	2.1302(6)	three
$Mo_2Br_4(dmpe)_2$	-	2.169	2.169(2)	-

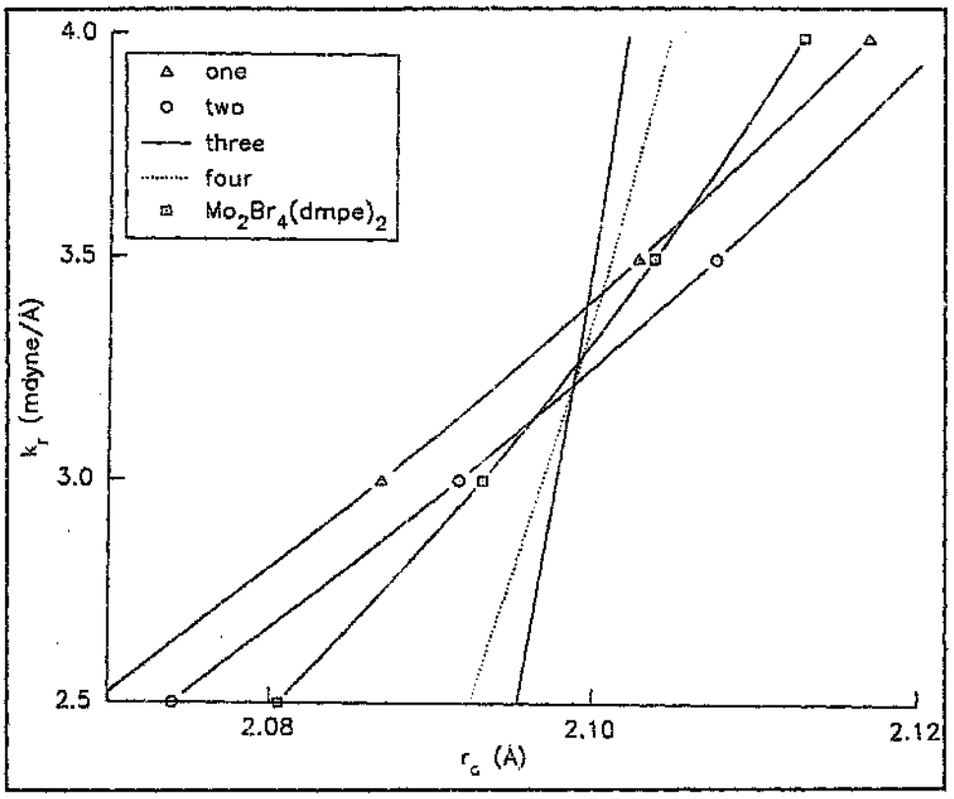


Figure 6.8 Molecular mechanics solution curves $\{k_r, r_o\}$ for the triply bonded Mo_2^{6+} centre.

Recall that the formally quadruple $Mo_2Br_4(dmpe)_2$, has a rotational twist about the Mo-Mo bond of 36°, which totally destroys the δ^2 component of the bond, as evidenced by the absence of an electronic contribution to the observed conformation. This molecule has a $\{k_r, r_o\}_{Mo-Mo}$ solution curve shifted down to r_o values characteristic of the triple Mo_2 molecules.

The positioning of the solution curves is similar to that for the quadruple compounds, with the bridged species shifted down to longer r_o values for smaller k_r with steeper curves. Again, compounds with similar Mo-Mo distances have coinciding solution curves.

Since the curves are clustered together, separate from

the higher bond orders, we may assume them to be of the same order.

The average $(k_r, r_o)_{Mo-Mo}$ = (3.37 mdyne/Å, 2.10 Å) of the overlap region is the most likely couple for the Mo-Mo triple bond.

The complete destruction of the δ^2 component results in a lengthening of the intrinsic Mo-Mo distance from 2.02 to 2.10 Å i.e. 0.08 Å/δ^2.

6.4.5 Experimental ν_{Mo-Mo} and the k_r(Mo-3-Mo) of 3.37 mdyne/Å.

The vibrational spectra of the Mo_2L_6 molecules are not subject to any simple, 'first-order' assignments. The Mo-Mo stretching mode appears to be extensively coupled to other internal coordinates, such as Mo-N(O) stretching or M-NC_2 rocking modes, thus precluding any simple assignment.

It is particularly interesting that these molecules do not show strong Raman bands which can be simply assigned to ν_{Mo-Mo}, since inorganic chemists have become accustomed to thinking that compounds with M-M bonds, especially those with multiple bonds, characteristically show easily recognizable Raman active bands assignable to M-M stretching frequencies. This reminds us of the care needed in empirically relating the observed frequencies to bond order.

However, the strongest feature in each solid-state Raman spectrum of the $[Mo_2(HPO_4)_4]^{2-}$ ions [134], is a line at 358 cm^{-1} for L_{ax} = H_2O, and a line at 361 cm^{-1} for L_{ax} = Cl. These are assigned to ν_{Mo-Mo} by analogy to the previously reported Mo-Mo stretching frequency of ca. 371 cm^{-1} for the sulfates. The Mo-Mo frequency for the phosphate

compounds is clearly lower than the previous values seen, in accord with its lower bond order.

The values of the harmonic force constants, 3.62 and 3.68 mdyne/Å, that yield the observed frequencies, 358 and 361 cm^{-1}, respectively, are quite close to the derived value of 3.37 mdyne/Å. Coupling of vibrational modes and possible anharmonic Mo-Mo bond deformation account for the small discrepancies.

6.5 The Mo-Mo Double Bond

Whenever the M-M bond is spanned by bridging ligands, it becomes difficult to distinguish unequivocally between the direct coupling of electron spins (M-M bonding) and indirect coupling through the bridges. No compound with a double bond, unsupported by bridging ligands, is available to serve as a landmark for the position of the $\{k_r, r_o\}_{Mo\text{-}2\text{-}Mo}$ solution curves.

From simple electron counting (Chapter 2), it is proposed that the $Mo_2(OBu^t)_6(\mu\text{-}CO)$ molecule has a double Mo-Mo bond. Structural evidence (Chapter 2) argues irrefutably for a direct bond between the Mo atoms in $Mo_2(OPr^i)_8$, and simple electron counting predicts a $\sigma^2\pi^2$ electron configuration. The Mo-Mo distances, 2.498(1) Å in $Mo_2(OBu^t)_6(\mu\text{-}CO)$ and 2.523(1) Å in $Mo_2(OPr^i)_8$, fall between those of Mo≡Mo and the single Mo-Mo bond, suggesting the possibility of a double bond.

6.5.1 Molecular Mechanics Modelling

These molecules were treated somewhat differently to previously modelled molecules. The adopted force field is rather incomplete, since the Mo-Mo-L and Mo-L_{br}-Mo angles are excluded from the force field i.e. they are a

consequence of the Mo-Mo and Mo-L_{br} distances, and other structural parameters. No lone pairs were included in the force field. They are not sterically important in matching the calculated and observed structures.

As discussed in Chapter 2, the configuration of oxygen atoms about each Mo atom in $Mo_2(OPr^i)_8$ is a slightly distorted trigonal bipyramid (Figure 2.19). The Mo_2O_8 central portion of the structure is therefore modelled as two MoO_5 trigonal bipyramids joined along a common axial-equatorial edge. The three equatorial bonds make almost perfect (120°) trigonal angles, the actual values being 120.9°, 120.2° and 118.9°, and the MoO_3 unit is planar within experimental error.

The coordination polyhedron about each Mo atom in $Mo_2(OBu^t)_6(\mu\text{-}CO)$ is a distorted square pyramid with the carbonyl C atom at the apex. The Mo atom is therefore modelled as having an ideal square pyramidal disposition of the attached ligands.

Force field parameters are given in Table 6.22.

The torsional parameter about all bonds is repulsive, $V_{\chi=60°} = 0.0049$ kcal/mol.

The distortion from ideal square pyramidal and trigonal bipyramidal arrangements is a consequence of steric interactions.

The Mo-Mo-L and Mo-L_{br}-Mo angles match the observed values despite their exclusion from the force field. The Mo-Mo and Mo-$(O/C)_{br}$ distances ensure the observed acuteness of the Mo-L_{br}-Mo angles.

Table 6.22 Details of the force field

Bond	k_r (mdyne/Å)	r_o (Å)
$Mo-O_{eq}$	2.00	1.88
$Mo-O_{ax}$	2.05	1.98
$Mo-C_{br}$	2.00	2.00
$Mo-O_{base}$	1.50	1.88
C=O	5.00	1.20
Angle	k_θ (mdyne.Å)	θ_o (rad.)
Mo-O-C	0.10	2.094
$Mo-C_{br}=O$	0.10	2.094
$O_{ax}-Mo-O_{ax}$	0.20	3.1416
$O_{ax}-Mo-O_{eq}$	0.80	1.571
$O_{eq}-Mo-O_{eq}$	1.00	2.094
$C_{apex}-Mo-O_{base}$	0.[illegible]0	1.780
$O_{base}-Mo-O_{base}$	0.80	2.723
$O_{base}-Mo-O_{base}$	0.80	1.524

6.5.2 The $\{k_r,r_o\}_{Mo-Mo}$ Solution Curves

It is rewarding to see the solution curves of these two molecules, in Figure 6.9, almost coinciding, indicative of them having at least identical Mo-Mo bond orders. Unfortunately, no unique $\{k_r,r_o\}_{Mo-Mo}$ value is immediately obvious from the results. The Mo-Mo distances match the observed distances within 0.001 Å.

However, in Chapter 7, we will see how the unique $\{k_r,r_o\}_{Mo-Mo}$ obtained from the solution curves for the Mo-Mo bond of orders 4.0, 3.5 and 3.0, enable the formulation of relationships between k_r and r_o, N and k_r,

and finally between N and r_o.
Application of these relationships to the non-intersecting solution curves of these molecules, very interestingly reveals the presence of a double Mo-Mo bond.

The intersection of the k_r vs. r_o analytical sampling curve, $k = 137.4/(r_o)^5$, with the solution curves is shown in Figure 6.9.

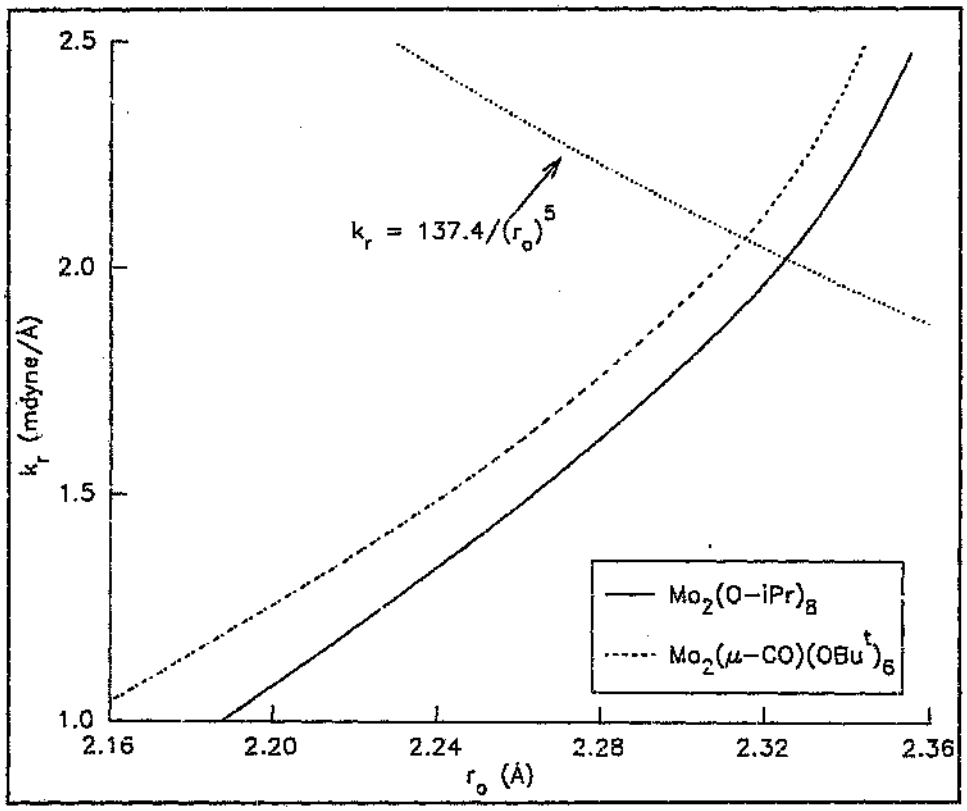


Figure 6.9 Molecular mechanics solution curves $\{k_r, r_o\}$ for the double Mo-Mo bond.

The average of the two intersections, **(2.04 mdyne/Å, 2.32 Å)**, is the unique couple for a Mo-Mo double bond. Verification of the bond order is obtained from the N vs. k_r or N vs. r_o analytical curves (see Chapter 7).

6.6 The Unbridged Mo-Mo Single bond

These $Mo_2(\eta^5\text{-}C_5R_5)_2L_6$ (R = H, Me, $(CH_2)_2CH_2(OH)$; L = CO, $CNCH_3$) complexes are typical piano-stool dimers in which two units share the leg coincident with the Mo-Mo vector. The Mo-Mo separations (ca. 3.2-3.3 Å) are quite long, ca. 0.5 Å longer than the sum of the metal radii.

The unsupported Mo-Mo bond obviously necessitates some Mo-Mo interaction. Simple electron-counting ideas and a recent (1992) molecular orbital approach based on extended-Hückel molecular orbital calculations with frontier molecular orbital analysis [135], suggest a σ^2 electron configuration.

6.6.1 Force Field Parameters

The molecular geometry is best modelled by attributing a square pyramidal configuration to each half of the molecule, with the Cp ring occupying the apical position, and the three L ligands and Mo-Mo bond completing the square base.

The adopted force field is given in Table 6.23.

Successful modelling of the Cp ring was achieved by specifying a bond between Mo and an interactionless 'pseudoatom' (Cen) at the centroid of the five membered ring. The Mo-Cen-C angles were restricted to 90° by specifying large force constants. Rigidity of the ring was ensured by fixing bond lengths in the same way. Interactions between Mo and carbons of the Cp ring were therefore ignored. This force field method produces correct structural features, as reported previously by Boeyens et al [136].

Table 6.23 Details of the force field

Bond	k_r (mdyne/Å)	r_o (Å)
Mo-CO	2.00	1.93
Mo-Cen	15.00	2.00
Mo-CNMe	2.05	1.98
C≡O	3.00	1.14
C=C (Cp)	999.0	1.39
Cen-C	7.50	1.19
Angle	**k_θ (mdyne.Å)**	**θ_o (rad.)**
Mo-Cen-C	999.0	1.571
Mo-C≡O	1.00	3.1416
Mo-C≡N	1.00	3.1416
Cen-Mo-Mo	0.20	1.780
Cen-Mo-CO	0.20	1.780
Cen-Mo-$CNCH_3$	0.20	1.780
Mo-Mo-CO(CNMe)	0.20	2.723
OC-Mo-CO	0.20	2.723
Mo-Mo-CO	0.30	1.524
(MeNC)OC-Mo-CO	0.30	1.524
C-C-C (Cp)	0.50	1.885
C-C-L (Cp)	0.50	2.199
C≡N-C	1.00	3.1416
C-O-H(L_p)	0.40	1.911

Torsional interactions, except those involving the Cp ring, were set at $V_{\chi=60°} = 0.0049$ kcal/mol. The ring has attractive interactions across the C-C bonds, with

$V_{\chi=0°}$ = 0.05 kcal/mol.

Constraints were placed on the angular movement (δ) of the atoms bound to cyclopentadienyl carbons out of the plane of the ring, with k_δ = 0.80 mdyne.Å for hydrogens, and 1.20 mdyne.Å for carbon atoms on the Cp ring.

6.6.2 The $\{k_r, r_o\}_{Mo-Mo}$ Solution Curves

The Mo-Mo bond was reproduced within 0.001 Å of the observed values (Table 6.24).

Table 6.24 Calculated and observed Mo-Mo distances

Molecule	Calc. (Å)	Obs. (Å)	Figure Label
$(\eta^5\text{-}C_5H_5)_2Mo_2(CO)_6$	3.233	3.235(1)	two
$(\eta^5\text{-}C_5Me_5)_2Mo_2(CO)_6$	3.280	3.281(1)	three
$(\eta^5\text{-}C_5H_5)_2Mo_2(CO)_5(CNMe)$	3.231	3.230(1)	two
$\{[\eta^5C_5H_4((CH_2)_2CH_2OH)]Mo(CO)_3\}_2$	3.22	3.213	one

The $\{k_r, r_o\}_{Mo-Mo}$ solution curves in Figure 6.10, are close together and separated from higher order solution curves.

However, as was the case for the double Mo-Mo bond, the curves are non-intersecting, precluding the deduction of the unique (k_r, r_o) couple for a single bond.

Intersection of the k_r vs. r_o analytical sampling curve with the solution curves is shown in Figure 6.10. The unique couple for a single bond is $(k_r, r_o)_{Mo-Mo}$ = **(1.01 mdyne/Å, 2.67 Å)**. Very intriguing, is the assignment of a strong Raman band at 193 cm^{-1} to the

Mo-Mo stretching frequency in $Mo_2(\eta^5\text{-}C_5H_5)_2(CO)_6$. The corresponding diatomic force constant value of 1.05 mdyne/Å, probably justifies the chemical validity of the analytical sampling curves.

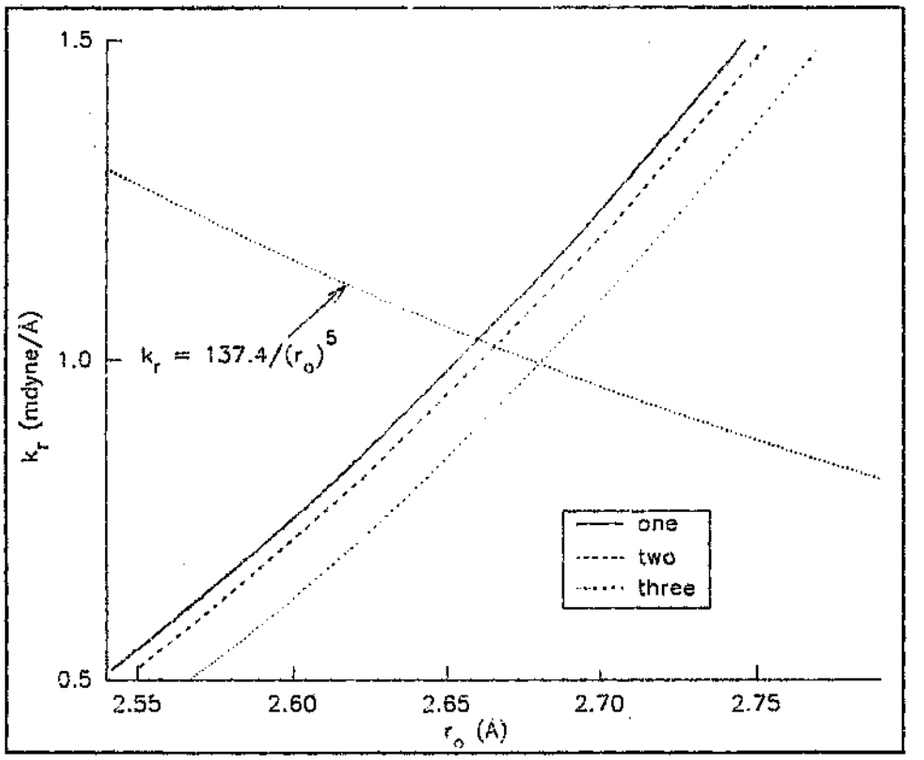


Figure 6.10 Molecular mechanics solution curves for the Mo-1-Mo bond.

The solution curves are of positive slope implying stretching of the Mo-Mo bond by steric forces. Because of the lower force constant (1.01 mdyne/Å), the Mo-1-Mo bond is more flexible and easily stretched from 2.67 Å to the observed 3.2 - 3.3 Å.

This contradicts the proposal made by the Italian researchers [135], that the observed Mo-Mo separations are a direct consequence of mainly electronic forces, and that steric factors are minor.

6.6.3 The Equilibrium Structures

The observed molecular geometry is pseudo-square pyramidal because of the distorting effects of steric interactions within the molecule. The long Mo-Mo distances are a result of the molecule being under considerable steric strain.
Additional features of interest are the trans disposition of the cyclopentadienyl rings, obviously sterically demanded, and the nonlinearity of the Mo-C≡O and Mo-C≡N groups.

There is considerable repulsion between the Cp ring and L_3 groups [L_3 = $(CO)_3$, $(CO)_2(CNMe)$] on a given Mo atom, let alone what steric crowding occurs in the presence of another such bulky $MoCp(CO)_3$ or $MoCp(CO)_2(CNMe)$ group.
Steric crowding between the Cp ring and CO groups (or CO and CNMe groups) on a given Mo atom is so large as to force two of the three CO groups (or the two CO groups) to lie over the Mo-Mo bond. This consequently introduces immense steric crowding and repulsion between these CO groups cis to the Mo-Mo bond and the Cp ring on the adjacent Mo atom. The other CO (or CNMe group) points well away from the region of contact, but contributes indirectly because its presence imposes a buttressing effect on the other two CO groups and Cp ring that make direct contact with the ligands on the adjacent Mo atom. The end against end repulsion is obviously severe.

The nonbonded interactions cause quite marked bending of the Mo-C≡O groups cis to the Mo-Mo, ca. 173°, and slight bending for the CO (or CNMe) trans to the Mo-Mo bond, ca.178°. The direction of bend is obviously away from the neighbouring $MoCpL_3$ group.

It is evident that these molecules are under considerable internal strain, and stretching of the Mo-Mo bond is a

direct consequence of the need to move, the already crowded, halves away from each other.

6.7 Brief Overview of the Mo-Mo Bond

The Mo-Mo bond order depends solely on the formal number of electrons available for bond formation. The ligand environment has an insignificant effect on this formal bonding.

There is overlap of observed Mo-Mo distances between bonds of different order, but each bond order has a characteristic r_o value.

We can conclude this chapter content that the availability of unique couples for, at least, the bonds of order four to three, allow for the derivation of analytical sampling curves to rationalize the wide range of observed dichromium distances.

Chapter 7
THE RELATIONSHIPS BETWEEN M-M BONDING VARIABLES FOR GROUP VIA METALS

7.1 Previous Analytical Curves

Two analytical sampling curves, based on the empirical rules of Badger [137] and of Gordy [138] have been proposed [139]. Reformulated in terms of k_r, r_o and bond order, N, these relationships have the form

$$k(r_o)^3 = \text{constant} \qquad \text{(Badger)}$$

$$k(r_o)^{1.5}/N = \text{constant} \qquad \text{(Gordy)}$$

In their original form both of these relationships are more complicated than shown here, to allow for differences in periodic position, electronegativity and oxidation state.
The Gordy curve represents a functional relationship for constant effective bond order. Since bonds of the same effective order have identical force constants, this is not a realistic relationship. Whatever the relationship, there clearly is a progressive decrease in force constant with bond order.

Badger's rule has been shown to apply to third row diatomic species and to transition metal oxides. However, this does not imply general extension of the relationship to compounds possessing dimetal bonds from period VIA.

Fortunately, a range of dimolybdenum crystal structures for each Mo_2 bond order has accumulated over the years, and a molecular mechanics method of directly probing the electronic component of the dimetal bond is available. We therefore do not need to rely on empirical relationships specific to other systems; the relationship appropriate to dimetal bonding within complexes is experimentally available.

7.2 The Relationship between k_r and r_o for the Mo-Mo Bond

The relationships derived from the experimental results on the Mo_2 system are assumed as representative of M-M bonding for all group VIA metals.
Also, these expressions are specific to the force field applied to the dimetal systems.

The three unique [k_r (mdyne/Å), r_o (Å)] values (4.07, 2.02), (3.63, 2.07) and (3.37, 2.10), for quadruple, 3.5 and triple Mo-Mo bonding respectively, serve as data points in the derivation of our relationships. The molecular mechanics force constant for Mo-1-Mo bonding is expected to be of the same magnitude as that derived from the experimentally observed Raman band, namely 1.05 mdyne/Å. This assists in validating the adopted expressions.

The experimental data obviously demands an inverse relationship between k_r and r_o. Two possible expressions are:

* a linear, inverse relationship between k_r and r_o:
  $k_r = -ar_o + c$, or
* a nonlinear, inverse relationship of the form
  $k_r = c/(r_o)^a$.

The former results in a k_r value for Mo-1-Mo ca. a tenth of that expected from Raman studies. Also, the existence

of a linear relationship seems too simple.

The latter expression is adopted. The relationship with the best fit to the experimental data is of the form

$$k_r = 137.4/(r_o)^5 \qquad 7.1$$

The analytical curve together with the experimental solution curves for the Mo-Mo bond of orders 4.0, 3.5 and 3.0 is shown in Figure 7.1.

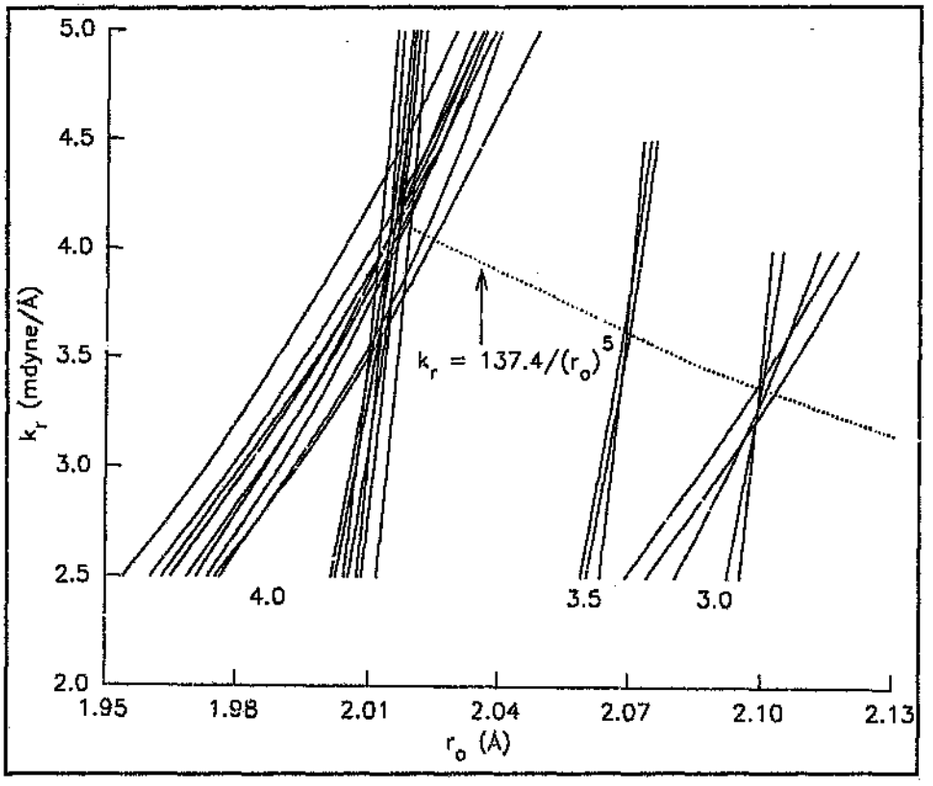


Figure 7.1 The k_r vs. r_o analytical curve and the solution curves for the Mo-Mo bond of orders 4.0, 3.5 and 3.0.

In Figure 7.2 error bars show the range of k_r and r_o values in the overlap regions of the solution curves for the Mo-Mo bond of orders 4.0, 3.5 and 3.0.

Figure 7.3 shows the analytical curve derived from the experimental (k_r, r_o) couples (filled circles) and the average of the points of intersection with the solution curves for the so-called double and the single Mo-Mo compounds (open circles).

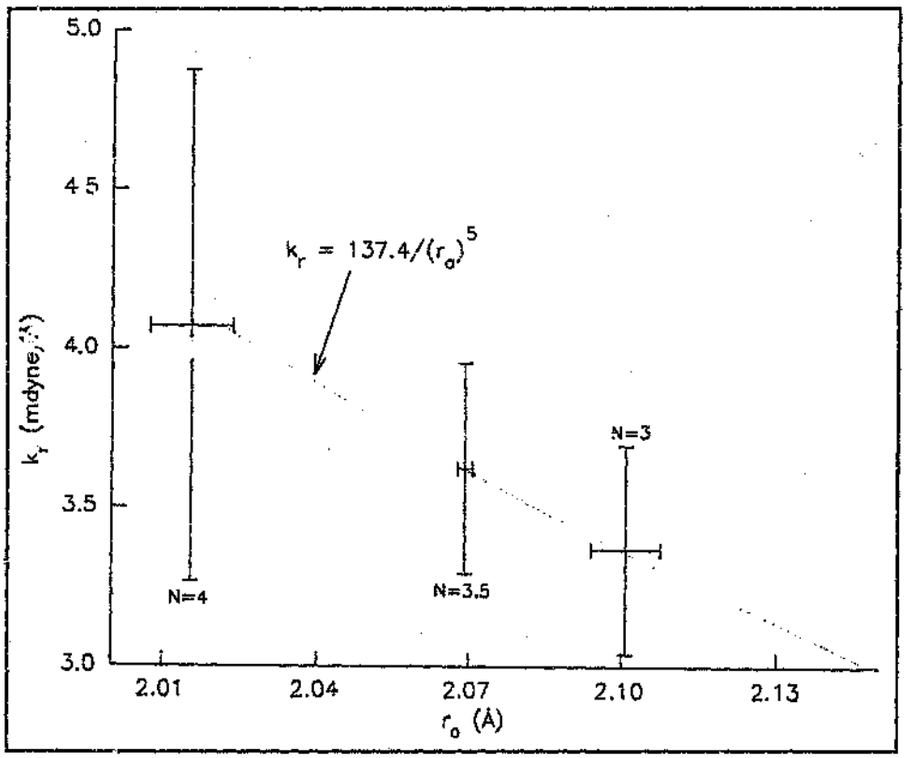


Figure 7.2 Error bars showing the range of k_r and r_o values for each Mo_2 bond order.

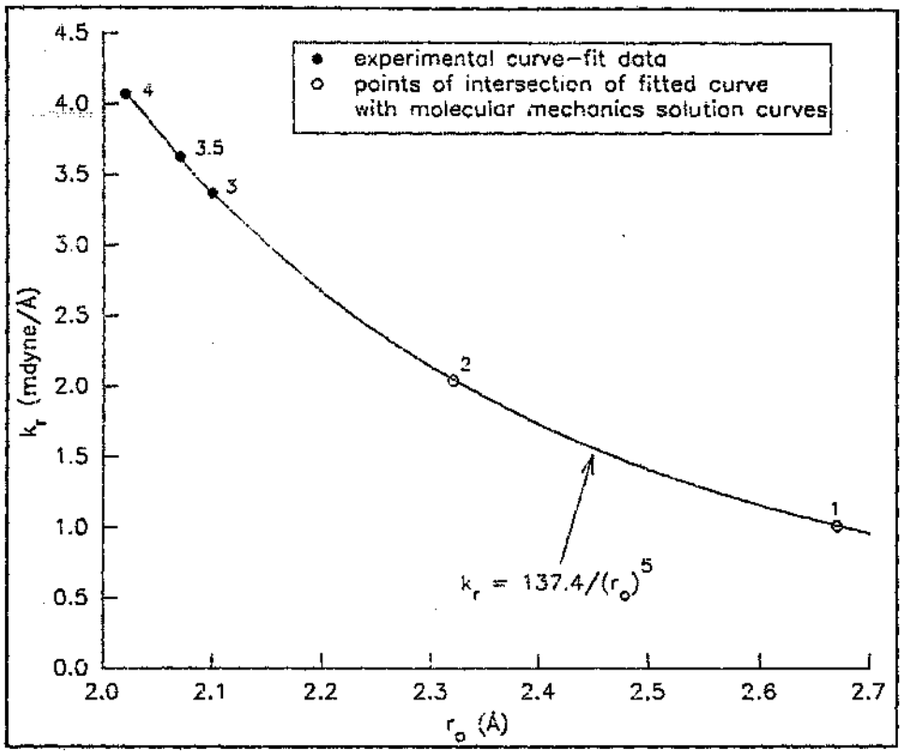


Figure 7.3 The relationship between k_r and r_o for the Mo-Mo bond of different orders.

7.3 The Relationships between N and k_r and N and r_o for the Mo-Mo Bond

From formal electron counting and molecular orbital calculations it is almost certain that the piano-stool compounds are held together by a single Mo-Mo bond. Uncertainty only exists for the so-called doubly bonded Mo_2 centres because of the presence of bridging ligands.

The experimental data suggests a near 1:1 relationship between bond order, N, and force constant, k_r. Using the data for the quadruple, 3.5, triple and single Mo-Mo bond the best fitted expression relating N and k_r has the form:

$$N = 0.9537\ (k_r) \qquad 7.2$$

This relationship is shown in Figure 7.4.

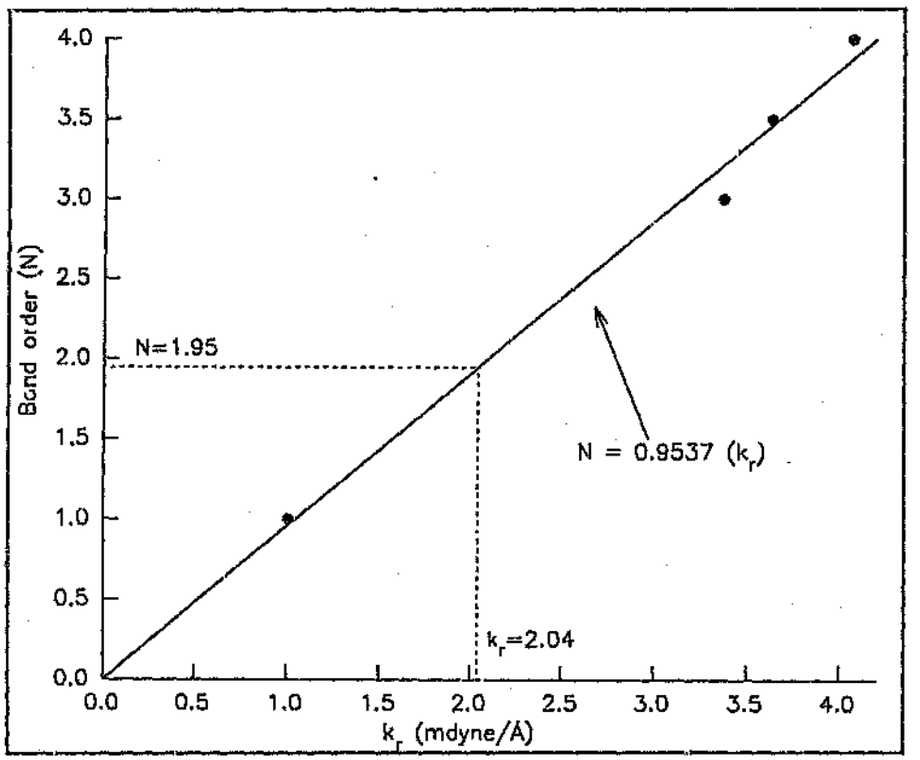


Figure 7.4 Relationship between N and k_r for the Mo-Mo bond in dimetal complexes. The true bond order for the so-called double Mo_2 bond is deduced from the experimental force constant.

From the k_r vs. r_o and N vs. k_r relationships, it follows that the relationship between N and r_o is:

$$N = 131.8/(r_o)^5 \qquad 7.3$$

The relationship is seen in Figure 7.5.

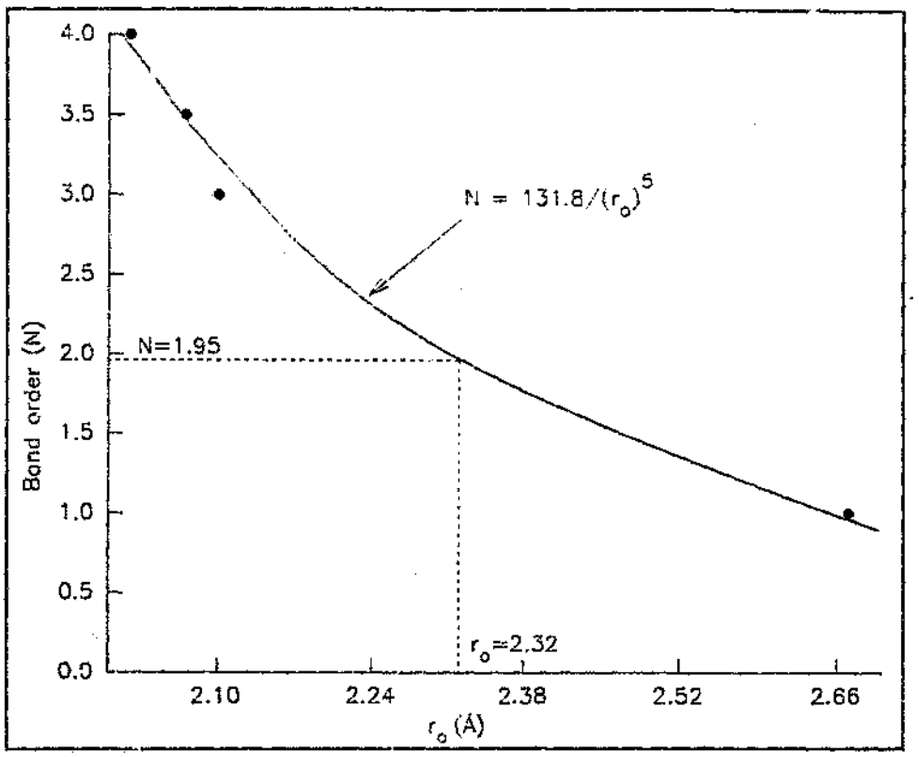


Figure 7.5 Relationship between N and r_o for the Mo-Mo bond. The true bond order for the so-called double Mo_2 bonds is deduced from the experimental r_o value.

The value of k_r for the so-called double Mo-Mo bond corresponds to a N of 1.95. We therefore conclude that these so-called double Mo_2 compounds are, within experimental error, of that order.

7.4 The General Relationships for Dimetal Bonds from Group VIA

Assuming the bonding in the dimolybdenum centre to be representative of that for M-M bonding between group VIA metals, we can generate more general expressions from those specific to Mo_2.

These equations are :

$$k_r = c/(r_o)^5 \qquad 7.4$$

$$N = b\ (k_r) \qquad 7.5$$

and

$$N = bc/(r_o)^5 \qquad 7.6$$

where the constants b and c are specific to the dimetal bond.

There may be other relationships that adequately fit the experimental data of the dimolybdenum system. The fact that the above relationships provide chemically reasonable explanations for the variability of the Cr_2 bond lengths, justifies their application to modelling dimetal bonding.

Chapter 8

THE Cr_2 SYSTEM AS ANALYZED BY THE M-M BONDING MODEL

8.1 Introduction

We have been interested for some time in the general question of how M-M bond strength in dimeric compounds is affected by the more important variables in the system, namely, the position of the metal in the periodic table, and the nature of the ligand environment.

In every case where there are relevant data, the length of a M-M multiple bond is increased by the introduction of axial ligands. However, the magnitude of the effect varies remarkably from one metal to another. The extent to which different M-M bonds vary in their sensitivity, to the presence of axial ligands has been illustrated in Chapters 2 and 3.

There are very interesting contrasts between dichromium and dimolybdenum species. For the bridged $Mo_2(XZY)_4$ the Mo-Mo distances are affected by only a few hundredths of an Angstrom. The $Cr_2(XZY)_4$ units, however, seem to have a powerful attraction for axial ligands, and the Cr-Cr bond lengths are markedly affected by the presence of such ligands. The Cr-Cr bond lengthens by ca. 0.7 Å in the presence of axial donors. This wide range has not yet been fully interpreted.

Ab initio calculations [104] show the quadruple bond configuration as making only a 16% contribution to the

ground electronic state at Cr-Cr distances of 2.16 - 2.56 Å. On the other hand, an SCF-Xα-SW calculation [103] for $Cr_2(O_2CH)_4$ at Cr-Cr = 2.20 and 2.36 Å gives an unambiguous result, showing that the ground state of the molecule does correspond to a $\sigma^2\pi^4\delta^2$ quadruple bond, but weaker than in the Mo compound. The ab initio calculations also suggest that only bridging ligands more basic than carboxylates will support 'supershort' Cr-Cr bonds. The electron diffraction study of $Cr_2(O_2CMe)_4$ with a dichromium distance of 1.96(1) Å appears to be completely at variance with the predictions from ab initio calculations.

From the experimental crystallographic results, it would seem difficult to escape the conclusion that while changes in both the bridging ligands and the axial ligands each have some influence on the Cr-Cr distance, the overwhelmingly more important factor seems to be whether there are any axial ligands present, and how strongly they donate.

Whatever the cause, such large differences in the Cr-Cr distances indicate that behind the formal concept of quadruple bonding the real bonding situation may be quite different.

8.2 Transfer of Mo_2 Force Field Parameters to the Cr_2 System

The bridging framework for a given $(XZY)^{-1}$ ligand is comparatively insensitive to changes in the dimetal bond length. All structures of this type can therefore be simulated by a virtually transferable force field.

Similarly, structural parameters for the ligating Me groups in $[M_2Me_8]^{4-}$ are transferable. The parameters k and p_o (p_o = bond or angle) for different structures are

assumed to remain constant for all interactions, except those involving the M-L and M-M units. These parameters transferred from the Mo_2 system to Cr_2, afford a match of the calculated and observed structure parameters within 0.1 Å for bond distances, and 3° for angles.

Obviously, bond length parameters involving the Cr centre are expected to change due to the different intrinsic sizes of Mo and Cr.

The geometry about each Cr atom in $Cr_2(XZY)_4$ and $[Cr_2Me_8]^{4-}$ is treated as being square planar; and octahedral for $Cr_2(XZY)_4L_2$. The k_θ and θ_o parameters for angles about the Cr atoms are the same as for the Mo_2 species.

Similarly, the torsional potential for rotation about a M-ligand or ligand-ligand bond, and out-of-plane deformation constants, is no different from that of the Mo_2 system. These observed parameters are matched to within 5°.

As was observed in the calculations for $Mo_2(XZY)_4$, no torsional parameter is needed to render the near-eclipsed conformation energetically favoured, due to the delocalization of the negative charge over the entire XZY group.

Coulombic interactions are needed in the simulation of the $[Cr_2Me_8]^{4-}$ ion, but are ignored if not present on atoms directly bonded to the Cr_2 centre. This is also an extension from Mo_2.

In short, the transfer of many parameters from the Mo_2 to the Cr_2 system greatly facilitate the molecular mechanics calculations.

Additional parameters are summarized in Tables 8.1 - 8.3.

Table 8 .1 Force field parameters for interacting pairs of atoms specific to $[Cr_2Me_8]^{-4}$ and $Cr_2(XZY)_4L_n$ (n = 0, 1 or 2)

Bond	k_r (Å)	r_o (Å)
$Cr-C^{-\frac{1}{4}}$	2.08	2.18
$Cr-N_{br}$	0.84	2.03
$Cr-O_{br}$	0.84	1.97
$Cr-C_{br}$	2.08	2.05
$C_{br}-O$ (CO_3)	3.00	1.26
$C_{ar}-N$	3.00	1.30
$Cr-Br_{ax}$	0.30	3.30
$Cr-Cl_{ax}$	0.20	3.20
$Cr-O_{ax}$	0.60	2.29
$Cr-O_{ax}$ $(inter.)_1$	0.40	2.30
$Cr-O_{ax}$ $(inter.)_2$	0.40	2.36
$Cr-N_{ax}{}^a$	0.70	2.32
$Cr-N_{ax}{}^b$	0.70	2.27
$Cr-O_{ax}$ $(Et_2O)_2$	0.60	2.22
$Cr-N_{ax}{}^c$	0.70	2.24

a :L_{ax} = pyrazine, 2-CN-py, 4-CN-py, py

b :L_{ax} = 4-NH_2-py, 4-CMe_3-py, 4-NMe_2-py

c :O_2CR = $O_2C(CF_2H)$ and L_{ax} = 4-NMe_2-py

Table 8.2 Angle bending parameters specific to Cr_2 species

Angle	k_θ (mdyne.Å)	θ_o (rad.)
C-N-C	0.10	1.911
C-N-L_p	0.40	1.911
O_{br}-C_{br}-O	1.00	2.094
O_{br}-C_{br}-C_{ar}	1.00	2.094
C-C-Cl	0.65	1.911
H-C-Cl	0.52	1.911
Cr-O-L_p	0.40	1.911
Cr-O-C	0.20	1.911
C-O-C	0.10	1.911
C-O-L_p	0.40	1.911
C_{ar}-N-H	0.60	2.094
H-N-H	0.50	2.094
H-C-F	0.52	1.911
C_{ar}-N-C	0.20	2.094

Table 8.3 Nonbonded parameters

Interaction	a (u)	b ($Å^{-1}$)	c ($u.Å^6$)
Cr--Cr	682.9	3.28	2.20
Cr--O	1485.0	3.89	2.22
Cr--H(L_p)	341.9	3.86	0.710
Cr--C	1907.6	3.88	2.13
Cr--N	1350.0	3.89	2.25
Cr--Br	348.8	3.02	8.22
Cr--Cl	1179.3	3.51	5.74
Cr--F	697.6	3.90	1.33

One can be confident that all the calculated parameters are of the correct order of magnitude and hence suitable for the generation of $\{k_r, r_o\}_{Cr\text{-}Cr}$ solution curves and calculation of barriers to rotation.

Within the Cr_2 system the supporting framework, including the $Cr\text{-}X_{br}$ bonds, is comparatively insensitive to changes in the Cr-Cr bond length. The force field parameters are assumed to remain constant for all interactions, except those involving both Cr centres. Observed structures are therefore simulated by energy minimization and adjustment of the force constant, k_r, and strain-free bond length, r_o, of the dichromium bond only.

8.3 The Quadruple Cr-Cr Bond

8.3.1 The Delta Contribution to the Quadruple Bond Strength

The only formally quadruple dichromium compound unsupported by bridging ligands is $[Cr_2Me_8]^{4-}$. The compound is isostructural and isoelectronic with the analogous Mo_2 compound. The presence of a δ bond receives strong support from the eclipsed nature of the Me ligands across the Cr-Cr bond.

The results of a driver calculation on $[Cr_2Me_8]^{4-}$ is shown, together with that for Mo_2, in Figure 8.1.

Again, the potential energy has a maximum at $\chi = 0°$, viz. the eclipsed conformation. This shows conclusively that an electronic factor, i.e. δ bonding, is also responsible for the stabilization of the observed conformation in Cr_2. The difference in potential energy, $(U_{\chi=0°} - U_{\chi=30°})$ = 9.5 kcal/mol, defines a lower limit for the δ contribution to the quadruple bond strength in Cr_2. This value is larger than the 7.5 kcal/mol for the analogous

Mo_2 compound; a reflection of the greater steric congestion in Cr_2 due to its smaller intrinsic size.

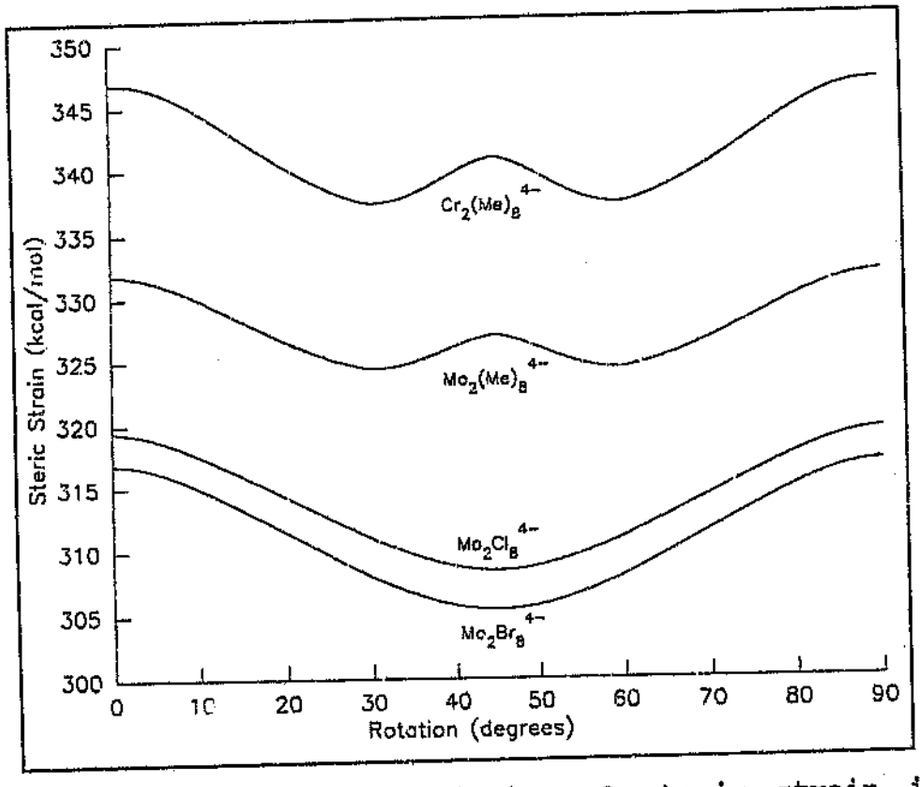


Figure 8.1 Angular variation of steric strain in quadruply bonded $[M_2X_8]^{4-}$ ions.

8.3.2 $\{k_r, r_o\}$ Solution Curves for the Cr_2 Centre

From the molecular mechanics $\{k_r, r_o\}_{Cr-Cr}$ studies, it was found that Cr-Cr compounds spanned by C^O- and N^N-bridging ligands have solution curves intersecting that of the $[Cr_2Me_8]^{4-}$ ion at the shortest r_o (Figure 8.2), and is therefore accepted as the most likely overlap region for a true quadruple Cr-Cr bond. The other Cr_2 bridged complexes have solution curves positioned at longer r_o, clearly separated from the C^O- and N^N-bridged compounds, indicative of a decrease in Cr-Cr bond order.

The calculated Cr-Cr distances match the observed values

within 0.001 Å. The calculated and observed Cr-Cr distances for compounds possessing true quadruple bonding are given in Table 8.4.

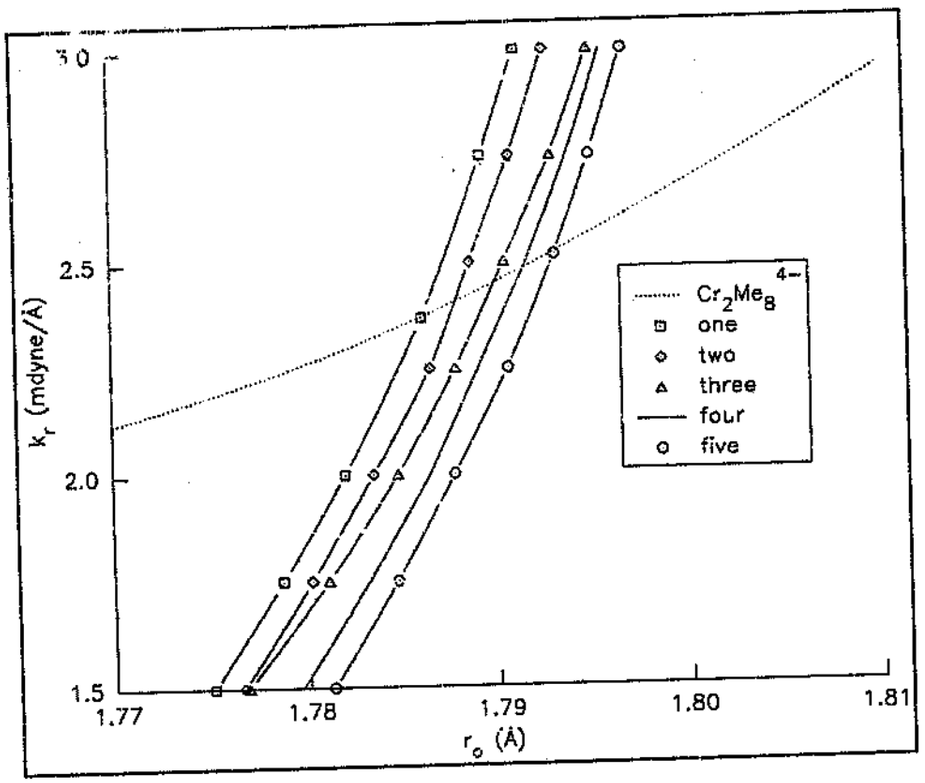


Figure 8.2 Molecular mechanics solution curves $\{k_r, r_o\}$ for the quadruple Cr-Cr compounds.

The slopes of the solution curves are all positive, indicative of the Cr-Cr bond being stretched from its electronic separation to the observed distance by steric forces.

The Br^- ions lie approximately along the extensions of the Cr-Cr axes (Cr-Cr-Br = 171°), but at such a great distance, 3.266(2)Å, that they are only weakly, if at all bonding. This weak axial interaction is reminiscent of that for Mo-L_{ax} interactions.

Table 8.4 Calculated and observed distances for the quadruple Cr-Cr centre

Molecule	Calc. (Å)	Obs. (Å)	Figure Label
$[Cr_2Me_8]^{4-}$	1.982	1.980(5)	
$Cr_2(DMP)_4$	1.847	1.847(1)	two
$Cr_2(TMP)_4$	1.847	1.849(2)	two
$Cr_2(2MeO\text{-}5MeC_6H_3)_4$	1.830	1.828(2)	one
$Cr_2(PhN\text{-}N\text{-}NPh)_4$	1.858	1.858(1)	four
$Cr_2(MAP)_4$	1.870	1.870(3)	five
$Cr_2(DMF)_4$	1.930	1.930(2)	three
$[Cr_2(o\text{-}C_6H_4C)_4(Br)_2]^{6-}$	1.831	1.830(4)	one

8.3.3 Steric Deformations

As discussed for Mo_2, the bridging group stretches the Cr-Cr bond toward the natural 'bite' distance. Partial stretching of the Cr-Cr bond to the 'bite' separation is compensated for by the opening of the Cr-Cr-X_{br} angles. This opening is symmetrical for the N^N-bridged complexes, but in the case of C^O-bridged compounds, the excessive 'bite' is compensated for almost entirely by the more obtuse Cr-Cr-O_{br} angles (ca. 102°) compared to the near orthogonal Cr-Cr-C_{br} angles (ca.92°). However, all the Cr-Cr-X_{br} angles are more obtuse (by ca. 3°) than the corresponding Mo-Mo-X_{br}, due to the shorter Cr-Cr and Cr-X_{br} bonds.

Further structural evidence of the increased steric crowding within the Cr_2 compounds is demonstrated by the larger N-Cr-Cr-N torsion angles in $Cr_2(PhN\text{-}N\text{-}NPh)_4$ (10.4°, 10.5°, 12.9°, 14.8°) and $Cr_2(DMF)_4$ (8.4°, 8.7°), compared to the near-eclipsing in the corresponding Mo_2

compounds. However, these small rotations have no effect on the strength of the δ^2 component of the quadruple Cr_2 bond, a result already demonstrated for the Mo_2 quadruple bond.

The Cr_2 bond in $[Cr_2Me_8]^{4-}$ experiences greater steric congestion than the analogous Mo_2 compound. This is demonstrated by the larger Cr-Cr-C$^{\frac{1}{2}}$ angles and the Cr-Cr bond being stretched further from its electronic separation. The lengthening of the Cr-Cr distance upon rotation about the Cr-Cr bond from 30° to the observed eclipsed conformation is also greater than that for $[Mo_2Me_8]^{4-}$.

8.3.4 The Unique $(k_r, r_o)_{Cr-Cr}$ Couple for Quadruple Bonding

The overlap region in Figure 8.2 results in an average $(k_r, r_o)_{Cr-Cr}$ = (2.45 mdyne/Å, 1.79 Å); accepted as the most likely couple for a quadruple Cr-Cr bond. This rather low force constant explains the longer observed Cr-Cr separations than might have been expected from the Mo-Mo bond lengths in comparable compounds. The ratio $r_o(Mo):r_o(Cr)$ = 1.13, is almost exactly the ratio of the covalent radii, namely 1.10.

Unfortunately, and very surprisingly, no vibrational frequency data are available for these quadruple Cr-Cr bonds to permit a comparison of experimental and calculated harmonic force constants. The calculated force constant implies a ν_{Cr-Cr} of 400 cm^{-1} for a 'pure' Cr-Cr stretch.

Very interestingly, calculations at the SCF level on $Cr_2(O_2CH)_4$ [102], show the SCF ground state to correspond to a quadruple bond configuration at Cr-Cr distances smaller than 1.8 Å. Beyond this distance, the nonbonded

configuration has a lower energy. This value is in accord with our electronic separation of 1.79 Å for a quadruple Cr-Cr bond.

8.4 The Relationships between Bonding Variables for Cr_2

The fixed quadruple (k_r, r_o) point allows for the generation of expressions specific to the Cr_2 system. The result is the following equations:

$$k_r = 45.02/(r_o)^5 \qquad 8.1$$

$$N = 1.633\ (k_r) \qquad 8.2$$

$$N = 73.51/(r_o)^5 \qquad 8.3$$

The relationship 8.1, together with error bars showing the experimental variation in k_r and r_o for the overlap region, is displayed in Figure 8.3.

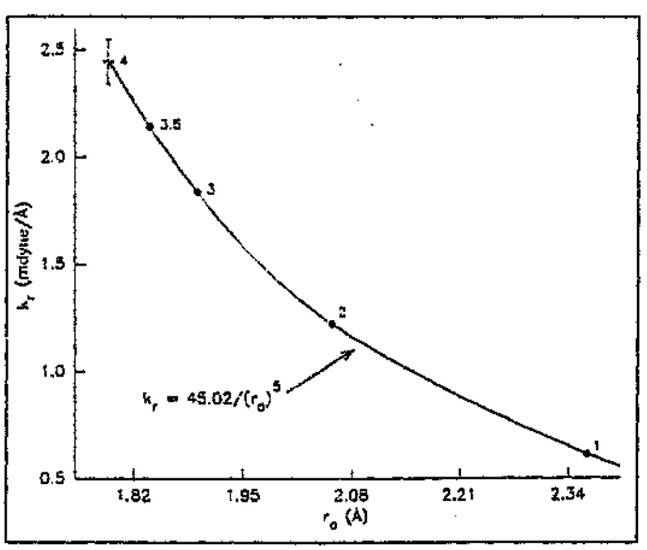


Figure 8.3 Relationship between k_r and r_o for Cr-Cr bonding in dimetal complexes. The (k_r, r_o) couples for Cr-Cr bonds of order 4 through to 1 is shown.

Seeing that the larger the constant c is, the less sensitive is the M-M bond, we suggest that c be called the 'index of inflexibility'.

8.5 Formally Quadruple, but Effectively of Slightly Lower Order

8.5.1 Molecular Mechanics Results

The molecular mechanics calculations indicate an electronic influence of the nature of the X^Y group on the Cr-Cr bond, a result predicted previously by ab initio calculations.

The solution curves for the Cr_2 compounds bridged by $(N\hat{}O)_4$, $(C\hat{}O)_2(O\hat{}O)_2$, and $(O\hat{}O)_4$ groups are shown in Figures 8.4 and 8.5. The solution curves for the C^O- and N^N-bridged Cr_2 compounds are included in Figure 8.4.

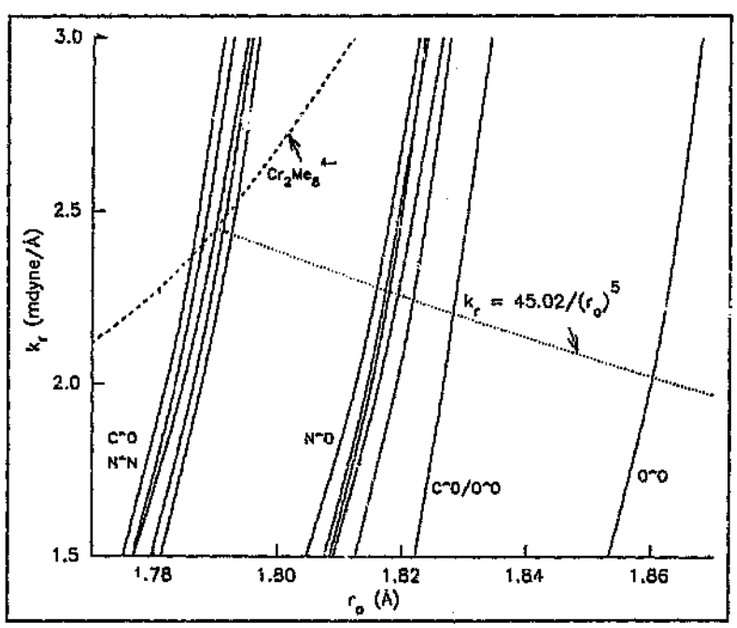


Figure 8.4 Molecular mechanics solution curves $\{k_r, r_o\}$ for the supported Cr_2 bond, in the absence of strong axial ligation.

Clearly they intersect the solution curve of the quadruple $[Cr_2Me_8]^{4-}$ ion at the shortest r_o value, therefore being the most likely overlap region for quadruple Cr-Cr bonding. It is also obvious that the solution curves of the different X^Y-bridged compounds do not intersect. A gradual change in Cr-Cr bond order on going from the C^O- and N^N- to N^O- to (C^O/O^O)- and finally to the O^O-bridging groups is implied by the relative positions of the solution curves.

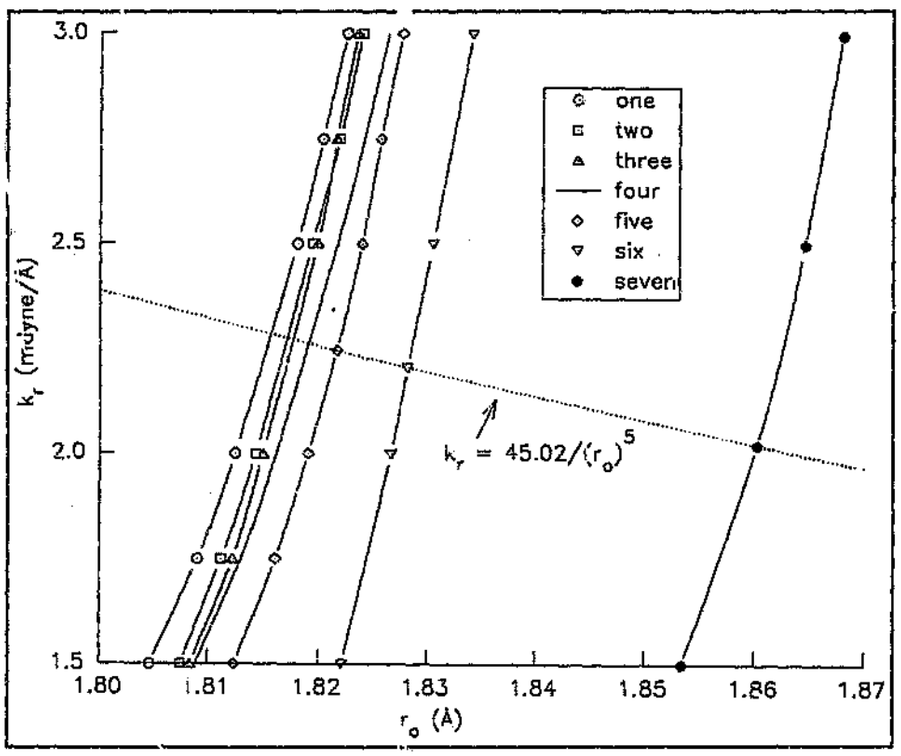


Figure 8.5 Molecular mechanics solution curves $\{k_r, r_o\}$ for the Cr-Cr bond of different bond orders. Intersection of the k_r vs. r_o relationship with the solution curves is shown.

The calculated Cr-Cr distances match the observed separations within 0.001 Å (Table 8.5). Again, molecules with similar Cr-Cr r_{obs} have essentially coinciding

solution curves.

Table 8.5 Calculated and observed Cr-Cr separations

$(X\text{-}Z\text{-}Y)_n$	$(L_{ax})_2$	Calc. (Å)	Obs. (Å)	Figure Label
$(PhN\text{-}C(Me)\text{-}O)_4$	-	1.871	1.873(1)	three
$(MHP)_4$	-	1.890	1.889(1)	one
$(DMHP)_4$	-	1.903	1.907(3)	one
$[(2,6xylyl)N\text{-}C(Me)\text{-}O]_4$	-	1.938	1.937(2)	two
$[(2,6xylyl)N\text{-}C(Me)\text{-}C]_4$	CH_2Cl_2	1.950	1.949(2)	five
$[(2,6xylyl)N\text{-}C(Me)\text{-}O]_4$	CH_2Br_2	1.958	1.961(2)	four
$(CHP)_4$	-	1.957	1.955(2)	four
$(o\text{-}Bu^tOC_6H_4)_2(O_2CMe)_2$	-	1.863	1.862(1)	six
$(O_2CMe)_4$ (g)	-	1.96	1.96(1)	seven

By extrapolation from the fixed point for a quadruple Cr-Cr bond, (2.45, 1.79), specific solutions, (k_r, r_o), for the family of compounds in Figure 8.5 can be obtained by systematic sampling, using the derived expressions for Cr-Cr bonding. Force constants and reference bond lengths were accordingly read from the points of intersection of the $k_r = 45.02/(r_o)^5$ relationship with the molecular mechanics solution curves.

Application of either equation 8.2 or 8.3 to the k_r or r_o values, respectively, allows the determination of the true bond orders. The solution curves for the N^O-bridged compounds are sufficiently close together to be

considered of the same Cr-Cr bond order, and obviously the average of the overlap region is used in the bond order determination. The deductions arrived at by applying the relationships are summarized in Table 8.6 and presented graphically in Figure 8.6.

Table 8.6 The sampled (k_r, r_o) couples and effective Cr-Cr bond orders for different bridging groups

$(X-Z-Y)_n$	$(k_r, r_o)_{Cr-Cr}$	Bond Order	ν_{Cr-Cr} $(cm^{-1})^a$
$(C-C-O)_4$, $(N-N-N)_4$, $(N-C-N)_4$	(2.45, 1.79)	4.00	400
$(N-C-O)_4$	(2.26, 1.82)	3.70	384
$(C-C-O)_2$ $(O-C-O)_2$	(2.21, 1.83)	3.60	380
$(O-C-O)_4$	(2.02, 1.86)	3.30	363

a :localized harmonic Cr-Cr stretch

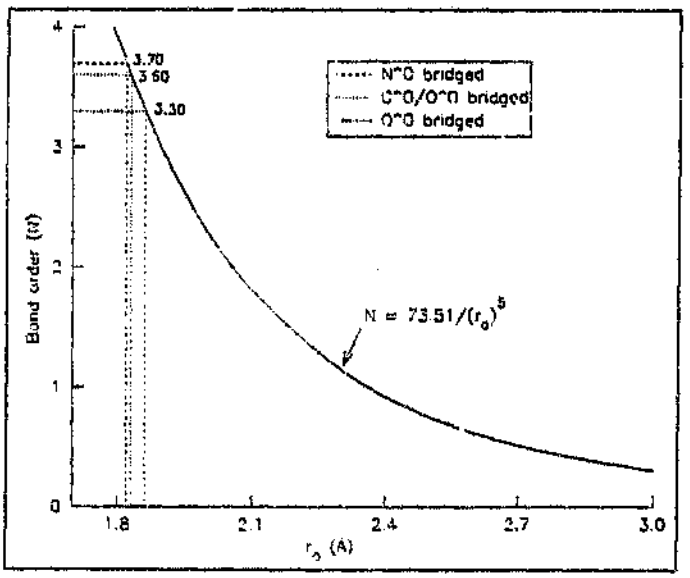


Figure 8.6 Deduction of bond order from experimental strain-free distances, r_o, for the $(N^O)_4$-$[(C^O)_2(O^O)_2]$-, and $(O^O)_4$-bridged Cr_2 bond.

Clearly, the electron density at the Cr_2 centre is being modified by the X-Z-Y bridging groups. These compounds are qualitatively similar to the corresponding Mo_2 compounds, but quantitatively there is a major difference, namely, the sensitivity of Cr_2 to the ligand environment.

8.5.2 Discussion

The results obtained allow a strict classification of the Cr_2 compounds in terms of the donor ability of the bridging group. The donor strengths of the bridging ligands are mainly a function of the kind of atoms (i.e. C, N, or O) in the 1 and 3 positions of the bridge, with the acidity decreasing in the order OH > NH > CH and the donor strengths of the corresponding anions increasing in the order $O^- < N^- < C^-$. The electron donor ability of the bridging groups, as deduced from the molecular mechanics calculations, C^O = N^N > N^O > (O^O/C^O) > O^O, is exactly that expected on electronegativity grounds.

It is very interesting that the Cr_2 bond spanned by $[(C^O)_2(O^O)_2]$ ligands has a bond order halfway between that of the Cr_2 bond bridged by $(C^O)_4$ groups and that spanned by $(O^O)_4$ groups.

The solution curves are all of positive slope due to the stretching of the Cr-Cr bond from r_o to the natural 'bite' distance of the bridging ligand. The impartial deformation of Cr-Cr to this 'bite', is compensated by the opening of the $Cr\text{-}Cr\text{-}L_{br}$ angles, more so than in the corresponding Mo_2 compounds. This again is due to the shorter Cr-Cr and $Cr\text{-}L_{br}$ bonds. For the N^O-bridged and the C^O portion of the $(C^O)_2(O^O)_2$ bridge, the 'bite' of the bridging group is larger than the Cr-Cr distance and the necessary increase in the $Cr\text{-}Cr\text{-}O_{br}$ and $Cr\text{-}Cr\text{-}(C/N)_{br}$

angles over 90° occurs mostly in the former.

The Cr-Cr bond exhibits sensitivity to the nature of the bridging group, however, the (k_r,r_o) used to model the Cr-L_{br} bonds in these compounds of different bond order, remains unchanged.

The N^O-bridged compounds with remote axial donation by CH_2X_2 (X = Cl, Br) (Cr--X ca. 3.4 Å) has the same Cr-Cr bond order as those lacking axial ligation. This clearly implies very weak, if at all, donation by these ligands. The slightly longer Cr-Cr distance in these axially coordinated compounds over that of the parent molecule is purely of steric origin.

It is now clear, that axial coordination is not uniquely influential in determining the strength of the Cr-Cr bond, the nature of the bridging ligand, X^Y, also plays a role.

The solid state Raman spectrum of $Cr_2(MHP)_4$ shows a very strong band at 556 cm^{-1}. This band was originally assigned to ν_{Cr-Cr}. However a band occurs at 548-554 cm^{-1} in the infra-red and Raman spectrum of all $M_2(MHP)_4$ compounds. Also, the electronic spectrum of $Cr_2(MHP)_4$ exhibits a progressional origin having a spacing of ca. 320 cm^{-1}. These experimental observations clearly rules out the previous 556 cm^{-1} assignment for the ground-state Cr-Cr stretch. It was concluded that the vibrational structure be assigned to a Cr-ligand stretching vibration in the excited electronic state. It appears that there is no band in the Raman spectrum that can be assigned to a pure Cr-Cr stretch.

8.5.3 The Existence of Fractional Cr-Cr Bond Orders

A common problem in the field of metal-metal bonding is the assignment of exact bond orders. In many cases bond orders actually appear to be fractional rather than integral. This is not always easy to rationalize in terms of the established models of multiple bonding. In terms of the screening mechanism proposed by Boeyens [140], bonds of exact integral order would be the exception rather than the rule. The method assumes that bond order derives essentially from changes in the repulsive part of covalent interactions and more specifically from a modification of the internuclear repulsion due to electronic screening. This electron density must be sensitive to the nature of any ligands attached to the bonded metal atoms. One therefore expects M-M bond orders spanning the whole region of orders instead of well-defined integral bond orders only. This is exactly what the Cr_2 system is experiencing.

8.5.4 Comparison with Previous Predictions

From studies of the photoelectron spectra of dimolybdenum and dichromium carboxylato-bridged compounds, it is believed that these two metal compounds have different electronic structures [100]. In contrast to the photoelectron spectra of the corresponding carboxylato complexes, essentially the same spectral profile is observed for both $Mo_2(MHP)_4$ and $Cr_2(MHP)_4$ [141].
The assignment problems encountered for the gas-phase photoelectron spectrum of Cr_2 carboxylato compounds, probably lies in the expectation of observing ionizations characteristic of a quadruple Cr-Cr bond. Assignment of the ionization bands should be clearer, now that the Cr-Cr bond is known to be of order 3.30.
The $Cr_2(MHP)_4$ compound is closer to being quadruple and therefore has similar ionization bands to the quadruple

$Mo_2(MHP)_4$ molecule.

Ab initio calculations including a limited amount of CI have predicted that the Cr_2 bond in the carboxylato compound has a minimum in the potential energy curve at ca. 2.40 Å [102] and has an effective bond order of 1.10. The potential energy minimum occurs at 1.93 Å for $Cr_2((NH)_2CH)_4$ corresponding to a Cr-Cr bond order of 2.57 [142]. The weight of the quadruple bond configuration in the C.I wavefunction is only 16% for the carboxylate, but makes up nearly 50% of the wavefunction for $Cr_2((NH)_2CH)$. Clearly there has been a dramatic change in the bonding.

Similarly $[Cr_2Me_8]^{4-}$ exhibits a minimum in the potential energy curve at 2.16 Å, with a calculated bond order of only 2.0 at 1.980 Å. The weight of the quadruply bonding configuration is only 42% at 1.980 Å. It was concluded [105] that the "'strong Cr-Cr quadruple bond' apparently does not exist".

Clearly the theoretical work is still seriously wanting, at least with respect to predicting Cr-Cr distances and bond orders. Quadruple Cr-Cr bonds do exist.
The shallow potential energy well found in the ab initio calculations, is one of the most frequently stated reasons for the wide range of Cr-Cr bond lengths since small changes in the compounds can create large changes in the Cr-Cr bond length without changing the total energy significantly. The bonding is explained as quadruple, but only as strong as a 'typical' double bond for $[Cr_2Me_8]^{4-}$, and as strong as 'typical' 2.57 and 1.10 Cr-Cr bond order for the (N-C-N)- and (O-C-O)-bridged compounds, respectively.
This is ludicrous; either the Cr-Cr bond is quadruple or of lower order. Perhaps more realistic results will be accomplished from further ab initio calculations now that the true bond orders are known.

At least the ab initio calculations predict

* a difference in Cr-Cr bonding for different bridging groups, and
* the existence of fractional Cr-Cr bond orders.

8.6 Further Electronic Weakening of the Cr-Cr Bond by Axial Donation.

8.6.1 Introduction

The Cr-Cr bonds with axial ligation, are far longer than might have been expected from the Mo-Mo bond lengths in comparable compounds. Since accepted bond radii of whatever specific form or origin are always at least a little smaller for Cr than for Mo, the Mo-Mo bond lengths might well have been considered an upper limit for the Cr-Cr bond in a homologous compound. The enormous observed lengthening of the Cr-Cr bond for a given (XZY) bridging type, shows that axial coordination is an important determining factor for the strength of the Cr-Cr bond.

Stretching of the dimetal centre originates purely from steric forces for the Mo_2 compounds. Since the Cr_2 bonding is modified simply by changes in the inductive nature of the X^Y bridging unit, electronic weakening by axial donation is more than expected.

The axial ligands affect the Cr-Cr bond primarily by introducing electrons into the d_{z^2}-d_{z^2} σ^* component of the bond. This first order effect is probably accompanied by 2nd-order effects stemming less directly from the addition of negative charge to the metal atoms.

It is notable that, without exception, the bonds to axial ligands are relatively long, indicating that even at their strongest, these bonds are weaker than those to the

equatorial ligand atoms. This is clearly evident from the longer r_o values for Cr-L_{ax} than Cr-L_{eq} in the force field used for the molecular mechanics calculations (Table 8.1). These r_o values for M-L_{ax} are, however, shorter for Cr than Mo, as expected from the intrinsically smaller size of chromium, although greater electronic Cr-L_{ax} interaction cannot be ruled out.

8.6.2 The Amidato-bridged Cr_2 Bond and Axial Coordination

All amidato-bridged Cr_2 compounds have Cr-Cr distances below 1.96 Å in the absence of axial ligands. Axial ligation increases this distance by ca. 0.3 Å.

(a) Molecular Mechanics Calculations

In is noteworthy that the $CrOC_2$ fragment of the axial THF molecules was modelled with a sp^2 geometry. Both oxygen lone pairs therefore contribute to the anti-bonding.

The $\{k_r, r_o\}$ solution curves are shown in Figure 8.7, together with the k_r vs. r_o sampling curve.

The observed Cr-Cr distances are reproduced to within 0.001 Å, as seen in Table 8.7.

The results of applying the relationship between bond order and k_r or r_o, are shown in Table 8.8. Graphical presentation of the (k_r, r_o) values are displayed in Figure 8.8.

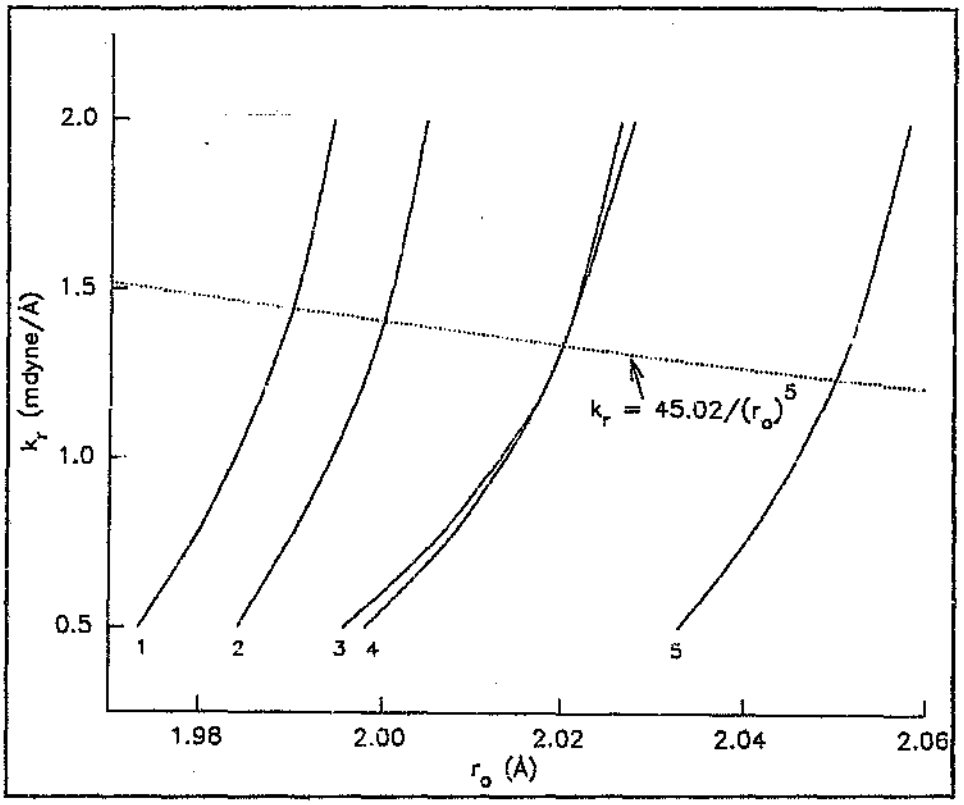


Figure 8.7 Molecular mechanics solution curves for the Cr-Cr centre spanned by N^O ligands, in the presence of axially coordinated THF.

Table 8.7 Calculated and observed Cr-Cr distances

$(XZY)_4$	$(L_{ax})_n$	Calc. (Å)	Obs. (Å)	Figure Label
$(4NMe_2\text{-}C_6H_4)N\text{-}C(Me)\text{-}O$	$(THF)_1$	2.006	2.006(2)	1
(2,6xylyl)N-C(Me)-O	$(THF)_1$	2.022	2.023(1)	2
(2,6xylyl)N-C(Me)-O	$(THF)_2$	2.220	2.221(3)	3
FHP	$(THF)_1$	2.151	2.150(2)	4
PhN-C(NHPh)-O	$(THF)_2$	2.246	2.246(2)	5

Table 8.8 Unique $(k_r, r_o)_{Cr\text{-}Cr}$ and deduced bond orders for the N^O-bridged dichromium complexes, coordinated axially by THF

$(XZY)_4$	$(L_{ax})_n$	(k_r, r_o)	Bond Order	$\nu_{Cr\text{-}Cr}$ $(cm^{-1})^a$
$(4NMe_2\text{-}C_6H_4)N$-C(Me)-O	$(THF)_1$	(1.44, 1.99)	2.36	307
(2,6xylyl)N-C(Me)-O	$(THF)_1$	(1.41, 2.00)	2.30	303
(2,6xylyl)N-C(Me)-O	$(THF)_2$	(1.3', 2.02)	2.19	296
FHP	$(THF)_1$	(1.34, 2.02)	2.19	296
PhN-C(NHPh)-O	$(THF)_2$	(1.24, 2.05)	2.03	285

a :localized harmonic Cr-Cr stretch

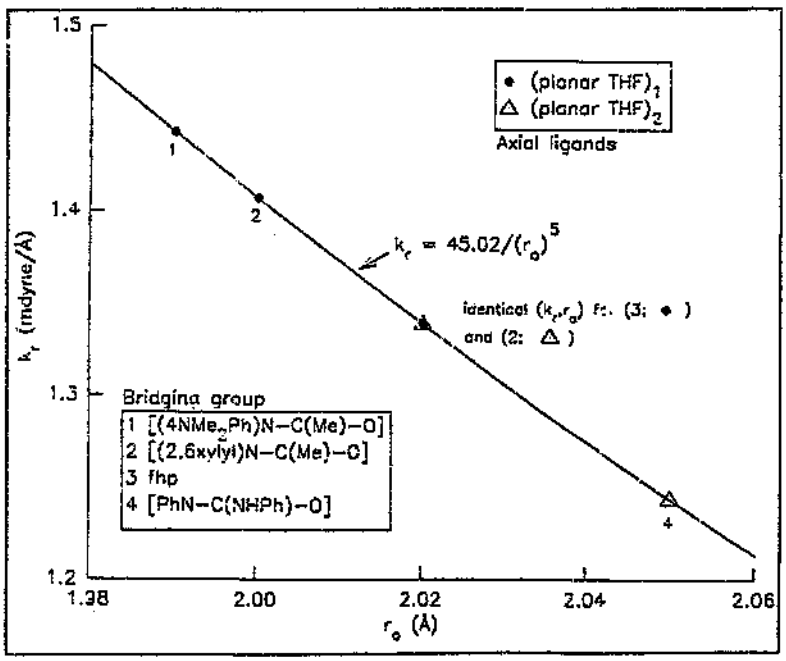


Figure 8.8 Graphical presentation of the variation in k_r and r_o for the Cr-Cr bond in the N^O-bridged compounds, coordinated axially by one or two THF molecules.

(b) Discussion

The results clearly reveal further weakening of the Cr-Cr bond bridged by N^O ligands due to axial donation by THF. In fact, the Cr-Cr bond strength is inversely related to the number of axial THF molecules, as demonstrated by the lower bond order for the $Cr_2[(2,6xylyl)NC(Me)O]_4$ molecule with two THF molecules as opposed to only one.

For the N^O-bridged Cr_2 compounds effectively lacking $Cr-L_{ax}$ interaction, the bond order remains 3.70 regardless of changes in the substituents on the bridging atoms.

Now, in the presence of axial interactions, these factors are somewhat enhanced by the fact that as the Cr-Cr bond weakens, it becomes more sensitive to such changes as ligand substitution. This is exemplified by the gradual decrease in Cr-Cr bond order on going from the bridging group $[(4NMe_2)N-C(Me)-O]$ to $[(2,6xylyl)N-C(Me)-O]$ to (FHP), all having only one axial THF molecule. In fact the bond order for $Cr_2(FHP)_4(THF)_1$ is identical to that of $Cr_2[(2,6xylyl)NC(Me)O](THF)_2$, despite the lesser degree of axial donation in the former compound. This illustrates the powerful effect on the Cr-Cr bond of the kind of substituents on the N-C-O bridge. There is obviously a synergic effect here, with weakly donating N^O groups causing increased donation by the axial O atoms of the THF ligands. The presence of the very electron-withdrawing F^- in the former complex enhances the axial donation by the sole THF, weakening the Cr-Cr bond to the order of 2.19 occurring in a compound having two axial THF molecules and a electron rich bridge.

The solution curves are all of positive slope due to the stretching of the Cr-Cr bond by both the bridging ligand to the natural 'bite', and the additional steric

congestion caused by the presence of axial ligands. The excessive 'bite' is once again compensated for almost entirely by the more obtuse Cr-Cr-O_{br} angles.
When there is only one axial THF molecule present, the Cr-Cr-L_{br} angles are more obtuse about the Cr atom having no Cr-L_{ax} interaction. This is purely a steric consequence.

The (k_r,r_o) couple for the Cr-L_{br} bond is unchanged by the varying Cr-Cr bond order. Any change in the observed Cr-L_{br} bond distances is of steric nature only.

It is quite remarkable that such weakly bound axial THF molecules can actually influence the Cr-Cr bonding pattern.

The bridging and axial ligands do not affect the Cr-Cr bonding independently, but cooperatively. It is therefore difficult to assign the weakening of the Cr-Cr bond to the interaction of specific orbitals. One possibility is donation of electron density by the axial ligand into Cr-Cr σ^* orbitals.

8.6.3 The Carboxylato-bridged Cr_2 Bond and Axial Coordination

The change in the Cr-Cr distance upon axial coordination is even more drastic for the carboxylato-bridged compounds, namely 0.6 Å compared to the 0.3 Å variation for the amidato-bridged complexes.

Previous experimental attempts at correlating Cr-Cr bond strength (as observed by changes in the Cr-Cr distance) with the nature of the bridging ligands, or the nature and proximity of axial donation in these carboxylato compounds, are rather loose and erratic. However, the results do seem to bear out the generally accepted

concept that increased strength of axial coordination and/or decreased donation by bridging groups lead to decreased strength of the M-M bond.
It was hoped that exclusion of steric factors would produce more intelligible results.

(a) Molecular Mechanics Calculations

A large range of crystallographically solved structures for the dichromium carboxylato-bridged compounds, with axial coordination, is available. This large data set allows for a study of the response of the Cr-Cr bond in $Cr_2(O_2CR)_4(L_{ax})_n$ (n = 1, 2) compounds to the character of R and to the strength of axial coordination.

As noted before, axial THF and H_2O can have orientations consistent with either a planar (sp^2) or a tetrahedral (sp^3) $CrOR_2$ fragment, donating either two or one lone pairs into antibonding Cr orbitals. Fortunately, the H positions for all the axial water molecules were found in the crystal structure making it possible to consider the detailed mode of interaction between the water molecule and Cr atom. Force field parameters for both arrangements have already been defined.

All structural parameters are modelled with the same accuracy as the previous calculations.
The molecular mechanics solution curves are presented in Figure 8.9 for the Cr_2 unit coordinated axially to oxygen donors, and in Figures 8.10 - 8.13 for the axial donors of pyridine and substituted pyridine. The corresponding calculated Cr-Cr distances are given in Tables 8.9 and 8.10.

The $\{k_r, r_o\}_{Cr-Cr}$ solution curve for $Cr_2Cp_2(CO)_6$, which is isostructural and isoelectronic to the analogous Mo_2

compound, is also given in Figure 8.9. The calculated Cr-Cr separation of 3.283 Å, is within 0.001 Å of the observed separation of 3.281(1) Å.

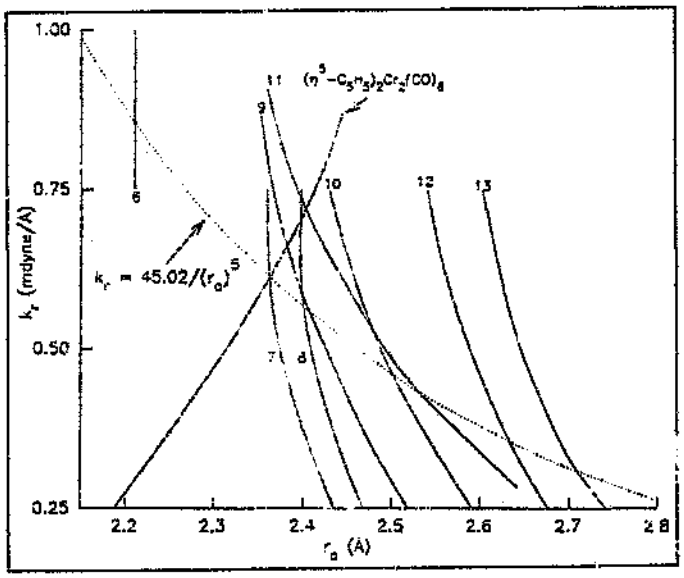


Figure 8.9 Molecular mechanics solution curves for the carboxylato-bridged Cr-Cr bond with O-donor axial ligands.

Table 8.9 Calculated and observed Cr-Cr distances for the $Cr_2(O_2CR)_4$ compounds with axial O-donors

R	$(L_{ax})_n$	Calc. (Å)	Obs. (Å)	Figure Label
carbonate (O)	$(H_2O)_2$ (sp^2)	2.214	2.214(1)	6
biph	$(inter.)_1$[a]	2.349	2.348(2)	7
Me	$(inter.)_2$[b]	2.286	2.288(2)	9
CMe_3	$(inter.)_2$[b]	2.390	2.388(4)	8
Me	$(H_2O)_2$ (sp^3)	2.360	2.362(1)	11
biph	$(THF)_2$ (sp^3)	2.316	2.316(3)	10
CF_2F	$(Et_2O)_2$ (sp^2)	2.490	2.490(3)	12
CF_3	$(Et_2O)_2$	2.541	2.541(1)	13

a :dimer of $Cr_2(O_2biph)_4$ dimers

b :intermolecular O donation from neighbouring molecule

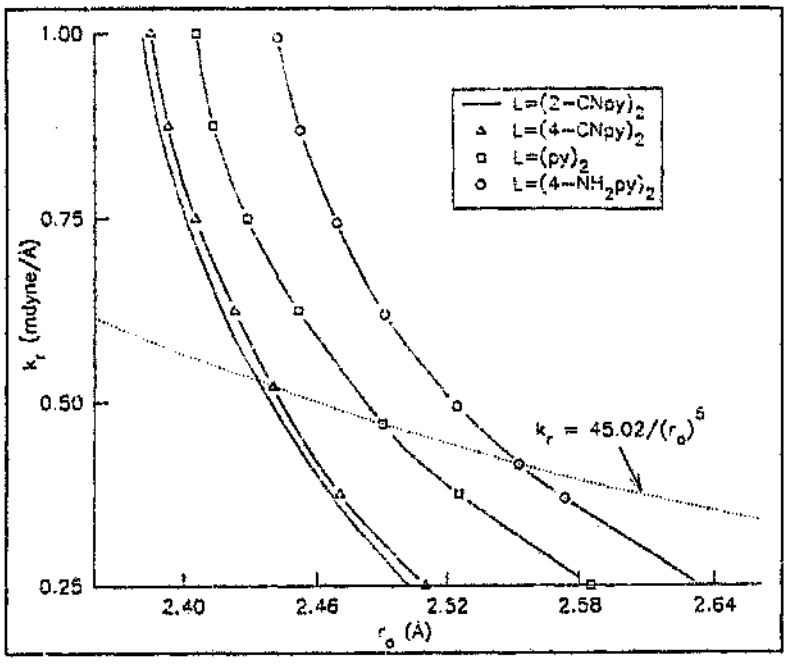


Figure 8.10 Molecular mechanics solution curves for $Cr_2(O_2CCMe_3)_4L_2$ with pyridine or substituted pyridine as axial donors.

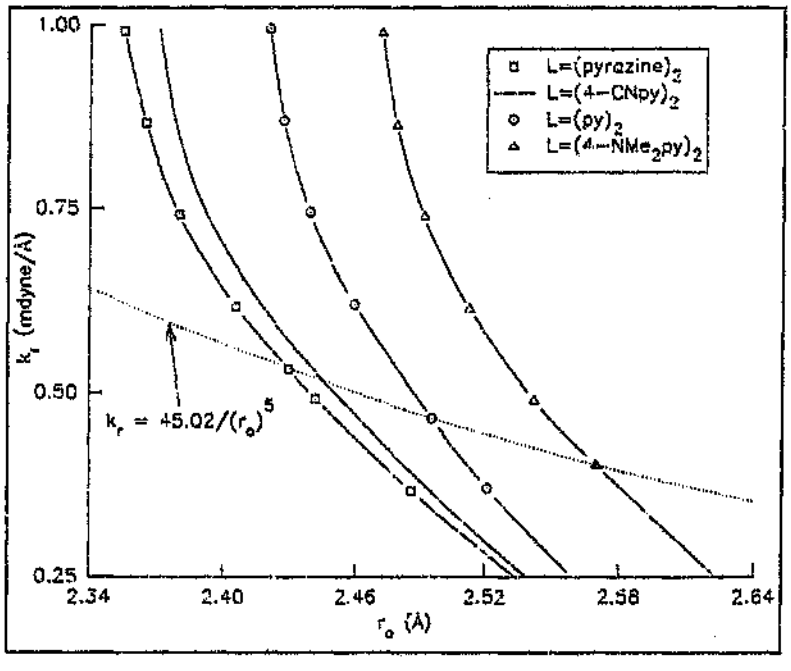


Figure 8.11 Molecular mechanics solution curves for $Cr_2(O_2CMe)_4L_2$ with N-donor axial ligands.

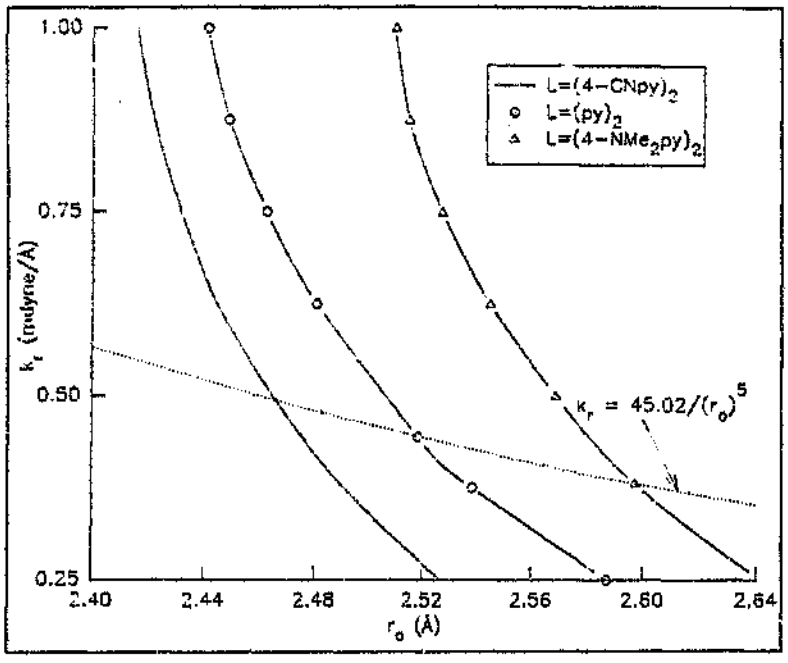


Figure 8.12 Molecular mechanics solution curves for $Cr_2(O_2CH)_4L_2$ with pyridine or substituted pyridine as axial donors.

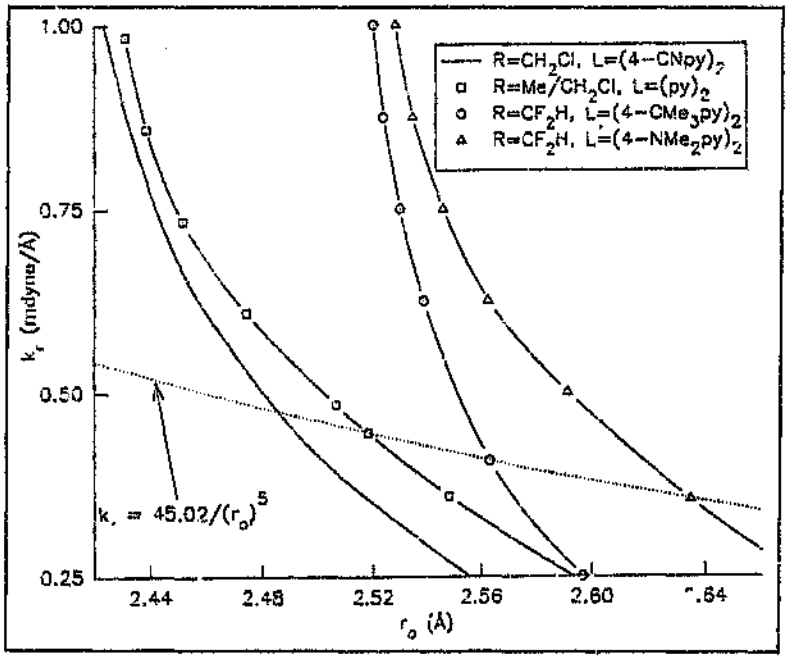


Figure 8.13 Molecular mechanics solution curves for $Cr_2(O_2CR)_4L_2$ with N-donor axial ligands.

Table 8.10 Calculated and observed Cr-Cr distances for $Cr_2(O_2CR)_4L_2$ with axial N-donors

R	$(L_{ax})_2$	Calc. (Å)	Obs. (Å)
CMe_3	2-CNpy	2.327	2.327(1)
CMe_3	4-CNpy	2.335	2.335(1)
CMe_3	py	2.358	2.359(3)
CMe_3	4-NH_2py	2.380	2.379(1)
Me	pyrazine[a]	2.295	2.295(2)
Me	4-CNpy	2.315	2.315(2)
Me	py	2.370	2.369(2)
Me	4-NMe_2py	2.410	2.411(1)
H	4-CNpy	2.385	2.385(3)
H	py	2.408	2.408(1)
H	4-NMe_2py	2.443	2.443(1)
CH_2Cl	4-CNpy	2.408	2.408(4)
Me/CH_2Cl	py	2.369	2.367(2)
CF_2H	4-CMe_3py	2.514	2.514(1)
CF_2H	4-NMe_2py	2.500	2.500(1)

a :bifunctional pyrazine forms a 1:1 complex with $Cr_2(OAc)_4$ linking the Cr_2 units into chains

The force constants and reference bond lengths are read from the points of intersection of the sampling curve with the molecular mechanics solution curves. The values so obtained are presented in Figure 8.14.

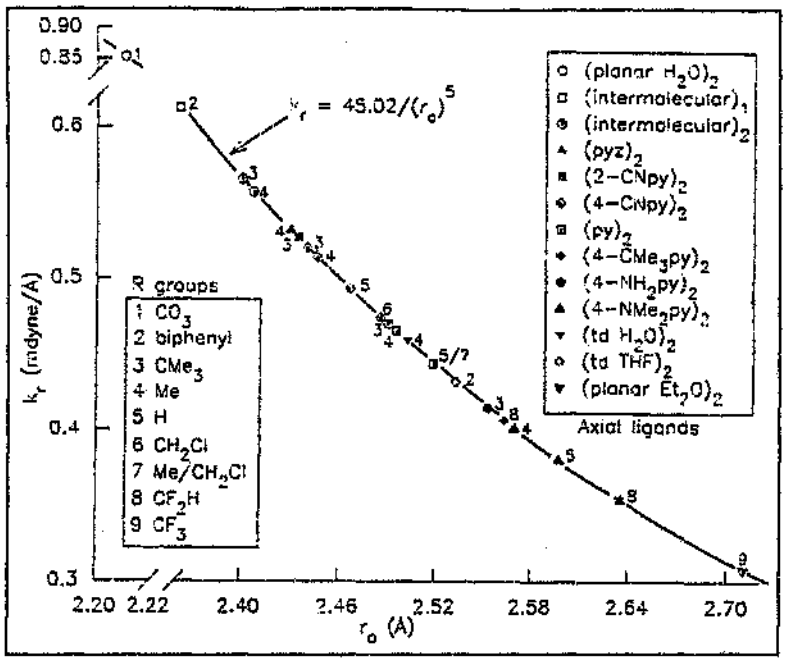


Figure 8.14 Trend in force constant and electronic separation for the Cr-Cr bond in $Cr_2(O_2CR)_4L_2$.

The bond orders derived from the k_r or r_o values are summarized in Tables 8.11-8.12 and exemplified in Figure 8.15.

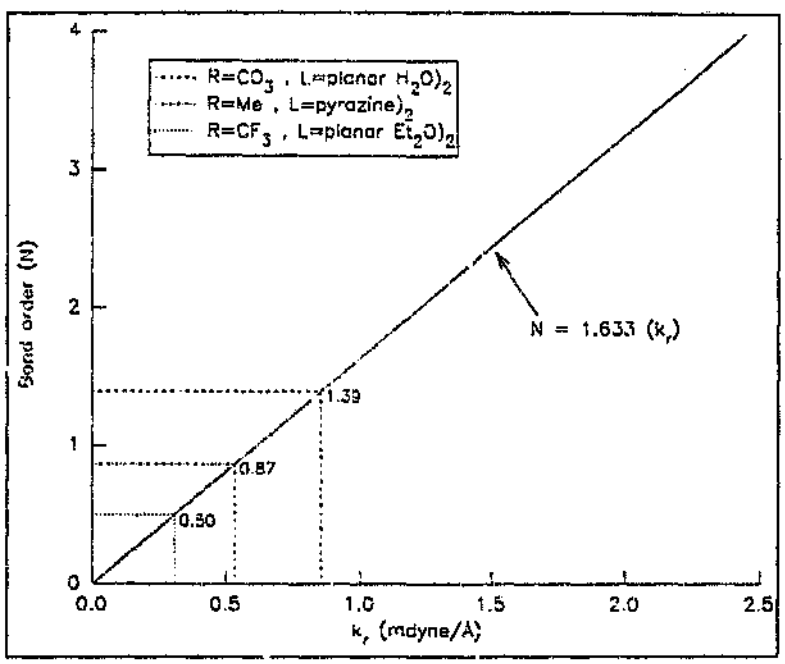


Figure 8.15 Deduction of the Cr-Cr bond order.

Table 8.11 Bonding parameters for the Cr-Cr bond in $Cr_2(O_2CR)_4L_2$ compounds with axial O-donors

R	$(L_{ax})_n$	(k_r, r_o)	Bond Order	ν_{Cr-Cr} $(cm^{-1})^a$
O (carbonate)	$(H_2O)_2$ (sp^2)	(0.85, 2.21)	1.39	236
biph	$(inter.)_1$	(0.61, 2.36)	1.00	200
CMe_3	$(inter.)_2$	(0.57, 2.40)	0.92	193
Me	$(inter.)_2$	(0.56, 2.41)	0.91	191
Me	$(H_2O)_2$ (sp^3)	(0.46, 2.50)	0.75	173
biph	$(THF)_2$ (sp^3)	(0.43, 2.53)	0.71	168
CF_2H	$(Et_2O)_2$ (sp^2)	(0.35, 2.63)	0.58	151
CF_3	$(Et_2O)_2$ (sp^2)	(0.31, 2.71)	0.50	142

a :localized harmonic Cr-Cr stretch

Table 8.12 Bonding parameters for Cr-Cr in $Cr_2(O_2CR)_4L_2$ with axial N-donors

R	$(L_{ax})_2$	(k_r, r_o)	Bond Order	ν_{Cr-Cr} $(cm^{-1})^a$
CMe_3	2-CNpy	(0.53, 2.43)	0.86	186
CMe_3	4-CNpy	(0.52, 2.44)	0.85	184
CMe_3	py	(0.47, 2.49)	0.77	175
CMe_3	4-NH_2py	(0.42, 2.55)	0.68	166
Me	pyrazine	(0.53, 2.43)	0.87	186
Me	4-CNpy	(0.51, 2.45)	0.84	182
Me	py	(0.47, 2.50)	0.76	175
Me	4-NMe_2	(0.40, 2.57)	0.66	162
F	4-CNpy	(0.49, 2.47)	0.81	179
H	py	(0.44, 2.52)	0.73	169
H	4-NMe_2py	(0.38, 2.60)	0.62	158
CH_2Cl	4-CNpy	(0.47, 2.49)	0.77	175
Me/CH_2Cl	py	(0.44, 2.52)	0.73	169
CF_2H	4-CMe_3py	(0.41, 2.56)	0.66	164
CF_2H	4-NMe_2py	(0.35, 2.63)	0.58	151

a :localized harmonic Cr-Cr stretch

It should be noted that the experimental results are reported to two decimals only; consequently identical reported (k_r,r_o) values may have dif. erent reported bond orders.

(b) Discussion

It is noteworthy that the sampling curve intersects the solution curve of $Cr_2Cp_2(CO)_6$ at (0.61, 2.36), corresponding to a Cr-Cr bond order of exactly 1.00. This result, in itself, leaves no doubt that the equations modelling the M-M bonding in these dimetal complexes are chemically valid. This molecule is discussed further in a later section.

The most obvious observation is that all Cr_2-carboxylato compounds with one or two Cr-L_{ax} interactions have much lower bond orders than the gaseous $Cr_2(O_2CMe)_4$ molecule. This confirms the strong influence of axial coordination on the bonding nature of Cr atoms in the binuclear complexes.

The electronic bond distance, r_o, for the carbonate is practically independent of k_r.
The r_o value for the each of the other compounds is longer than the observed Cr-Cr separation. The molecular mechanics slopes are different to those generated for previous Cr_2-bridged compounds. In these low-order Cr_2 compounds the Cr-O bonds of the CrO_4 units are bent towards the Cr-Cr bonds simply because the Cr-Cr bond length is greater than can be accommodated without distortion by the 'bite' of the carboxy ligands. In fact, the bridging groups work to compress the Cr-Cr bond from the long r_o values to the shorter natural 'bite' distance of ca. 2.2 Å.

Sterically bulky ligands in the axial positions

counteract this compression. Thus, it is reasonable to see a weakly donating axial ligand have a long observed Cr-Cr distance, longer than a stronger axial donor, simply because it has a greater steric resistance to contraction of the carboxylate framework. This is illustrated by the effect of axial pyridine. For R = Me, it is less effective than water in electronically weakening the Cr-Cr bond, but since it sterically inhibits contraction of the carboxylate framework, the observed bond length is longer than for the hydrate.

The equilibrium Cr-Cr separation is a result of rather complex steric forces, and simple deduction of the Cr-Cr bond strength from inspection of these observed Cr-Cr distances is totally misleading and unscientific.
The negative slopes show, however, that the steric forces exerted by the bridging ligands are still more important.

Even though the axial donation is relatively weak, as demonstrated by the long r_o values for the Cr-L_{ax} interactions, they have a decisive influence on the Cr-Cr bonding. Although the Cr-Cr bond is modified by the electronic influence of the coordinated ligands, the Cr-O_{br} force field parameters remain unchanged.

The force constants obtained from the molecular mechanics calculations can be used to derive ν_{Cr-Cr}, assuming localized harmonic vibration. Unfortunately, there is no vibrational spectral data on $Cr_2(O_2CR)_4$-type compounds, gaseous or solid.

The calculated bond order of 0.5 for $Cr_2(O_2CCF_3)(Et_2O)_2$ is in accord with its experimentally observed paramagnetism (μ_{eff} = 0.85 BM at 25°C). This serves to justify the chemical validity of the relationships used to model the M-M bond in these binuclear complexes.

(c) Cr-Cr Bond Order Trends within the Cr_2 Carboxylates

The variations in Cr-Cr bond order cannot be accounted for solely by postulating linear and independent dependencies on the inductive effect of the R groups and the donor ability of the axial ligands.

The pK_a of the acid from which the bridging ligand is derived gives an appropriate measure of the donor strength of the bridging ligand. On this basis, weak acids yield strongly donating anionic ligands and strong acids weakly donating anionic ligands.

The more electron-withdrawing the character of R, the greater the donation by a given axial ligand. There is obviously a synergic effect here, as was observed in the amidato-bridged compounds bound axially by THF molecules. In the presence of axial ligands, the sensitivity of the Cr-Cr bond to the nature of the substituents on the O-C-O bridging atoms is enhanced, a consequence of the weaker Cr-Cr bond.

The role played by the axial and bridging ligands can be investigated by employing sets of compounds in which the carboxyl groups remain unchanged while the axial ligands are varied, or, conversely, the axial ligand is fixed and the R groups are varied.

The carboxylato-compounds with pyridine or its derivatives as axial ligands provides such an opportunity.

The dependence of the Cr-Cr bond strength on the pK_a of the acids, from which the bridging ligand is derived, is clearly demonstrated in Figure 8.16. Here, compounds with the same bridging ligand are located at the same ordinate, of course, and the Cr-Cr bond order for a given

axial ligand is decreased as the bridging ligand becomes a weaker donor. The compounds with the same axial ligands give essentially straight lines (experimental error may cause slight deviations). The positive slope indicates a positive relationship between Cr-Cr bond order and the donor strength of the bridging ligands. In fact, the change in bond order for a given change in axial N-donor is approximately constant for any given pair of bridging groups.

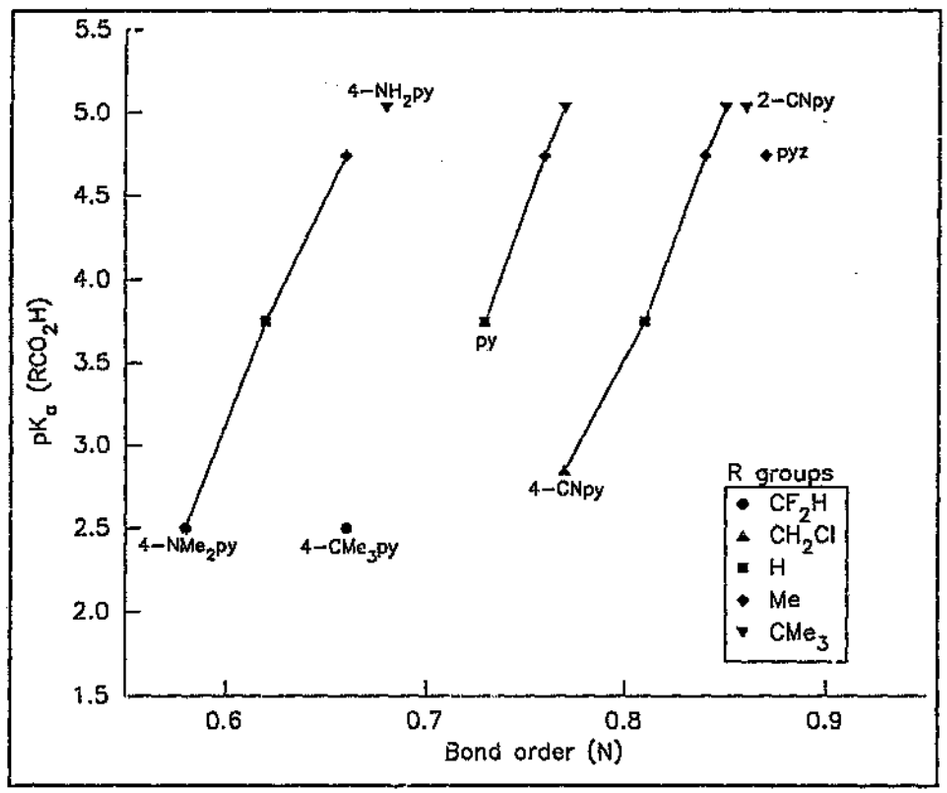


Figure 8.16 Relationship between pK_a (RCO_2H) and calculated bond order for the dichromium carboxylates with N-donor axial ligands.

It might be expected that as the axial ligand becomes a better donor (i.e. more basic, as evidenced by a higher value of pK_a for the protonated base) the Cr-Cr bond order would decrease. For a given bridging group, the axial donation is approximately a linear function of its

σ-donor ability as shown by the [pK_a (axial ligand) vs. bond order] plot in Figure 8.17. Here, compounds with the same bridging ligand are located on essentially straight lines. It is clear from the data that as the bridging group becomes less electron donating, so the Lewis acidity of the Cr-Cr bond towards a given axial ligand increases, as indicated by the decrease in bond order. This increase in acidity is essentially constant for a given change in bridging group, irrespective of the axial N-donor.

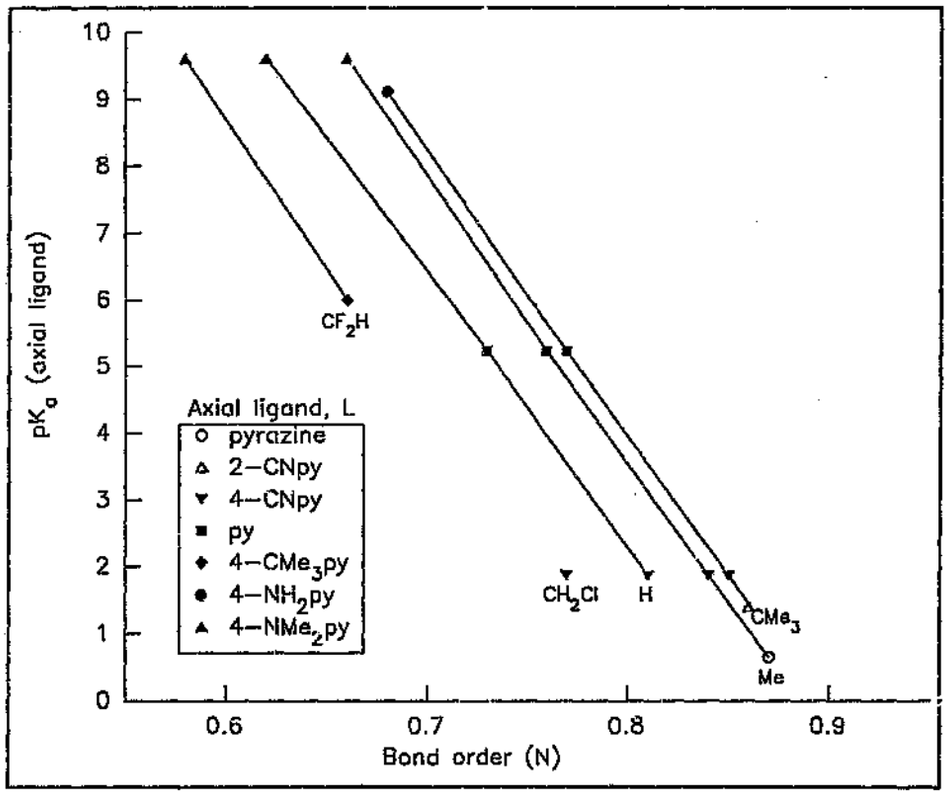


Figure 8.17 Relationship between pK_a (axial ligand) and calculated Cr-Cr bond order for $Cr_2(O_2CR)_4I_2$ compounds with axial N-donors.

The molecular mechanics data suggest that the Cr-Cr bond strength is more sensitive to the change in bridging ligand for a given axial donor, than to the change in axial ligation for a given bridge. This is supported by

the steeper slopes for the [$pK_a(L_{ax})$ vs N] plot.

It would have been interesting to plot the r_o values for the Cr-Cr bond against those of Cr-N_{ax}. However, the observed structures were reproduced with (k_r, r_o) values of (0.70, 2.32) for pyridine, pyrazine, 2CN- and 4CN-pyridine; and (0.70, 2.27) for the $4NH_2$-, $4CMe_3$-, and $4NMe_2$- derivatives of pyridine. These values need not necessarily be the unique couples; they only provide a matching of the observed Cr-N_{ax} distances. However, the different r_o needed to model the two sets of N-donors clearly demonstrates the greater basicity of the latter set.

The $Cr_2(O_2CR)_4$ compounds with O-donation by intermolecular association have bond orders greater than all the other oxygen axial donors, besides that of the carbonate. The formation of a 4-membered ring containing two Cr atoms and two bridging oxygens forces the axial oxygen off the Cr-Cr axis. This together with the longer Cr-O_{ax} distance, works to strengthen the σ contribution of the Cr-Cr bond.

Interestingly though, the dimer of dimers, $[Cr_2(O_2Cbiph)_4]_2$, has a stronger Cr_2 bond than the compounds with intermolecular association at both Cr atoms. Here, the nature of the axial donation dominates. Also R = CMe_3 has a stronger Cr-Cr bond than R = Me, both having intermolecular association.

The $(CO_3)^-$ bridging group represents the one extreme of the donor strength of bridging groups. The axial water molecules donate two lone pairs to the Cr atoms, and yet this molecule has the strongest Cr-Cr bond. This demonstrates the decisive role played by the bridging group here. The strongly electron donating $(CO_3)^-$ group results in poor axial donation, poorer than even intermolecular association.

At the other extreme we have the R = CF_3 bridging group with planar Et_2O groups axially coordinated to the Cr atoms. This molecule has the weakest Cr-Cr bond, as expected from the greater axial donation by two lone pairs and the weaker inductive character of the bridging group.

Between these two extremes are found the R = Me, L_{ax} = $(sp^3\ H_2O)_2$; and R = biph, L_{ax} = $(sp^3\ THF)_2$ molecules, with Cr-Cr bond orders of 0.75 and 0.71 respectively. These axial ligands donate only one lone pair to each Cr atom, yet the Cr-Cr bond is of a lower order than the carbonate. The explanation lies in the fact that the weaker bridging groups (Me, biph) promote greater axial donation, so that the Cr-Cr bond experiences greater weakening by a single oxygen lone pair, than two in the presence of the stronger carbonate bridge.

One may perhaps conclude that for bridging groups of intermediate donor strength the nature of the axial donation is more important, as demonstrated by the decreased Cr-Cr strength in the order of axial donation: $(\text{intermolecular O})_1$ > $(\text{intermolecular O})_2$ > $(1\ L_p\ O)_2$, for R = CMe_3, Me, and biph. However, strongly donating bridging groups, such as carbonates, may reverse the expected donor strength of an axial ligand. Very weakly donating bridging groups, such as CF_2H and CF_3, would just reinforce the expected donor ability of an axial ligand, resulting in a weaker Cr-Cr bond for axial donation by only one oxygen lone pair, than that for axial donation by two lone pairs in the presence of bridging groups of intermediate strength.

In short, there is a cooperative electronic influence of the axial and bridging groups on the Cr_2 bond. As stated before, it is therefore difficult to assign the weakening

of the Cr-Cr bond to the interaction of specific orbitals.

8.6.4 Comparing the Carboxylato-and Amidato-bridged Compounds

The N^O-bridged Cr_2 bond is less weakened by axial coordination than the O^O-bridged compounds. In fact, the difference in bond order between the N^O- and O^O-bridged compounds is enhanced in the presence of axial donation. Since O^O is a weaker donor than N^O, the Cr_2 unit in the carboxylates is an even stronger Lewis acid and so axial donation is greater.

However, carboxylato and carboxanilide complexes of Cr_2 both show a marked sensitivity toward axial coordination. The molecular mechanics calculations have clearly elucidated the cooperative role played by the ligand environment in determining the effective Cr-Cr bonding.

8.6.5 Comparison with Previous Predictions

Ab initio calculations caused some controversy as to the effect of axial ligands on the Cr-Cr bond.

In 1983, Benard [102] calculated a change of only 0.05 Å upon addition of axial water ligands to $Cr_2(O_2CH)_4$ using CI calculations on HF orbitals, whereas changing the bridging ligand from formato to formamidato causes a decrease of 0.5 Å in the equilibrium bond length. This implies that the influence of bridging ligands is far more important.

However, in 1989, Davy et. al. [143], using the GVB method of calculation, predict a lengthening of the Cr-Cr bond by 0.11 Å for formato and 0.18 Å for amidinato upon addition of axial water molecules. Thus, in their

calculations, the amidinato complex is twice as sensitive to axial ligation as the formato complex. This is quite the reverse of the molecular mechanics results. It is logical that the weaker carboxylates be more sensitive. They did, however, predict a steady increase in the Cr-Cr bond strength as the basicity of the bridging ligand increases.

The prediction of Kok et. al. [107] from generalized molecular orbital and CI calculations that "the amidato species do not bind axial ligands as readily as the carboxylato species do", is in agreement with our results.

8.7 The Unsupported Cr-Cr Single Bond

As mentioned in Section 8.6.3 (b), the sampling curve intersects the $\{k_r, r_o\}_{Cr-Cr}$ solution curve of $Cr_2(\ ^5\text{-}C_5H_5)_2(CO)_6$ at a bond order of exactly 1.00, justifying the equations used to model M-M bonding.

8.7.1 Force Field Parameters

The force field parameters defined for the Mo_2 system are transferable to the analogous Cr_2 molecule. The only differences are the Cr-L parameters given in Table 8.13.

Table 8.13 Force field parameters for Cr-L bond deformations

Bond	k_r (mdyne/Å)	r_o (Å)
Cr-CO	2.08	1.85
Cr-Cen	15.00	1.84

8.7.2 Steric Deformations

The most arresting feature is the very long Cr-Cr distance, 3.281(1) Å. It is longer by several tenths of an Å than would naively have been expected by simple reference to the Mo-Mo separation in the analogous compound. The explanation is to be found in the presence of substantial nonbonded repulsions.

The $M_2Cp_2(CO)_6$ molecules are exceptionally sterically crowded, particularly with regard to the interaction between the two halves. It is well to stress that this interaction results from the proximity of three ligands on each metal, viz., the two CO groups which are cis to the M-M bond and the Cp group, with the corresponding three ligands on the other metal atom. The other two CO groups point well away from the region of contact and make no direct contribution to it, although they contribute indirectly because their presence imposes a buttressing effect on each set of three ligands that do make the direct contacts.

The end-against-end repulsion is more severe for the Cr compound because the various Cr-ligand distances are all shorter than the corresponding Mo-L distances by ca. 0.15 Å.
Because of its lower force constant, 0.61 mdyne/Å, the Cr-1-Cr bond is more flexible and easily stretched from 2.36 Å to minimize steric strain at 3.281(1) Å.

Chapter 9

CONCLUDING REMARKS OF GROUP VIA METAL-METAL BONDING

9.1 Overview

9.1.1 Mo_2 vs. Cr_2

Important differences have been noticed in the M-M bonding of the binuclear complexes of transition metals belonging to the same group in the periodic table.

In the case of Mo_2, the ligand environment does not influence the bonding character of the Mo atoms. The situation is not so simple in the case of binuclear complexes of Cr. The extreme variability in observed Cr-Cr distances, not observed for corresponding Mo and W compounds, is a direct consequence of the electronic weakening of the Cr-Cr bond.

The range of Cr-Cr bond orders has been explained by the perturbing effects of the ligands, axial and equatorial, on the bonding character of the Cr_2 centre. These Cr_2^{4+} centres are all formally quadruple, but the 'true' Cr-Cr bonding is an extremely sensitive function of the amount of electron density donated along both the equatorial and outer extensions of the Cr-Cr bond. This donation by the bridging and axial ligands is cooperative, with weakly donating bridging groups enhancing the donation by axial ligands.

9.1.2 Effect of Torsion on the Delta Bond

Another interesting facet of this elaborate molecular mechanics study concerns the barrier to rotation about the M-M bond. The structures of several $Mo_2X_4(L\hat{}L)_2$ molecules in which the steric properties of the bridging bidentate ligand, L^L, serve to change the torsion angle, facilitated a study of this effect. It was found that the quadruple bond could withstand rotation about the Mo-Mo axis as large as ca. 26°, but a twist of 36° destroyed the δ bond and a triply bonded Mo_2 centre resulted.

9.1.3 Other Aspects

Concern has been shown in the literature as to the exact role played by the bridging (XZY) groups in restricting the M-M separation. It is clear from the range of Cr-Cr bond orders supported by such ligands, that the bridging ligands merely keep the metal atoms close enough to interact according to their own electronic requirements, but allow the actual M-M distance to vary enormously as those electronic requirements may dictate.

The last point concerns the relationship between observed M-M distances and M-M bond orders. Bond order is a purely electronic concept whereas bond length depends not only on bond order but also on steric factors. These steric factors become progressively less important with increasing bond order, bond strength, and force constant. Each M-M bond order therefore has a unique electronic separation, r_o, but a range of sterically-modified M-M distances. The efforts of many experimental and theoretical chemists at correlating observed M-M separations with bond strength are in vain, and have resulted in several erroneous attempts at resolving the dichromium controversy.

9.2 What makes Cr_2 Unique?

Chromium exhibits a remarkable and unique variability of bond order not seen for the analogous compounds of Mo_2. The obvious question raised by this result is "what makes chromium so different?"

The precise reason for this difference in behaviour of the formally quadruple Mo-Mo and Cr-Cr bonds is still under study.
It has been suggested from SCF-Xα-SW studies on $M_2(O_2CH)_4$ [144], that there is increased (n+1)s contribution to the M-M σ bonding for Mo_2 and W_2 over that in Cr_2. In fact, there is essentially no 4s atomic orbital participation to the 3d-3d σ bond of $Cr_2(O_2CH)_4$, whereas they [144] find a significant contribution of Mo 5s and W 6s atomic orbital participation to the 4d-4d and 5d-5d σ bond, respectively.

The importance of the s-s σ bonding orbital in the Mo and W systems, is that it provides another mechanism by which the symmetric $(L_{ax})_n$ orbital can interact with the dimetal core, without electronic weakening of the M-M bond. This, of course, is a possible explanation for the insensitivity of Mo_2 to axial ligation. What about the insensitivity of Mo_2 to the inductive nature of the bridging groups?

We defined the constant in the equation relating k_r to r_o to be the 'index of flexibility'. This constant is smaller for the Cr_2 system (45.02), than the Mo_2 system (137.4). This means that the Cr_2 bond is more flexible and hence more sensitive to the perturbing effects of the ligand environment.

9.3 The Value of Molecular Mechanics

Theory has not yet been able to give explicit compound-by-compound predictions. It is therefore very rewarding to present the results of the molecular mechanics calculations done in this thesis.

Molecular mechanics has proved to be a useful technique in probing the nature of M-M bonding in these dimeric complexes. A wealth of information has originated from these studies. The molecular mechanics force constants are presented as a guide to further experimentation, such as photoelectron and M-M vibrational spectroscopy.

9.4 Further Studies

The 'index of inflexibility' is seen to increase as one descends group VIA in the periodic table. It is expected that the W_2 system will be less flexible than Mo_2 and would therefore have a larger force constant for a given bond order. This could be verified by similar molecular mechanics calculations for the range of W_2 complexes available in the literature.

In fact, this method can be extended to dimetal complexes belonging to other groups in the periodic table. In this way, the 'true' bonding within any given dimetal complex can be firmly deduced from simple inspection of its ligand environment.

Chapter 10

MOLECULAR MECHANICS OF SINGLE BONDS IN TETRAKIS(CARBOXYLATO)DIRHODIUM SYSTEMS

The work discussed in this Chapter forms part of the publication:

Françoise M. O'Neill, Jan C.A. Boeyens, *Inorganic Chemistry*, 1990, 29, 1301.

10.1 Introduction

For a dirhodium(II) compound isostructural with $Mo_2(O_2CR)_4$, there are 14 electrons available for occupation of the M-M MO's. Thus in terms of the simple qualitative M-M bonding picture, the Rh-Rh bond order is one.

On the basis of comparisons with Rh-Rh bonds which are unambiguously single and have bond lengths in the range 2.68 - 2.94 Å, it has been suggested that the Rh_2-carboxylato compounds have multiple Rh-Rh bonds, probably of order three.
However, extensive SCF-Xα-SW calculations [145] are in favour of a single Rh-Rh bond, which is now believed to have settled the longstanding bond order controversy.

It is interesting that paralleling the ambiguity about the bond order, there has also been uncertainty about the frequency of the Rh-Rh stretching mode.

The initial indications of San Filippo and Sniadoch [127], subsequently supported by Kharitonov et. al. [146] and Kireeva et. al. [147] were in favour of the range 150-170 cm^{-1} for ν_{Rh-Rh} in a variety of complexes of the type $Rh_2(O_2CR)_4L_2$. This value seems quite consistent with a single bond.

On the other hand, Ketteringham and Oldham [148], who also studied a range of complexes of this sort, favoured the range 288-351 cm^{-1} for ν_{Rh-Rh}, which seems somewhat high for a single bond.

Recent electronic, infrared, Raman and resonance Raman studies [149, 150] have shown that ν_{Rh-Rh} should rather be assigned to the band at ca. 300 cm^{-1}.

10.2 Molecular Mechanics Calculations

It is of interest to see if this assignment could be sustained by molecular mechanics simulation of the known dirhodium system, using the corresponding harmonic force constant of 2.73 mdyne/Å.

Calculations were done on a series of $Rh_2(O_2CR)_4L_2$ systems [151-155], allowing for the variation of both the carboxyl group and the axial ligands.

Force field parameters not already defined for Mo_2- and Cr_2-carboxylato compounds and transferable to the Rh_2 system, are summarized in Tables 10.1 and 10.2.

Since the hydrogen positions were not found in the crystal structure of $Rh_2(O_2CR)_4(H_2O)_2$, both sp^3 and sp^2 geometries were modelled for the O atom.
Since we have a single Rh-Rh bond, the torsions are of a repulsive nature with $V_{\chi=45°} = 0.0033$ kcal/mol.

Table 10.1 Force field parameters for bond and angle deformations

Bond	k_r (mdyne/Å)	r_o (Å)
$Rh-O_{br}$	0.84	2.03
S-C	3.50	1.80
$S-L_p$	6.00	1.00
As-C	3.50	1.90
Sb-C	3.50	2.09
$Rh-O_{ax}$ (H_2O)	0.80	2.29
$Rh-O_{ax}$ (Me_2SO)	0.80	2.21
$Rh-S_{ax}$	0.80	2.35
$Rh-P_{ax}$	0.80	2.44
$Rh-As_{ax}$	0.80	2.55
$Rh-Sb_{ax}$	0.80	2.71
Angle	k_θ (mdyne.Å)	θ_o (rad.)
$L_p-O=S$	1.00	2.094
$L_p-S=O$	1.00	1.911
O=S-C	1.00	1.911
C-S-C	0.10	1.911
L_p-S-C	1.00	1.911
S-C-H	0.65	1.911
$C_{ar}-L_{ax}{}^a-C_{ar}$	0.1	1.911
$L_{ax}{}^a-C_{ar}-C_{ar}$	0.65	2.094
Rh-O=S	0.20	2.094
Rh-S=O	0.10	1.911
Rh-S-C	1.00	1.911
$Rh-L_{ax}{}^a-C_{ar}$	0.10	1.911

a :L_{ax} = As, Sb, P

Table 10.2 Nonbonded parameters

Interaction	a (u)	b ($Å^{-1}$)	c (u.$Å^6$)
Rh--Rh	24.0	2.40	4.00
Rh--O	217.0	3.32	2.46
Rh--H(L_p)	42.7	3.13	1.17
Rh--C	220.0	3.22	2.88
Rh--F	215.6	3.44	1.90
Rh--S	25.0	3.02	7.48
Rh--P	516.1	3.17	6.50
Rh--As	129.1	2.70	10.21
Rh--Sb	125.5	2.53	16.5

The results are summarized in Table 10.3.

Table 10.3 Calculated and observed Rh-Rh distances (k_r = 2.73 mdyne/Å) together with the tabulated values of r_o

R	$(L_{ax})_2$	Calc. (Å)	Obs. (Å)	r_o (Å)	Ref.
CMe_3	H_2O (sp^3)	2.371	2.371(1)	2.42	151
CMe_3	H_2O (sp^2)	2.371	2.371(1)	2.41	151
Me	H_2O (sp^3)	2.385	2.3855(5)	2.43	152
Me	H_2O (sp^2)	2.385	2.3855(5)	2.42	152
C_2H_5	Me_2OS	2.407	2.407(1)	2.43	153
Me	Me_2OS	2.406	2.406(1)	2.44	151
Me	PPh_3	2.450	2.4505(2)	2.46	154
Me	$AsPh_3$	2.427	2.427(1)	2.44	155
Me	$SbPh_3$	2.420	2.421(4)	2.43	155
CF_3	Me_2SO	2.420	2.419(1)	2.45	153

All structures were simulated satisfactorily by using values of r_o within the range 2.41 - 2.46 Å, which is considered to be within experimental error.

10.3 Discussion

The conclusion to be drawn is that the Rh-Rh bond order is unity in all cases and that the observed variations in bond length are due entirely to steric factors that are governed by the nature of the bridging or axial donor groups. The $[RCO_2]^-$ ligands have the effect of drawing the metal atoms together, which is obviously counteracted by the presence of axial ligands, more so for the bulky LPh_3 (L= P, As, Sb) ligands.

The compression of the Rh-Rh bond from a long r_o distance to the natural 'bite' of the bridging group, provides a rationale for the shortness of the Rh_2 bond, which in the absence of bridging ligands would be closer to 2.7 Å. The study on Rh_2 has revealed, once again, the extreme caution needed in assuming that observed distances reflect bond strength.

In a previous analysis [122] of the dirhodium centre by molecular mechanics, a harmonic force constant of 0.88 mdyne/Å, calculated from a measured Rh-Rh vibration frequency of 170 cm^{-1}, was used in the force field for Rh-Rh single bonds.

It is therefore necessary to point out, once again, that any given molecular property can always be simulated in molecular mechanics by a matched pair of parameters (k, p_o), consisting of a force constant and a characteristic value. In general, where neither is fixed by experimental evidence, a solution set can be chosen over an extensive range without affecting the simulation.

This is exactly what was done in the analysis of M-M bonding for the Mo_2 and Cr_2 systems. The ultimate aim is to have both parameters fixed experimentally. This has been achieved, via elaborate molecular mechanics calculations, for the group VIA Mo_2 and Cr_2 bonds of various orders. A shorter means to the unique couple is frustrated by wrong vibrational band assignments, and, if correctly assigned, by extensive coupling of different modes.

'.. when the tangled web of our experience is transformed into symmetries of pristine order and the chemical equivalent of the rich diversity of pattern of an oriental carpet - it is then that one encounters a moment of intellectual pleasure that really makes one feel good about being a chemist.'

Ronald Hoffman (1982)

Refinement of the Standard Expression for Threefold Rotational Barriers

The molecular mechanics program currently used by our research group is not too well adapted to the study of dimetal compounds and delocalized systems.

In the original software, all torsional contributions to steric strain are simply calculated from the expression commonly used for threefold rotational barriers, ie, $U = V/2[1 + \cos3(\chi-(\chi_o - 180^\circ))]$, with this term being considered to be zero for all torsion angles, χ, greater than 60°.

This potential adequately models the repulsive torsional interactions between bonding electron groups adjacent to the M-M bond (bond order 3.0 or less) in $L_3M\text{-}ML_3$ dimers. Here, the repulsion between the electron groups favours a staggered ($\chi_o = 60^\circ$) conformation.
However, this threefold potential has minima at $\chi = |60^\circ|$ and $\chi = |180^\circ|$, which can result in false energy minimization of the molecular structure. The symmetry of the original expression was therefore reduced to ensure a single minimum at $\chi = |60^\circ|$.

The original threefold potential has, however, no physical meaning when applied to rotation about the M-M bond (bond order 4.0 or 3.5) in $L_4M\text{-}ML_4$ dimers, or to delocalized systems. Here, it is not the repulsion but rather the attraction of the electron groups adjacent to the reference bond that favours the eclipsed conformation. Hence, onefold torsional potentials which

describe the attraction of the electron groups ($\chi_o = 0^\circ$) are physically more correct.

For $L_4M\text{-}ML_4$ dimers with a M-M bond order of 3 or less, a repulsive interaction between electron groups adjacent to the M-M bond favours a staggered ($\chi_o = 45^\circ$) conformation. The original threefold potential has therefore no physical meaning in such a system. A onefold potential describing the repulsion between the electron groups at $\chi < |45^\circ|$, is more correct. Here, the repulsive interactions approach zero as $\chi \rightarrow 45^\circ$.

In summary, the original threefold potential has been refined so as to provide a more meaningful analysis of various systems, as well as to eliminate possible false energy minimization.

REFERENCES

1. L. Pauling, *The Nature of the Chemical Bond*, 3rd Ed., Cornell University Press, Ithaca, N.Y., 1960.

2. F.A. Cotton et al, *Science*, 1964, 145, 1305.

3. F.A. Cotton, *Inorg. Chem.*, 1965, 4, 334.

4. F.A. Cotton, C.B. Harris, *Inorg. Chem.*, 1965, 4, 330.

5. K.H. Johnson, *Adv. Quantum Chem.*, 1973, 7, 143.

6. J.G. Norman Jr., H.J. Kolari, *J. Chem. Soc., Chem. Comm.*, 1974, 303.

7. J.G. Norman Jr., H.J. Kolari, *J. Am. Chem. Soc.*, 1975, 97, 33.

8. A.P. Mortola, J.W. Moskowitz, N. Rosch, *Int. J. Quantum Chem., Symp. No. 8*, 1974, 161.

9. A.P. Mortola, J.W. Moskowitz, N. Rosch, C.D. Cowman, H.B. Gray, *Chem. Phys. Lett.*, 1975, 32, 283.

10. M. Benard, A. Viellard, *Nouv. J. Chim.*, 1977, 1, 97.

11. M. Benard, *J. Am. Chem. Soc.*, 1978, 100, 2359.

12. J.G. Norman Jr., H.J. Kolari, *J. Chem. Soc., Chem. Comm.*, 1975, 649.

13. J.G. Norman Jr., H.J. Kolari, H.B. Gray, W.C. Trogler, *Inorg. Chem.*, 1977, 16, 987.

14. F.A. Cotton, G.G. Stanley, B.J. Kalbacher, J.C. Green, E. Seddon, M.H. Chisholm, *Proc. Nat. Acad. Sci. USA*, 1977, 74, 3109.

15. B.E. Bursten, F.A. Cotton, J.C. Green, E.A. Seddon, G.G. Stanley, *J. Am. Chem. Soc.*, 1980, 102, 4579.

16. J.V. Brencic, F.A. Cotton, *Inorg. Chem.*, 1969, 8, 7.

17. J.V. Brencic, I. Leban, P. Segedin, *Z. Anorg. Allg. Chem.*, 1976, 427, 85.

18. F.A. Cotton, J.M. Troup, T.R. Webb, D.H. Williamson, G. Wilkinson, *J. Am. Chem. Soc.*, 1974, 96, 3824.

19. F.A. Cotton, M.W. Extine, T.R. Felthouse, B.W.S. Kolthammer, D.G. Lay, *J. Am. Chem. Soc.*, 1981, 103, 4040.

20. M.D. Hopkins, W.P. Schaefer, M.J. Bronikowski, W.H. Woodruff, V.M. Miskowski, R.F. Dallinger, H.B. Gray, *J. Am. Chem. Soc.*, 1974, 96, 3824.

21. F.A. Cotton, L.M. Daniels, G.L. Powell, A.J. Kahaian, T.J. Smith, E.F. Vogel, *Inorg. Chim. Acta*, 1988, 144, 109.

22. F.A. Cotton, K.J. Wiesinger, *Inorg. Chem.*, 1990, 29, 2594.

23. E.H. Abbot, F.A. Cotton, *Inorg. Chem.*, 1978, 17, 3240.

24. F.A. Campbell, F.A. Cotton, G.L. Powell, *Inorg. Chem.*, 1984, 23, 4222.

25. P.A. Agaskar, *J. Am. Chem. Soc.*, 1984, 106, 1851.

26. F.L. Campbell, F.A. Cotton, G.L. Powell, *Inorg. Chem.*, 1985, 24, 177.

27. P.E. Fanwick, W.S. Harwood, *Inorg. Chim. Acta*, 1986, 122, 7.

28. F.A. Cotton, Z.C. Mester, T.R. Webb, *Acta Crystallogr.*, 1974, B30, 2768.

29. F.A. Cotton, J.G. Norman Jr., B.R. Stults, T.R. Webb, *J. Coord. Chem.*, 1976, 5, 217.

30. F.A. Cotton, J.G. Norman Jr., *J. Coord. Chem.*, 1971, 1, 161.

31. F.A. Cotton, M. Extine, L.D. Gage, *Inorg. Chem.*, 1978, 17, 172.

32. F.A. Cotton, R.A. Walton, *Multiple Bonds between Metal Atoms*, John Wiley and Sons, 1982.

33. F.A. Cotton, J.G. Norman Jr., *J. Am. Chem. Soc.*, 1972, 94, 5967.

34. F.A. Cotton, J.L. Thompsom, *Inorg. Chem.*, 1981, 20, 3887.

35. S.N. Kelley, M. Fink, *J. Chem. Phys.*, 1982, 76, 1407.

36. F.A. Cotton, S.A. Koch, M. Millar, *Inorg. Chem.*, 1978, 17, 2087.

37. F.A. Cotton, P.E. Fanwick, R.H. Niswander, J.C. Sekutowski, *J. Am. Chem. Soc.*, 1978, 100, 4725.

38. F.A. Cotton, W.H. Ilsley, W. Kaim, *Inorg. Chem.*, 1980, 19, 1453.

39. F.A. Cotton, L.R. Falvello, S. Han, W. Wang, *Inorg. Chem.*, 1983, 26, 4106

40. F.A. Cotton, R.H. Niswander, J.C. Sekutowski, *Inorg. Chem.*, 1978, 17, 3541.

41. F.A. Cotton, R.H. Niswander, J.C. Sekutowski, *Inorg. Chem.*, 1979, 18, 1152.

42. S. Baral, F.A. Cotton, W.H. Ilsley, W. Kaim, *Inorg. Chem.*, 1982, 21, 1644.

43. S. Baral, F.A. Cotton, W.H. Ilsley, *Inorg. Chem.*, 1981, 20, 2696.

44. F.A. Cotton, W.H. Ilsley, W. Kaim, *J. Am. Chem. Soc.*, 1980, 102, 3475.

45. F.A. Cotton, W.H. Ilsley, W. Kaim, *Inorg. Chem.*, 1980, 19, 3586.

46. A. Bino, F.A. Cotton, W. Kaim, *Inorg. Chem.*, 1979, 18, 3030.

47. F.A. Cotton, X. Feng, M. Matusz, *Inorg. Chem.*, 1989, 28, 584.

48. F.A. Cotton, G.W. Rice, J.C. Sekutowski, *Inorg. Chem.*, 1979, 18, 1143.

49. C.L. Angell, F.A. Cotton, A.F. Bertram, T.R. Webb, *J. Chem. Soc., Chem. Comm.*, 1973, 399.

50. F.A. Cotton, A.F. Bertram, E. Pederson, T.R. Webb, *Inorg. Chem.*, 1975, 14, 391.

51. F.A. Cotton, B.A. Frenz, T.R. Webb, *J. Am. Chem. Soc.*, 1973, 95, 4431.

52. A. Bino, F.A. Cotton, D.O. Marler, *Inorg. Chim. Acta*, 1987, 133, 295.

53. A. Bino, F.A. Cotton, *Inorg. Chem.*, 1979, 18, 1159.

54. M.H. Chisholm, F.A. Cotton, M. Extine, B.R. Stults, *Inorg. Chem.*,1976, 15, 2252.

55. M.H. Chisholm, F.A. Cotton, C.A. Murillo, W.W. Reichert, *Inorg. Chem.*, 1977, 16, 1801.

56. M. Akiyama, M.H. Chisholm, F.A. Cotton, M.W. Extine, C.A. Murillo, *Inorg. Chem.*, 1977, 16, 2407.

57. M.H. Chisholm, F.A. Cotton, M.W. Extine, C.A. Murillo, *Inorg. Chem.*, 1978, 17, 2338.

58. M.H. Chisholm, D.A. Haitko, K. Folting, J.C. Huffman, *J. Am. Chem. Soc.*, 1981, 14, 4046.

59. A. Bino, F.A. Cotton, *Angew. Chem., Int. Ed. Engl.*, 1979, 18, 462.

60. A. Bino, F.A. Cotton, *Inorg. Chem.*, 1979, 18, 3562.

61. M.H. Chisholm, J.C. Huffman, W. van der Sluys, *Inorg. Chim. Acta*, 1986, 116, L13.

62. M.H. Chisholm, F.A. Cotton, M.W. Extine, R.L. Kelley, *J. Am. Chem. Soc.*, 1979, 101, 7645.

63. M.H. Chisholm, F.A. Cotton, M.W. Extine, R.L. Kelley, *Inorg. Chem.*, 1978, 17, 2944.

64. M.H. Chisholm, F.A. Cotton, M.W. Extine, R.L. Kelley, *J. Am. Chem. Soc.*, 1978, 100, 3354.

65. R.D. Adams, M. Brice, F.A. Cotton, *J. Am. Chem. Soc.*, 1973, 95, 6594.

66. W. Clegg, N.A. Compton, R.J. Errington, N.C. Norman, *Acta Cryst.*, 1988, C44, 568.

67. T.S. Coolbaugh, R.J. Coots, D.J. Benard, R.H. Grubbs, *Inorg. Chim. Acta*, 1985, 98, 99.

68. J.Krausse, G. Marx, G. Schödl, *J. Organomet. Chem.*, 1970, 21, 159.

69. F.A. Cotton, B.G. de Boer, M.D. LaPrade, J.R. Pipal, D.A. Ucko, *J. Am. Chem. Soc.*, 1970, 93, 2926.

70. idem, *Acta Crystallogr. B*, 1971, 27, 1664.

71. B.N. Figgis, R.L. Martin, *J. Chem. Soc.*, 1956, 3837.

72. F.A. Cotton, *Rev. Pure Appl. Chem.*, 1967, 17, 25.

73. F.A. Cotton, C.E. Rice, G.W. Rice, *J. Am. Chem. Soc.*, 1977, 99, 4704.

74. F.A. Cotton, M.W. Extine, G.W. Rice, *Inorg. Chem.*, 1978, 17, 176.

75. F.A. Cotton, G.W. Rice, *Inorg. Chem.*, 1978, 17, 2004.

76. F.A. Cotton, T.R. Felthouse, *Inorg. Chem.*, 1980, 19, 328.

77. F.A. Cotton, J.L. Thompson, *Inorg. Chem.*, 1981, 20, 1292.

78. F.A. Cotton, W. Wang, *Nouveau J. de Chimie*, 1984, 8, 331.

79. F.A. Cotton, S.A. Koch, M. Millar, *J. Am. Chem. Soc.*, 1977, 99, 7372.

80. F.A. Cotton, S.A. Koch, M. Millar, *Inorg. Chem.*, 1978, 17, 2087.

81. F.A. Cotton, M. Millar, *Inorg. Chim. Acta*, 1977, 25, L105.

82. F.A. Cotton, S.A. Koch, M. Millar, *Inorg. Chem.*, 1978, 17, 2084.

83. F.A. Cotton, M. Millar, *Inorg. Chem.*, 1978, 17, 2014.

84. F.A. Cotton, S.A. Koch, *Inorg. Chem.*, 1978, 17, 2021.

85. F.A. Cotton, R.H. Niswander, J.C. Sekutowski, *Inorg. Chem.*, 1978, 17, 3541.

86. F.A. Cotton, P.E. Fanwick, R.H. Niswander, J.C. Sekutowski, *J. Am. Chem. Soc.*, 1978, 100, 4725.

87. F.A. Cotton, R.H. Niswander, J.C. Sekutowski, *Inorg. Chem.*, 1979, 18, 1152.

88. F.A. Cotton, W.H. Ilsley, W. Kaim, *Inorg. Chem.*, 1980, 19, 1453.

89. F.A. Cotton, G.W. Rice, J.C. Sekutowski, *Inorg. Chem.*, 1979, 18, 1143.

90. A. Bino, F.A. Cotton, W. Kaim, *J. Am. Chem. Soc.*, 1979, 101, 2506.

91. A. Bino, F.A. Cotton, W. Kaim, *Inorg. Chem.*, 1979, 18, 3030.

92. S. Baral, F.A. Cotton, W.H. Ilsley, *Inorg. Chem.*, 1981, 20, 2696.

93. F.A. Cotton, T. Ren, *J. Am. Chem. Soc.*, 1992, 114, 2237.

94. F.A. Cotton, W.H. Ilsley, W. Kaim, *Angew. Chem., Int. Ed. Engl.*, 1979, 18, 874.

95. F.A. Cotton, W.H. Ilsley, W. Kaim, *J. Am. Chem. Soc.*, 1980, 102, 3475.

96. F.A. Cotton, W.H. Ilsley, W. Kaim, *J. Am. Chem. Soc.*, 1980, 102, 3464.

97. F.A. Cotton, L.R. Falvello, S. Han, W. Wang, *Inorg. Chem.*, 1983, 22, 4106.

98. S.N. Ketkar, M. Fink, *J. Am. Chem. Soc.*, 1985, 107, 338.

99. R.D. Adams, D.E. Collins, F.A. Cotton, *J. Am. Chem. Soc.*, 1974, 96, 749.

100. C.D. Garner, I.H. Hillier, M.F. Guest, J.C. Green, A.W. Coleman, *Chem. Phys. Lett.*, 1976, 41, 91.

101. M.F. Guest, I.H. Hillier, C.D. Garner, *Chem. Phys. Lett.*, 1977, 48, 587.

102. M. Benard, A. Viellard, *Nouv. J. Chim.*, 1977, 1, 97.

103. F.A. Cotton, G.G. Stanley, *Inorg. Chem.*, 1977, 16, 2668.

104. M.F. Guest, C.D. Garner, I.H. Hillier, *J. Chem. Soc., Faraday II*, 1978, 74, 2092.

105. M. Benard, *J. Am. Chem. Soc.*, 1978, 100, 2354.

106. P.M. Atha, J.C. Campbell, C.D. Garner, I.H. Hillier, A.A. MacDowell, *J. Chem. Soc., Dalton Trans.*, 1983, 1085.

107. R.A. Kok, M.B. Hall, *J. Am. Chem. Soc.*, 1983, 105, 676.

108. R. Wiest, M. Benard, *Chem. Phys. Lett.*, 1983, 98, 102.

109. J.C.A. Boeyens, *J. S. Afr. Chem. Inst.*, 1973, 26, 94.

110. M. Born, R. Oppenheimer, *Ann. Phys.*, 1927, 84, 457.

111. N.L. Allinger, *Molecular Mechanics*, Am. Chem. Soc., 1982.

112. J.C.A. Boeyens, *Struct. and Bonding*, 1985, 63, 66.

113. K.S. Pitzer, *Adv. Chem. Phys.*, 1959, 2, 59.

114. D.A. Brant, P.J. Flory, *J. Am. Chem. Soc.*, 1965, 87, 2788.

115. R.A. Scott, H.A. Scheraga, *J. Chem. Phys.*, 1965, 42, 2209.

116. K.S. Pitzer, *Adv. Chem Phys.*, 1959, 2, 367.

117. J. Ketelaar, *Chemical Constitution*, Elsevier, Amsterdam, 1953.

118. R.H. Boyd, *J. Chem. Phys.*, 1968, 49, 2574.

119. G.M. Sheldrick, *Computing in Crystallography*, Eds: H. Schenk , R. Olthof-Hazelkamp, H. van Koningsveld and G.C. Bassi, Delft University Press, Holland.

120. M.D. Hopkins, T.C. Zietlow, V.M. Miskowski, H.B. Gray, *J. Am. Chem. Soc.*, 1985, 107, 510.

121. F.A. Cotton, J.C. Eglin, B. Hong, C.A. James, *J. Am. Chem. Soc.*, 1992, 114, 4915.

122. J.C.A. Boeyens, F.A. Cotton, S. Hans, *Inorg. Chem.*, 1985, 24, 1750.

123. J.C.A. Boeyens, *Inorg. Chem.*, 1985, 24, 4149.

124. F.A. Cotton, K.M. Dunbar, R. Poli, *Inorg. Chem.*, 1986, 25, 3700.

125. P.E. Fanwick, W.S. Harwood, R.A. Walton, *Inorg. Chim. Acta*, 1986, 122, 7.

126. F.A. Cotton, P.E. Fanwick, J.W. Fitch, H.D. Glicksman, R.A. Walton, *J. Am. Chem. Soc.*, 1979, 101, 1752.

127. J. San Filipo Jr., H.J. Sniadoch, *Inorg. Chem.*, 1973, 12, 2326.

128. B. Hutchinson, J. Morgan, C.B. Cooper, Y. Mathey, D.F. Shriver, *Inorg. Chem.*, 1979, 18, 2048.

129. M.C. Manning, W.C. Trogler, *J. Am. Chem. Soc.*, 1983, 105, 5311.

130. A.P. Sattelberger, J.P. Fackler, *J. Am. Chem. Soc.*, 1977, 99, 1258.

131. W.K. Bratton, F.A. Cotton, M. Debeau, R.A. Walton, *J. Coord. Chem.*, 1971, 1, 121.

132. A.P. Ketteringham, C. Oldham, C.J. Peacock, *J. Chem. Soc., Dalton Trans.*, 1976, 1640.

133. A. Loewenschuss, J. Shamin, M. Ardon, *Inory. Chem.*, 1976, 15, 238.

134. M.D. Hopkins, V.M. Miskowski, H.B. Gray, *J. Am. Chem. Soc.*, 1986, 108, 959.

135. C.G. Arena, F. Faraone, M. Fochi, M. Lanfranchi, R.S. Mealli, A. Tiripicchio, *J. Chem. Soc., Dalton Trans.*, 1992, 1847.

136. P. Johnston, L. Denner, C.F Marais, J.C.A. Boeyens, N.J. Coville, *J. Crystall. and Spectros. Research*, 1988, 18, 403.

137. R.M. Badger, *J. Chem. Phys.*, 1934, 2, 128.

25×

138. W. Gordy, *J. Chem. Phys.*, 1946, 14, 305.

139. J.C.A. Boeyens, *Private Communication.*

140. J.C.A. Boeyens, D.J. Ledwidge, *Inorg. Chem.*, 1983, 22, 3587.

141. C.D. Garner, I.H. Hillier, A.A. MacDowell, I.B. Walton, M.F. Guest, *J. Chem. Soc., Faraday Trans. 2*, 1979, 75, 485

142. R.A. Kok, M.B. Hall, *Inorg. Chem.*, 1985, 24, 1542.

143. R.D. Davy, M.B. Hall, *J. Am. Chem. Soc.*, 1989, 111, 1268.

144. B.E. Bursten, D.L. Clark, *Ployhedron*, 1987, 6, 695.

145. J.G. Norman Jr., H.J. Kolari, *J. Am. Chem. Soc.*, 1978, 100, 791.

146. Y.Y. Kharitonov, G.Y. Mazo, N.A. Knyazera, *Russ. J. Inorg. Chem.*, 1970, 15, 739.

147. I.K. Kireeva, G.Y. Mazo, R.N. Shchelokov, *Russ. J. Inorg. Chem.*, 1979, 24, 220.

148. A.P. Ketteringham. C. Oldham, *J. Chem. Soc., Dalton Trans.*, 1973, 1067.

149. R.J.H. Clark, A.J. Hempleman, *Inorg. Chem.*, 1988, 27, 2225.

150. R.J.H. Clark, A.J. Hempleman, C.D. Flint, *J. Am. Chem. Soc.*, 1986, 108, 518.

151. F.A. Cotton, T.R. Felthouse, *Inorg. Chem.*, 1980, 19, 323.

152. F.A. Cotton, B.G. de Boer, M.D. LaPrade, J.R. Pipal, D.A. Ucko, *Acta Crystallogr.*, 1971, B27, 1664.

153. F.A. Cotton, T.R. Felthouse, *Inorg. Chem.*, 1980, 19, 2347.

154. G.G. Christoph, J. Halpern, G.P. Khare, Y.B. Koh, I.C. Romanowski, *Inorg. Chem.*, 1981, 20, 3029.

155. R.J.H. Clark, A.J. Hempleman, C.D. Flint, H.M. Dawes, M.B. Hursthouse, *J. Chem Soc., Dalton Trans.*, 1985, 1775.

Author: O'Neill Francoise Marcelle Mary.

Name of thesis: Molecular mechanics calculations of dimetal bonds,

PUBLISHER:

University of the Witwatersrand, Johannesburg
©2015

LEGALNOTICES:

Copyright Notice: All materials on the University of the Witwatersrand, Johannesburg Library website are protected by South African copyright law and may not be distributed, transmitted, displayed or otherwise published in any format, without the prior written permission of the copyright owner.

Disclaimer and Terms of Use: Provided that you maintain all copyright and other notices contained therein, you may download material (one machine readable copy and one print copy per page)for your personal and/or educational non-commercial use only.

The University of the Witwatersrand, Johannesburg, is not responsible for any errors or omissions and excludes any and all liability for any errors in or omissions from the information on the Library website.